

DENDROCOLOGY OF WHITE SPRUCE (*PICEA GLAUCA* [MOENCH] VOSS)
IN SOUTHERN SASKATCHEWAN

BY

BRYAN J. MOOD

A thesis submitted to the
Department of Geography and Environment
Mount Allison University
in partial fulfillment of the requirements for the
Bachelor of Science degree with Honours

15 April 2013

Table of Contents

List of Tables.....	iv
List of Figures.....	v
Abstract.....	vi
Acknowledgements.....	vii
1. Introduction.....	1
1.1 Literature Review.....	1
1.1.1 Dendrochronology in Saskatchewan.....	1
1.1.2 Current and Future Climate of Saskatchewan.....	2
1.1.3 The Boreal Forest Treeline.....	2
1.1.4 Tree-Rings and Climate.....	2
1.2 Filling the Gap.....	3
1.3 Research Objectives.....	3
1.3 Accessible Science.....	4
1.5 References.....	5
Statement of Co-authorship	7
2. Observed growth thresholds of <i>Picea glauca</i> in Saskatchewan and its implications for climate change induced range migration.....	8
2.0 Abstract.....	9
2.0.1 Keywords.....	9
2.1 Introduction.....	10
2.2 Study Area.....	12
2.3 Methods.....	14
2.4 Results.....	16
2.5 Discussion.....	17
2.6 Conclusion.....	19
2.7 Acknowledgements.....	20
2.8 References.....	21
2.9 Tables.....	25
2.10 Figures.....	28
3. Conclusions.....	34

3.1	References.....	36
4.	Appendices	37
	Appendix A: Standardized Radial Growth Chronologies.....	37
	Appendix B: DendroCLIM2002 Figures.....	40
	Appendix C: Local Moran’s I (LISA) Clustering Analysis Results.....	52
	Appendix D: Eigenvector Analysis Data Tables.....	75
	Appendix E: Tree-Ring Annual Growth Estimator (TRiAGE) Program.....	81

List of Tables

- Table 2.9.1 Study site sampling information for all locations. MSI = mean series intercorrelation and demonstrates strength of correlation between samples at the same location based of 30-year segments. MTA = mean tree age. MS = mean sensitivity which demonstrates mean year-to-year variability of radial growth within the chronology.
- Table 2.9.2 Frequency of significant response functions found using the statistical program DENDROCLIM2002.
- Table 2.9.3 Radial growth and climate eigenvector component percentage values of explained variance.

List of Figures

Figure 2.10.1 Study area with climate and site locations in southern Saskatchewan (Supplementary sites are not shown on this figure).

Figure 2.10.2 Map demarcating thresholds of growth for white spruce in southern Saskatchewan. Thresholds are quantified through mean sensitivity: normal (<0.300), stressed (0.300 – 0.400), super-stressed (0.400-0.500), and intolerable (>0.500).

Figure 2.10.3 Histogram representing frequency of significant correlations (95% confidence) to monthly climate variables between April of the previous year and the current October climate data. Capitalized month abbreviations (e.g., APR, MAY, JUN) indicate previous year, non-capitalized month abbreviations (e.g., Apr, May, Jun) indicate present year. Lines indicate average correlations and bar plots indicate frequency of significant correlations. Supplementary study sites are not used for this analysis.

Figure 2.10.4 Radial growth eigenvector (RGE) analysis loadings spatially mapped in southern Saskatchewan: A) RGE I, B) RGE II, and C) RGE III. Number values within maps indicate the percentage of explained variance. Supplementary study sites were not used for this analysis.

Figure 2.10.5 Climate eigenvector loadings spatially mapped in southern Saskatchewan. Twenty-four eigenvectors were created. The three observably similar eigenvectors are displayed: A) June precipitation, B) May precipitation, C) June temperature, all other data is not displayed.

Abstract

Southern Saskatchewan's shelterbelts present a unique opportunity to examine the boreal forest's southern range limits. This thesis fills a research gap regarding spatial relationships by employing tree-ring analysis techniques throughout southern Saskatchewan to quantify the changes in the southern range limits of the boreal forest at a regional scale. This is the first study specifically dedicated to understanding how climate change will affect the redistribution of white spruce (*Picea glauca* [Moench] Voss) at its southern range limit rather than at the latitudinal treeline. We have also made the science and results accessible to landowners throughout Saskatchewan through an internet based program.

This study used four linear transects, two north-south and two east-west, to acquire a spatial representation of white spruce growth in southern Saskatchewan and utilized supplementary data from the International Tree-Ring Data Bank (ITRDB). Twenty-three radial growth chronologies were developed from primary sampling with seven supplementary sites in northern Saskatchewan. These chronologies were examined spatially using a geographic information system as well as standard dendroclimatology and dendroecology techniques.

Dendroclimatological results indicate that June temperature, June precipitation, and May precipitation are dominant factors in the growth of white spruce. It was also found that mean sensitivity, year-to-year variance in radial growth, has a significant relationship to latitude and longitude with the highest measures found in southwestern Saskatchewan. These results in addition to predicted changes to future temperature and weather patterns suggest that white spruce will be under increased physiological stress in these same zones where they currently illustrate the highest mean sensitivity values.

Acknowledgements

This research project was facilitated through a number of financial and other contributions. Data analysis was provided by the Mount Allison Dendrochronology Laboratory (MAD Lab) and funding was provided by the Agricultural Greenhouse Gas Project (AGGP).

A *titanic* thanks to Colin (*Cee-Doc*) Laroque. You took me under your wing and encouraged me to try and achieve things I only dreamt about. I honestly have no idea how you put up with my constant complaining and bickering but without your help there is no doubt that I would still be thinking of a title for this thesis. “Beverages” on me anytime or at least once I get a job(s).

Dear MAD Labbers – Cecilia (*CC*) Jennings, Emma (*Pumps*) Davis, Sarah (*Trixie*) Quann, Emily (*Chuckles*) Hogan, Jay (*Chick Allen*) Maillet, Geoff (*Jiffy*) Kershaw, Stuart (*Stooge*) Murray, Logan (*Bonecrusher*) Laroque, Jacqueline (*Jack*) Carverhill, et al. – thank you for making my summers so fantastic. My gut and cholesterol do not thank you for the many potlucks and beers but it was 100% worth it.

And a huge thanks to my Mother and Father for your support both financially and mentally, I highly doubt that I could have done anything without the two of you to lean on when I was down. And of course, thank you Kaitlin, without you I would not be the person I am today. You taught me so, so many things about life, school, and love. I would consider myself lucky if I ever become half the person or half as smart as you are.

1.0

Introduction

Global warming has resulted in changes to regional weather patterns as well as increased temperatures (IPCC 2007). The outcome of these changes is a potential rapid redistribution of plant and animal species throughout North America (Harsch et al. 2009), assessing how and why these abrupt changes are occurring is important for understanding where major reorganizations of ecosystems will take place (McKenney et al. 2007). Using dendrochronology, the study of tree rings (Fritts 1976), it is feasible to understand how tree species are migrating and reacting to climate change in the southern range limits within Saskatchewan.

Dendrochronology analyzes variation in tree-ring radial growth which acts as a repository for environmental information. With this information it is possible to relate tree-ring growth to the surrounding ecosystem and climate using dendroecology and dendroclimatology, respectively. These two sub-disciplines for dendrochronology can answer two important questions: dendroclimatology can indicate what causes the trees to grow; and dendroecology is able to determine where and how they are growing through time and space.

1.1 Literature Review

1.1.1 Dendrochronology in Saskatchewan – To date, only one dendrochronological study on shelterbelt trees has taken place in southern Saskatchewan by Davis et al. (2013). The study examined the potential for tree-ring studies on these trees in southern Saskatchewan for nine common species: *Salix acutifolia* (Acute willow), *Caragana arborescens* (caragana), *Picea pungens* (Colorado spruce), *Fraxinus pennsylvanica* (green ash), *Populus sp.* (hybrid poplar), *Acer negundo* (Manitoba maple), *Ulmus pumila* (Siberian Elm), and *Picea glauca* (white spruce). The study determined that white spruce, a common and representative boreal forest species (Takhtajan 1986), was the best overall species for further dendrochronological studies throughout the region. Other tree-ring studies in the province are limited to northern Saskatchewan, namely a dendrohydrology study by Beriault and Sauchyn (2006) which reconstructed streamflow in the Churchill Basin. This study noted that samples of white spruce taken were in the higher range of mean sensitivity (0.200-0.250) and located near a water source.

1.1.2 Current and Future Climate of Saskatchewan – Saskatchewan has a highly continental climate with extremely variable temperatures in the summer and winter. Over the past 50 years a number of changes to climate have occurred. There is a general trending of increased temperatures throughout Saskatchewan which is likely to continue (IPCC 2007). Precipitation has been shown to be increasing through time (Akinremi et al. 2001) and it is predicted that this trend will continue, however overall precipitation during the spring months will decrease while winter snowfall will increase (Cutforth et al. 1999) resulting in a potential water crisis (Wetherald and Manabe 1999; Schindler and Donahue 2006). This also means that there will be an increase and earlier spring runoff each year (Cutforth et al. 1999).

1.1.3 The Northern Boreal Forest Treeline – A number of studies have observed and recorded the changes to the northern treeline of the boreal forest and other forest systems. It has been determined that at least 52% of treelines are advancing, 1% receding, and 47% are at equilibrium at a global scale (Harsch et al. 2009). These results may be slightly skewed regarding the number of advancing treelines, as well due to the sporadic nature of recruitment events, which is determined by local, landscape, and regional-scale factors and has been found not to be uniform (Danby and Hik 2007a). In addition to the notion that there is a general advance of treelines globally, future projections of climate-envelopes suggest that they will continue to advance well into the next century (McKenney et al. 2007) while there is a predicted contraction in the southern limits of species climate-envelopes.

1.1.4 Tree-Rings and Climate – Climate often has a large influence on tree-ring annual radial growth (Fritts 1976). Alterations in the patterns of growth may indicate the favorable and unfavorable climatic conditions which result in greater or less average growth. Using eigenvector (principal component) analysis, a statistical procedure of data reduction used when data sources exhibit high dimensionality and a more essential pattern of causal growth factors is desired (Zuur et al. 2007), it is possible to extract relationships between climate and tree-rings. Eigenvector analysis is especially applicable in this study as it is able to extract macroscale climatic signals (Brubaker 1980) rather than microclimatic factors that cause minuscule changes in growth due to their exposure within shelterbelts. DendroCLIM2002, a statistical program using eigenvector analysis, response functions, and regressions (Biondi and Waikul 2004) is a commonly used tool for interpreting this association. These relationships are often used to reconstruct past climate

(Fritts 1976) where climate data (e.g., summer temperature reconstructions [Wilson and Luckman 2003]) is not readily available prior to direct human observations. In the case of this research project, we use the linkages between trees and climate to comprehend limiting factors associated with the possibility of heightened physiological stress.

1.2 Filling the Gap

There have been a number of studies looking at the general northward migration of boreal forest species throughout North America (e.g., McKenney et al. 2007; Danby and Hik 2007*a*; Harper et al. 2011). The northern latitudinal treeline has been extensively studied because it demarcates the boreal-tundra ecotone (Harper et al. 2011) and is easily defined. The latitudinal treeline is defined primarily by frost damage which causes immediate mortality for many species (Loehle 1998). The threshold where frost damage stops trees from recruiting in the northern range limitation is changing, allowing for tree species ranges to migrate further northward through sporadic recruitment events (Danby and Hik 2007*a*). The body of the boreal forest has also been studied by McKenney et al. (2007) where they quantified a number of important projected migrations of tree species in Canada's boreal forest. The study determined that tree species will migrate northward between 330 and 700 km depending on the climate scenario used (McKenney et al. 2007).

There is a noticeable gap in the current scientific literature attempting to study the southern range limits of many of the boreal forest tree species. This is primarily due to the large scale gradient associated with the southern limitations compared to the abrupt limits in the north. Where the northern treeline is caused by frost damage, the southern treeline is caused primarily by temperature (Loehle 1998). Trees in the south are also able to live outside of their natural range in gardens and shelterbelts as introduced species (Loehle 1998). This is the first study where the southern natural range limit and the range of introduction will be defined and investigated in regard to its potential migration and the causal factors.

1.3 Research Objectives

The objectives of this research project are to:

- examine the radial growth trends of white spruce in southern Saskatchewan (Chapter 2; Appendix A; Appendix C)
- analyze the relationship between radial growth and climatic variability (Chapter 2; Appendix B; Appendix D)
- determine the growth thresholds of white spruce in southern Saskatchewan and determine its relationship to the boreal forest (Chapter 2)
- make this science accessible to landowners that would find this information useful through an internet based program (Appendix E)

1.4 Accessible Science

The radial-growth chronologies developed through this research project as well as previous (e.g., Davis et al. 2013) and future initiatives will be accessible to the public through a web-based program (Appendix E). The purpose of this program is to assist landowners when they decide to plant new shelterbelts in southern Saskatchewan. The program prompts the user to input several key pieces of information, namely: the global climate model, tree species, and their location. These inputs are given to the program as variables and the output is a future radial growth forecast for the option they have chosen. A working version of the model can be found at: <http://www.mta.ca/madlab/GHG//Model/program-send.php> .

1.5 References

- Akinremi, O.O., McGinn, S.M., and Cutforth, H.W. 2001. Seasonal and spatial patterns of rainfall trends on the Canadian Prairies. *Journal of Climate*, 14, 2177-2182.
- Berriault, A. L. and Sauchyn, D.J. 2006. Tree-ring reconstructions of streamflow in the Churchill River Basin, Northern Saskatchewan. *Canadian Water Resources Journal*, 31(4), 249-262.
- Cutforth, H.W., McConkey, B.G., Woodvine, R.J., Smith, D.G., Jefferson, G., and Akinremi, O.O. 1999. Climate change in the semiarid prairie of southwestern Saskatchewan: Late winter-early spring. *Canadian Journal of Plant Sciences*, 79, 343-350.
- Danby, R.K. and Hik, D.S. 2007a. Variability, contingency and rapid change in recent subarctic alpine tree line dynamics. *Journal of Ecology*, 95, 352-363.
- Danby, R.K. and Hik, D.S. 2007b. Responses of white spruce (*Picea glauca*) to experimental warming at a subarctic alpine treeline. *Global Change Biology*, 13, 437-451. doi: 10.1111/j.1365-2486.2006.01302.x
- Davis, E.L., Laroque, C.P., and Van Rees, K. 2013. Evaluating the suitability of nine shelterbelt species for dendrochronological purposes in the Canadian Prairies. *Agroforestry Systems*. doi: 10.1007/s10457-012-9591-8.
- Fritts, H.C. 1976. *Tree Rings and Climate*. Academic Press, London, 567 pp.
- Harper, K.A., Danby, R.K., De Fields, D.L., Lewis, K.P., Trant, A.J., Starzomski, B.M., Savidge, R., and Hermanutz, L. 2011. Tree spatial pattern within the forest-tundra ecotone: a comparison of sites across Canada. *Canadian Journal of Forest Research*, 41, 479-489. doi: 10.1139/X10-221
- Harsch, M.A., Hulme, P.E., McGlone, M.S., and Duncan, R.P. 2009. Are treelines advancing? A global meta-analysis of treeline response to climate warming. *Ecology Letters*, 12, 1040-1049. doi: 10.1111/j.1461-0248.2009.01355.x

- [IPCC] Intergovernmental Panel on Climate Change. 2007. Climate Change 2007: The Physical Science Basis. Summary for Policy Makers (17 November 2012; <http://www.ipcc.ch/>).
- Loehle, C. 1998. Height growth rate tradeoffs determine northern and southern range limits for trees. *Journal of Biogeography*, 25, 735-742.
- McKenney, D.W., Pedlar, J.H., Lawrence, K., Campbell, K., and Hutchinson, M.F. 2007. Potential impacts of climate change on the distribution of North American trees. *Bioscience*, 57, 939-948.
- Schindler, D.W. and Donahue, W.F. 2006. An impending water crisis in Canada's western prairie provinces. *PNAS*, 103, 7210-7216.
- Wetherald, R.T. and Manabe, S. 1999. Detectability of summer dryness caused by greenhouse warming. *Climatic Change*, 43, 495-511.

Statement of Co-authorship

All data analysis was completed by Bryan J. Mood with support from M. Graham Clark. Sample design and development was completed by Bryan J. Mood with input and logistical support from Colin P. Laroque.

Manuscript preparation from Chapter 2 (“Observed growth thresholds of *Picea glauca* in Saskatchewan and its implication for climate change induced range migration”) was completed by Bryan J. Mood, with comments and editorial suggestions from Colin P. Laroque. This manuscript is planned to be submitted to Global Change Biology.

2.0

Observed growth thresholds of *Picea glauca* in Saskatchewan and its implications for climate change induced range migration

Bryan J. Mood^{1,2}, M. Graham Clark¹, and Colin P. Laroque¹

¹ Mount Allison Dendrochronology Laboratory

Department of Geography and Environment

Mount Allison University

Sackville, New Brunswick, E4L 1A7

Phone (506) 364-2390

Fax (506) 364-2625

E-mail:

bjmood@mta.ca

gclark@mta.ca

claroque@mta.ca

² corresponding author

2.0 Abstract

Climate change has resulted in the northward migration of many tree species in Canada and is likely to continue as greenhouse gas emissions alter weather patterns. The northern range limit and expansion of trees has been frequently studied but there has been little research concerning the effects of climate change on the fluctuations that will occur at the southern range margins of some of the same species. White spruce (*Picea glauca*) shelterbelts, an agroforestry product in southern Saskatchewan, represent a unique opportunity that offers significant insight into the future physiological stresses on the boreal forest in central and northern Saskatchewan. A regional pattern of radial growth for white spruce in both shelterbelts and natural forests throughout Saskatchewan was constructed using dendrochronological techniques. Thirty chronologies were established ranging from 36 to 188 years old and it was found that mean sensitivity had a significant relationship with latitude and longitude ($R^2 = 0.790$; $p < 0.0000$). Using eigenvector analysis it was found that white spruce growth variance is associated with June temperature, spring precipitation, and changes in soil characteristics.

Using mean sensitivity as a measure of physiological stress on white spruce, two implications can be interpreted. First, results of past growth taken in combination with future climate predictions of increasing surface temperature and changes in precipitation patterns suggest a physiological stress imposed on white spruce in southern Saskatchewan. And second, a future contraction of the optimum climate-envelope of white spruce in the southern boreal forest range margins will likely occur.

2.0.1 Keywords: boreal forest, climate change, climate-envelope, dendrochronology, dendroecology, eigenvector analysis, mean sensitivity, *Picea glauca*, tree migration, white spruce.

2.1 Introduction

Dendrochronology can be used as a reliable proxy for observation of climate variability and vulnerability (Fritts 1976). In southern Saskatchewan, dendrochronological methods may be useful to assess the present and future vulnerability of white spruce (*Picea glauca* [Moench] Voss) within shelterbelts as well as in the southern range margins of the boreal forest. As plant species begin to migrate northward (McKenney et al. 2007) they direct their energy towards recruitment strategies in higher latitudes (Woodall et al. 2009) and succumb to mortality events in the southern regions of their range. Determining the physiological stress and potential for mortality events in the southern range limits of the boreal forest is crucial in order to determine the contraction of the white spruce climate-envelope (McKenney et al. 2007), described as the current ecological niche for each species.

Nationally, tree species climate-envelopes are projected to migrate northward in the next century, as tree recruitment in the north increases in frequency and mortality events increase in the south (Woodall et al. 2009). McKenzie et al. (2007) suggested two extreme scenarios for tree migration: 1) a full-dispersal scenario where species move entirely into their future climate-envelopes or 2) a no-dispersal scenario where species do not move out of their current niches. The first scenario demonstrates a northward shift of 700 km, and the second scenario suggests a migration of approximately 330 km from their current locations. In both cases the optimum climate-envelope for each species is expected to contract. Regionally, species-specific results indicate that the white spruce's climate-envelope could advance between 190 km (B1 climate scenario) and 560 km (A1 climate scenario) northward by the year 2100 in Saskatchewan (McKenney et al. 2007) due to increased physiological stress and frequency of mortality events in the southern range margins (Woodall et al. 2009). These results suggest a marked potential redistribution and increased probability of mortality throughout Saskatchewan. Although these results demonstrate redistributions of many tree species, the causal factors have been left undetermined in addition to a quantifiable measure of white spruce species vulnerability.

No research initiatives have focused their attention on tree species at the southern range margins or their response to climatic changes in Saskatchewan. Northern range margins and the core of the boreal forest have been studied extensively (e.g., Danby and Hik 2007a, 2007b; McKenzie et al. 2007; Harper et al. 2011) because tree recruitment at latitudinal and altitudinal

treelines are readily available for study with recognizable changes in biota at the forest-tundra ecotone (Harper et al. 2011). The southern range margin is problematic for scientific inquiries because many species have the ability to grow farther south than the accepted range limit, in gardens and acceptable microclimates (Woodall et al. 2009), contrasting the northern limitations where the length of winter dormancy and frost damage become a key limiting factor (Loehle 1998) regarding northward migration. Traditionally, an optimal temperature has assumed to exist for the growth of a tree species (Loehle 1998) but recent studies have indicated that northern white spruce treeline advances are determined by beneficial recruitment events that occur abruptly and sporadically at local and regional levels (Danby and Hik 2007a). In the south temperature (Loehle et al. 1998), drought, and temperature induced-drought events (Barber et al. 2000) have been associated with regional mortality events. With recent estimates predicting an increase in global mean temperatures of 2.4 to 6.4 degrees Celsius (°C) (IPCC 2007) there is a need to quantify the vulnerability of white spruce at its southern range limitations within Saskatchewan now and in the future.

Large-scale weather systems affect tree growth by modifying the microenvironment of individual trees (Brubaker 1980) and represent an opportunity to understand climate-growth variability (Hughes 2002). Using dendroclimatology, the use of tree rings to reconstruct and study effects of climate on tree rings (Kaennel and Schweingruber 1995), it is possible to identify variations in tree ring radial growth associated with macroclimatic factors such as temperature and precipitation (Fritts 1976). If the response of tree growth to climate related variables is sufficiently strong, there will be a predictable relationship of annual growth among stands which are influenced by the same weather patterns on an annual basis (Brubaker 1980) although local differences vary greatly (e.g., elevation, slope, soil type). In order to infer relationships between trees and climate, trees should not be complacent in their growth indicated by mean sensitivity (MS), a measure of year-to-year variation, which is considered to be below 0.100 (Grissino-Mayer 2001). Instead, the trees under study should exhibit variation that reflects their daily and seasonal growth limiting processes (Beriault and Sauchyn 2006). In stressed environments tree-ring chronologies and individual trees typically exhibit MS above 0.200 indicating the physiological stresses imposed on tree ring radial growth is highly variable (Grissino-Mayer 2001). Mean sensitivity may be considered a measure of physiological stress on individual trees, directly related to the severity and number of limiting factors for radial growth (Beriault and

Sauchyn 2006), making them preferred for detecting climatic influences (Sakulich 2011). Therefore it is also an excellent measure to empirically determine the likelihood of a mortality event for an individual tree or tree stand by understanding that as mean sensitivity increases, the probability of mortality is also increased.

The purpose of this study is to (1) examine the causal factors for variability in white spruce radial growth throughout southern Saskatchewan and; to (2) investigate the current variability of radial growth as it relates to the boreal forest and demarcate the increasingly stressed areas of white spruce growth throughout southern Saskatchewan as previously suggested by Davis et al. (2013). This study uses a number of techniques to interpret the variability of white spruce growth and the causal factors. Eigenvector (principal component) analysis is used to determine the macroclimatic effects on trees throughout southern Saskatchewan. This will help to determine the causal factors for increasing physiological stress in white spruce shelterbelts. Mean sensitivity will be used to determine growth thresholds of white spruce throughout southern Saskatchewan, and combined with the results from the previous analyses, will result in a holistic understanding of current and future physiological stresses and growth thresholds for white spruce in the study area.

2.2 Study Area

Previously only one dendrochronological analysis of shelterbelts trees has occurred in Saskatchewan by Davis et al. (2013) determining the fitness of nine shelterbelt species for further analysis. The study determined that white spruce was the most appropriate species for further studies and was therefore chosen to be used in this study as it is also found throughout the boreal forest. The white spruce found in southern Saskatchewan is genetically the same as those found in higher latitudes (de Lafontaine et al. 2010) and is considered to be the species most representative of the boreal forest (Takhtajan 1986) because it can be found throughout the Canadian boreal forest in abundance.

Data collection took place in southern Saskatchewan, south of the boreal forest-grasslands ecotone, in shelterbelts located on agricultural land. Each study site was located near a location where long-term homogenized climate data was available for analysis (Environment Canada 2010). Site selection was based primarily on accessibility and location, although certain

criteria had to be met in order for sampling to advance. Study locations were taken along four theoretical linear transects throughout southern Saskatchewan (Figure 2.10.1) to create an acceptable and dispersed representation of growth throughout southern Saskatchewan. The number of white spruce trees at a study location was required to be at a minimum 10 trees, although above 20 was preferred to allow for more random sampling within a site. In addition, landowners were consulted prior to sampling to provide preliminary information (e.g., age of shelterbelt) that helped to determine whether sampling should commence. Shelterbelts that had previously been significantly modified through anthropogenic activity (e.g., consistent watering or fertilizing) were disregarded in this study.

Southern Saskatchewan is classified as tall grass prairie with Chernozemic soils, and parent material of fluvial and glaciofluvial origins (Dale and Lewry 2007). The climate of the region is highly variable with warm summers in a continental climate (DfB) (Environment Canada 2010). Saskatchewan has had significant increases in both rainfall amount and frequency, except in southwestern Saskatchewan, which has received relatively little increase in overall precipitation in comparison with the other Canadian Prairie provinces (Akinremi et al. 2001). Spring precipitation patterns diverge from the national average by as much as +120 mm in south-central Saskatchewan (Environment Canada 2010). The projected increases in surface temperature (IPCC 2007) indicate that further increases in precipitation amounts and frequency are to be expected (Akinremi et al. 2001) although southern Saskatchewan is not expected to follow this trend (Ripley 1986).

Supplementary data from the International Tree Ring Data Bank (ITRDB) was used to increase the sample depth and spatial coverage of study sites, as well as to verify hypothesis as they relate to the greater boreal forest. Seven white spruce chronologies were available from the ITRDB. The chronologies were deposited by Beriault and Sauchyn (2006) as part of streamflow reconstructions in the Churchill Basin of Northern Saskatchewan. The Churchill Basin begins in east-central Alberta, drains a large part of Saskatchewan before passing into Manitoba and emptying into Hudson Bay (Beriault and Sauchyn 2006). The area has short, cool summers and cold winters. Streamflow in the area is dominated by snowmelt runoff and summer precipitation. The sample sites were targeted towards likely moisture-stressed environments (Beriault and Sauchyn 2006), resulting in perhaps higher mean sensitivity measurements.

2.3 Methods

At each of the 23 site locations, white spruce trees were identified and 20 individuals were randomly selected for sampling when available. Landowners were questioned prior to actual sampling to determine if the trees were of the minimum 30 years old but preferably over 50 years in age. Two core samples were taken at right angles from one another at each tree. The samples were collected at breast height using a 5.1 mm increment borer and stored in straws for transportation. Sample preparation in the laboratory was conducted by gluing the tree cores into slotted mounting boards and then sanding them with progressively finer sand paper (80-600 grit) until their annual rings were clearly visible.

The samples were initially visually crossdated (pattern matched) for common marker years of suppressed or increased radial growth (Stokes and Smiley 1968). The annual-ring widths of the cores were then measured using a Velmex measuring stage and viewed through a 63X microscope, with a precision of 0.001 mm. Measurements were digitized and recorded using Measure J2X software (Voortech 2011), and then statistical crossdating was conducted utilizing the computer program COFECHA (Holmes 1983). In a few cases, some series of individual increment core measurements were eliminated due to irresolvable pattern matching errors.

COFECHA produces a number of statistical outputs that provide insight into the characteristics for a series of tree-ring measurements including sample depth, time-span of the series, the total rings within the series, interseries correlation, average mean sensitivity, and the mean tree age. Interseries correlation measures the strength of the common growth signal that is being expressed within and between trees at a site location. An interseries correlation value of 0.4226 was required to exceed the 99% confidence interval to be considered significant in our study. Mean sensitivity is a descriptive statistic of how responsive or how vulnerable the growth of a particular tree is to its surrounding environment (Fritts 1976; Grissino-Mayer 2001). A high degree of sensitivity indicates a high degree of changes in annual radial growth from year-to-year which is influenced by environmental parameters (Davis et al. 2013). Mean sensitivity from each study site location and supplementary location from ITRDB was correlated with latitude and longitude, and then mapped spatially to infer gradients of climatic vulnerability and probability of tree mortality in Saskatchewan.

Once a final master chronology was completed for a study location, the computer program ARSTAN (Cook 1985) was used to standardize the measurements. This was done to remove inherent biological growth trends of decreasing width from pith to bark (Brubaker 1980) whereby each measurement series was fit with a negative exponential curve. These newly standardized master chronologies were used to analyze and compare radial growth between sites and against climate.

The standardized measurements for each site and homogenized climate data from local climate stations over the same time-span were input into the program DendroClim2002 to determine the main climate factors influencing annual-radial growth (Biondi and Waikul 2004). The months of April of the previous-growth year, to September of the current-growth year, for both monthly temperature and precipitation variables, were selected for this analysis. This window was selected as it is considered to include the months that will most likely influence radial growth in white spruce. DendroClim2002 conducts both correlation and response function analyses, and provides an output that indicates which climatic variables are significantly correlated to growth (Biondi and Waikul 2004). The degree of significance of the correlation and response function tests are provided and are useful in demonstrating which climate factors are likely to be the strongest predictors of radial growth in terms of months in the current, and/or previous year, as well as in terms of a temperature and/or precipitation variable (Biondi and Waikul 2004).

Eigenvector analysis was conducted according to methods established by LaMarche and Fritts (1971), Blasing and Fritts (1976), and Brubaker (1980), although tree selection was not as comprehensive due to the lack of adequate sample selection in shelterbelts (e.g., tree age was not optimal). The dataset consisted of 23 standardized radial growth chronologies from southern Saskatchewan over a common interval (1975 – 2010). Lower order eigenvectors represent the most important large-scale anomaly patterns and higher order vectors reflect small-scale growth anomaly relationships (Brubaker 1980) that can be discarded for the purposes of this study. The major eigenvectors were then related visually to climate eigenvectors developed from homogenized climate stations throughout Saskatchewan to determine the significance of temperature and precipitation on growth variance.

2.4 Results

Sites ranged from 101.7°E to 108.3°E in longitude and 49.2°N to 57.9°N in latitude, covering a large percentage of Saskatchewan with the highest frequency of sites occurring in the south. Twenty-three radial growth chronologies were developed ranging from 36 to 88 years, with mean sensitivities values varying between 0.207 and 0.531 in southern Saskatchewan (Table 2.9.1), indicating a wide range of values from intermediate to extremely high environmental sensitivity compared to the previously established thresholds (Low: 0.10-0.19, Intermediate: 0.20-0.29, and High: >0.30, Grissino-Mayer 2001). The seven supplementary radial growth chronologies from northern Saskatchewan (ITRDB 2012) spanned between 112 and 174 years old with mean sensitivities ranging from 0.218 to 0.276. Site interseries correlation ranged between 0.460 and 0.788, all significant to 99%.

When mean sensitivity values were correlated to its geographic location several significant relationships arise. Longitude explains the data with an R^2 of 0.467 ($p = 3 \times 10^{-5}$), latitude presents an R^2 of 0.342 ($p = 7 \times 10^{-4}$), and when both are used in a multivariate regression, the R^2 is 0.790 ($p = 7 \times 10^{-10}$) (Table 2.10.2). When the regression models are further analyzed in association with spatial interpolation techniques (Figure 2.10.2) a gradient of increasing sensitivity from southwest to northeast in southern Saskatchewan is evident. Figure 2 demonstrates four distinctive thresholds of sensitivity: Normal (< 0.300), Stressed (0.300 – 0.400), Super-Stressed (0.400 – 0.500), and Intolerable (> 0.500). This measure was used as a measure for likelihood of tree mortality. The site 12QL200 was considered to have a relative low mean sensitivity in this study due to its close proximity to a water source.

The results of the climate analysis from DendroClim2002 are represented in Table 2.9.3 and Figure 2.10.3. These results demonstrated a high frequency of significant correlations and response functions between the months of May and September with a markedly higher number of significant values found for precipitation. The majority of sample sites are positively correlated to precipitation and negatively associated with temperature. Of the 36 variables June precipitation of the current year illustrated the highest overall frequency of significant correlations (17), the highest average correlation value across all sites (0.305), and the highest frequency of significant response functions (13). Other prominent climate factors included:

current June temperature, current May precipitation, previous August precipitation, and previous September precipitation.

Eigenvector analysis on radial growth chronologies produced three principal components explaining significant variance (> 5%), radial growth eigenvector (RGE) I explains 44%, RGE II explains 9.2%, and RGE III explains 8.6% of the tree-ring variance (Figure 2.10.4). The remaining 20 eigenvectors were representative of regional scale growth variance and not included in this study. Additionally, eigenvector analysis on monthly temperature and precipitation variables from January to December were produced. Only the first two eigenvectors explained significant variance and were therefore used in this study (Table 2.9.3). When the RGE and climate eigenvectors analysis are visually compared against one another, larger scale causes for variation are explained. It was determined that RGE I was observably similar to May and June precipitation's first eigenvectors. RGE II was observed to be similar in shape to soil type, and RGE III was determined to be observably similar to eigenvector I of June temperature.

2.5 Discussion

Using mean sensitivity as a measure to determine physiological stress imposed on trees proves to be successful in the determination of shifting growth regimes in southern Saskatchewan and has profound implications in the future climate-envelope of white spruce proposed by McKenney et al. (2007). The gradient of changing MS values supports the "abundant centre hypothesis" that has long been considered an ecological rule (Wulff 1943; Hengvald 1990; Brown et al. 1995). This hypothesis is based on a multi-dimensional niche concept where a species has high and low abundance depending on the environmental conditions. Where optimal conditions are met, a species will show the greatest abundance. As distance increases from these optimal habitats, a species will become more sensitive and vulnerable to its local non-optimal conditions therefore decreasing in abundance. Other dendrochronological studies have investigated this phenomenon though no significant results have been found (e.g., Sakulich 2011). In contrast, white spruce in this study shows a strong relationship between sensitivity and distance from its native range, and for arguments sake, considered its current optimal range, the boreal forest.

June precipitation has been shown to be the primary radial growth factor driving white spruce growth in southern Saskatchewan, agreeing with Davis et al. (2013). All significant values found for white spruce regarding June precipitation were positively correlated establishing that increased yearly June precipitation will likely result in above average growth. This relationship may be extended to May precipitation, to a lesser degree. Contrasting these results, June temperature demonstrated the highest frequency of significant results negatively correlated to radial growth. Due to the frequency of significant response functions and correlations it is determined that June precipitation and temperature, as well as May precipitation, patterns are the primary large-scale weather systems driving white spruce growth in southern Saskatchewan. Changes to these weather patterns will result in variation in change to annual radial growth patterns in white spruce.

Eigenvector analysis results indicate major climatic forcing imposed on white spruce in southern Saskatchewan. Observable similarities between May and June precipitation with RGE I indicates that spring precipitation is an important factor for the growth of white spruce. Although overall precipitation in the Canadian Prairies is projected to increase (Sauchyn et al. 2008), spring and summer dryness is likely to increase as a result of greenhouse gas emissions (Wetherald and Manaybe 1999) suggesting an impending water crisis in the Canadian Prairies (Schindler and Donahue 2006). This indicates that radial growth will likely be inhibited under future climatic scenarios, as 44% of the variance in growth can be explained through May and June precipitation. RGE II, explaining 9.2% of the variance is related to physical factors that will not likely change in the future. RGE III is observably similar to June temperature, which negatively affects white spruce in the most southern regions of Saskatchewan suggesting that predicted increases in temperature (IPCC 2007) will result in further inhibited growth and variation. The increased dryness and temperature of the area in the near future will have a dramatic effect on the physiologically stressed white spruce in the intolerable, super-stressed, stressed, and parts of the normal growth thresholds. Temperature induced drought and the increased dryness will result in increased MS and likelihood of mortality events in southern Saskatchewan due to decreases in May and June precipitation and increasing June temperatures in future climate scenarios (IPCC 2007).

2.6 Conclusion

This study has produced a comprehensive network of white spruce radial growth chronologies throughout southern Saskatchewan. In doing so, we have created a useful proxy measure to determine the potential future stresses imposed on the boreal forest through the study of shelterbelt systems. This study illustrates strong gradients and conclusive evidence of spatial patterns of white spruce radial growth throughout the study sites further demonstrating the viability of shelterbelts for tree-ring research initiatives.

Results have shown that the primary causal factors of radial growth have been determined to be primarily precipitation. May and June precipitation and June temperature of the current growth year have been shown to have a significant impact on white spruce radial growth, discerned through both eigenvector and dendroclimatological analysis. Precipitation has been shown to provide a positive impact but increased temperature has been shown to have a primarily negative impact on white spruce radial growth. This suggests that under future climate scenarios, where spring and summer precipitation are projected to diminish and surface temperatures continue to rise, white spruce growth will be negatively affected. Future studies should focus on how these spatial climate patterns may affect shelterbelts in the future.

The results of this study show that as white spruce extends from its natural range they become increasingly sensitive and vulnerable to climate. Four thresholds of growth were determined: 1) “normal”, which indicates white spruce are under moderate physiological stress ($MS < 0.300$); 2) “stressed”, which indicates the tree species is experiencing higher than average stress and year-to-year variation ($MS = 0.300-0.400$); 3) “super-stressed”, which indicates white spruce are under very high physiological stress – the likelihood of a mortality event in this growth threshold is high ($MS = 0.400-0.500$), and; 4) “intolerable”, which indicates the tree species is experiencing extremely high physiological stress and year-to-year variation which leads to a high probability of a mortality event ($MS > 0.500$). These thresholds are likely to expand and migrate northward and should be examined in future studies using similar techniques but with different species.

2.7 Acknowledgements

We acknowledge financial assistance from the Agricultural Greenhouse Gas Program (AGGP). Additionally, we would like to thank Emma Davis, Emily Hogan, Sarah Quann, Cecilia Jennings, Jay Maillet, Stuart Murray, and Logan Laroque for assistance in the field as well as the Geospatial Modeling Laboratory for their help with GIS related materials.

2.8 References

- Akinremi, O.O., McGinn, S.M., and Cutforth, H.W. 2001. Seasonal and spatial patterns of rainfall trends on the Canadian Prairies. *Journal of Climate*, 14, 2177-2182.
- Barber, V.A., Juday, G.P., and Finney, B.P. 2000. Reduced growth of Alaskan white spruce in the twentieth century from temperature-induced drought stress. *Nature*, 405, 668-673.
- Beriault, A. L. and Sauchyn, D.J. 2006. Tree-ring reconstructions of streamflow in the Churchill River Basin, Northern Saskatchewan. *Canadian Water Resources Journal*, 31(4), 249-262.
- Biondi, F. and Waikul, K. 2004. DENDROCLIM2002: a C++ program for statistical calibration of climate signals in tree-ring chronologies. *Computers and Geosciences*, 30, 303-311.
- Blasing, T.J. and Fritts, H.C. 1976. Reconstruction of past climate anomalies in the North Pacific and western North America from tree-ring data. *Quaternary Research*, 6, 563-579.
- Brown, J.H., Mehlman, D.W., and Stevens, G.C. 1995. Spatial variation in abundance. *Ecology*, 76, 2028-2043.
- Brubaker, L.B. 1980. Spatial patterns of tree growth anomalies in the Pacific Northwest. *Ecology*, 61(4), 798-807.
- Choat, B., Jansen, S., Brodribb, T.J., Cochard, H., Delzon, S., Bhaskat, R., Bucci, S.J., Feild, T.S., Gleason, S.M., Hacke, U.G., Jacobsen, A.L., Lens, F., Maherali, H., Martinez-Vilalta, J., Mayr, S., Mencuccini, M., Mitchell, P.J., Nardini, A., Pittermann, J., Pratt, R.B., Sperry, J.S., Westoby, M., Wright, I.J., and Zanne, A.E. 2012. Global convergence in the vulnerability of forests to drought. *Nature*, 491, 753-757. doi:10.1038/nature11688.
- Cook, E.R. 1985. A time series analysis approach to tree ring standardization. Ph.D. Dissertation, University of Arizona, Tucson.
- Dale, J.E., and Lewry, M.L. 2007. Geology and geomorphology. In: Canadian plains research centre, Saskatchewan: geographic perspectives. *Friesens, Altona*, 11-28 pp.

- Danby, R.K. and Hik, D.S. 2007a. Variability, contingency and rapid change in recent subarctic alpine tree line dynamics. *Journal of Ecology*, 95(2), 352-363. doi:10.1111/j.1365-2745.2006.01200.x
- Danby, R.K. and Hik, D.S. 2007b. Responses of white spruce (*Picea glauca*) to experimental warming at a subarctic alpine treeline. *Global Change Biology*, 13(2), 437-451. doi:10.1111/j.1365-2486.2006.01302.x
- Davis, E.L. Laroque, C.P., and Van Rees, K. 2013. Evaluating the suitability of nine shelterbelt species for dendrochronological purposes in the Canadian Prairies. *Agroforestry Systems*. doi: 10.1007/s10457-012-9591-8.
- de Lafontaine, G., Turgeon, J., and Payette, S. 2010. Phylogeography of white spruce (*Picea glauca*) in eastern North America reveals contrasting ecological trajectories. *Journal of Biogeography*, 37, 741-751. doi: 10.1111/j.1365-2699.2009.02241.x
- Environment Canada 2010. Climate Change - Climate Data and Model Output - Adjusted and Homogenized Canadian Climate Data Temperature Precipitation Pressure Wind Contact Information SiteMap Proactive Disclosure Proactive Disclosure Adjusted and Homogenized Canadian Climate Data.
- Fritts, H.C. 1976. Tree Rings and Climate. Academic Press, London, 567 pp.
- Grissino-Mayer, H.D. 2001. Evaluating cross-dating accuracy: a manual and tutorial for the computer program COFECHA. *Tree-Ring Research*, 57, 205-221.
- Harper, K.A., Danby, R.K., De Fields, D.L., Lewis, K.P., Trant, A.J., Starzomski, B.M., Savidge, R., and Hermanutz, L. 2011. Tree spatial pattern within the forest-tundra ecotone: a comparison of sites across Canada. *Canadian Journal of Forest Research*, 41, 479-489.
- Hengvald, R. 1990. Dynamic Biogeography. Cambridge University Press, Cambridge.
- Holmes, R.L. 1983. Computer-assisted quality control in tree-ring dating and measurement. *Tree-ring bulletin*, 43, 69-78.

- Hughes, M.K. 2002. Dendrochronology in climatology – the state of the art. *Dendrochronologia*, 20, 95-116.
- [IPCC] Intergovernmental Panel on Climate Change. 2007. Climate Change 2007: The Physical Science Basis. Summary for Policy Makers (17 November 2012; <http://www.ipcc.ch/>).
- Kaennel, M. and Schweinengruber, F.H. (eds) 1995. *Multilingual Glossary of Dendrochronology*. Paul Haupt Berne, Switzerland, 467pp.
- LaMarche, V.C., Jr., and Fritts, H.C. 1971. Anomaly patterns of climate over the western United States, 1700-1930, derived from principal component analysis of tree-ring data. *Monthly Weather Review*, 99, 138-142.
- Loehle, C. 1998. Height growth rate tradeoffs determine northern and southern range limits for trees. *Journal of Biogeography*, 25, 735-742.
- McKenney, D.W., Pedlar, J.H., Lawrence, K., Campbell, K., and Hutchinson, M.F. 2007. Potential impacts of climate change on the distribution of North American trees. *BioScience*, 57(11), 939-948.
- Ripley, E.A. 1986. Is the prairie becoming drier? *Drought: the impending crisis? Proc. 16th Canadian Hydrology Symposium*, Ottawa, ON, Canada, National Research Council, 50-60.
- Sakulich, J.B. 2011. A dendrochronological approach for analyzing the geographic range structure of tree species. Ph.D. dissertation, University of Tennessee, 221pp.
- Sauchyn, D., Kulshreshtha, S., et al. 2008. Prairies. *In: From Impacts to Adaptation: Canada in a Changing Climate 200*, edited by D. Lemen et al., Government of Canada, Ottawa.
- Schindler, D.W. and Donahue, W.F. 2006. An impending water crisis in Canada's western prairie provinces. *PNAS*, 103(19), 7210-7216.
- Stokes, M.A. and Smiley, T.L. 1968. An introduction to tree-ring dating. The university of Arizona Press, Tucson.
- Tahktajan, A.L. 1986. *Floristic regions of the world*. University of California Press, Berkeley.

VoorTech 2011. Project J2X. VoorTech consulting. <http://www.voortech.com/projectj2x/>

Wetherald, R.T. and Manabe, S. 1999. Detectability of summer dryness caused by greenhouse warming. *Climatic Change*, 43, 495-511.

Woodall, C.W., Oswalt, C.M., Westfall, J.A., Perry, C.H., Nelson, M.D., and Finley, A.O. 2009. An indicator of tree migration in forests of the eastern United States. *Forest Ecology and Management*, 257(5), 1434-1444. doi:10.1016/j.foreco.2008.12.013.

Wulff, E.V. 1943. An introduction to historical plant geography. Chronica Botanica Co., Waltham, MA.

2.9 Tables

Table 2.9.1: Study site sampling information for all locations. MSI = mean series intercorrelation; demonstrates strength of correlation between samples at the same location based on 30-year segments. MTA = mean tree age. MS = mean sensitivity; demonstrates mean year-to-year variability of radial growth within the chronology.

Site Code	Latitude	Longitude	Altitude (m asl)	No. of cores	Time-span	Length	MSI	MTA	MS
11ANL200	50° 26' 53.4"	106° 53' 41.6"	721	39	1922-2010	88	0.788	78.2	0.449
11GL200	52° 45' 08.9"	108° 05' 57.1"	581	38	1948-2010	62	0.687	55.3	0.435
11JL200	52° 04' 40.2"	107° 18' 50.5"	548	40	1945-2010	65	0.725	57.4	0.458
12AAL200	50° 04' 42.7"	108° 18' 10.1"	901	39	1952-2011	59	0.718	56.8	0.488
12ACL200	50° 21' 37.2"	105° 33' 33.7"	564	40	1963-2011	48	0.524	34.6	0.397
12ADL200	50° 31' 11.3"	104° 52' 27.0"	571	18	1952-2011	59	0.754	56.1	0.455
12AEL200	49° 08' 42.7"	104° 18' 01.7"	724	38	1970-2011	41	0.726	34.8	0.43
12AFL200	50° 16' 30.7"	103° 01' 37.8"	681	39	1953-2011	58	0.77	52.7	0.393
12AHL200	50° 55' 13.9"	101° 55' 13.9"	539	40	1970-2011	41	0.638	35.3	0.327
12AIL200	51° 37' 06.8"	102° 04' 32.5"	481	39	1971-2011	40	0.604	35	0.207
12AJL200	51° 41' 37.7"	102° 41' 50.7"	505	39	1953-2011	58	0.622	51.6	0.304
12AKL200	51° 56' 44.4"	104° 33' 03.6"	524	40	1971-2011	40	0.674	32.4	0.375
12ALL200	52° 08' 02.3"	106° 03' 19.3"	581	27	1957-2011	54	0.581	46.8	0.41
12AML200	51° 42' 29.1"	108° 35' 16.5"	636	35	1958-2011	53	0.46	45.5	0.504
12ANL200	51° 12' 42.8"	107° 21' 50.0"	692	40	1960-2011	51	0.653	42	0.524
12GL200	51° 57' 40.8"	103° 47' 40.8"	543	38	1945-2011	66	0.744	56.3	0.342
12HL200	52° 41' 50.2"	104° 53' 05.9"	539	39	1947-2011	64	0.754	58.9	0.373
12LL200	49° 23' 29.3"	103° 22' 09.3"	581	40	1975-2011	36	0.764	33.3	0.394
12ML200	49° 50' 18.7"	103° 25' 52.3"	610	40	1946-2011	65	0.712	58	0.374
12NL200	51° 07' 29.6"	103° 38' 36.3"	679	40	1953-2011	58	0.761	53.7	0.3
12OL200	51° 43' 54.9"	103° 50' 54.9"	568	38	1948-2011	63	0.696	55.5	0.33
12QL200	50° 34' 17.1"	104° 03' 46.9"	683	40	1950-2011	61	0.797	56.7	0.27
12ZL200	51° 31' 57.1"	108° 03' 33.5"	606	40	1973-2011	38	0.797	34.2	0.531

Table 2.9.2: Frequency of significant response functions found using the statistical program DENDROCLIM2002 with the 23 study sites in southern Saskatchewan.

Year	Month	Temperature	Precipitation
Previous	April	0	0
	May	1	2
	June	1	2
	July	2	0
	August	4	3
	September	2	4
	October	1	2
	November	2	2
	December	1	2
	Present	January	2
February		0	3
March		0	1
April		1	0
May		0	6
June		2	13
July		1	2
August		0	0
September		0	0

Table 2.9.3: Radial growth and climate eigenvector component percentage values of explained variance.

Radial growth eigenvectors							
	I	47					
	II	9.7					
	III	8.8					
Climate eigenvectors		Jan	Feb	Mar	Apr	May	Jun
Temp.	I	95	93.5	93.4	92.1	90.2	89.9
Precip.	I	53.1	47	52.2	50.6	54.2	52.9
		Jul	Aug	Sep	Oct	Nov	Dec
Temp.	I	86.9	92.3	93.4	91.7	94.2	94.6
Precip.	I	42.5	57.6	50.6	63.1	56.5	44.4

2.10 Figures

Figure 2.10.1: Study area with climate station locations, latitudinal and longitudinal transects, and site locations in southern Saskatchewan. Black-filled circles represent climate stations, X'd circles indicate sample locations.

Figure 2.10.2: Map demarcating thresholds of growth for white spruce in southern Saskatchewan. Thresholds are quantified through mean sensitivity: normal (<0.300), stressed ($0.300 - 0.400$), super-stressed ($0.400-0.500$), and intolerable (>0.500). The method of spatial interpolation was ordinary spherical kriging with a 1 km resolution.

Figure 2.10.3: Histogram representing frequency of significant correlations (95% confidence) to monthly climate variables between April of the previous year and the current October climate data. Capitalized month abbreviations (e.g., APR, MAY, JUN) indicate previous year, non-capitalized month abbreviations (e.g., Apr, May, Jun) indicate present year of growth. Line charts are average correlations and bar plots indicate frequency of significant correlations.

Figure 2.10.4: Radial growth eigenvector (RGE) analysis loadings spatially mapped in southern Saskatchewan: A) RGE I, B) RGE II, and C) RGE III. Number values within maps indicate the percentage of explained variance.

Figure 2.10.5: Climate eigenvector loadings spatially mapped in southern Saskatchewan. Twenty-four eigenvectors were created. The three observably similar eigenvectors are displayed: A) June precipitation, B) May precipitation, C) June temperature, all other data is not displayed.

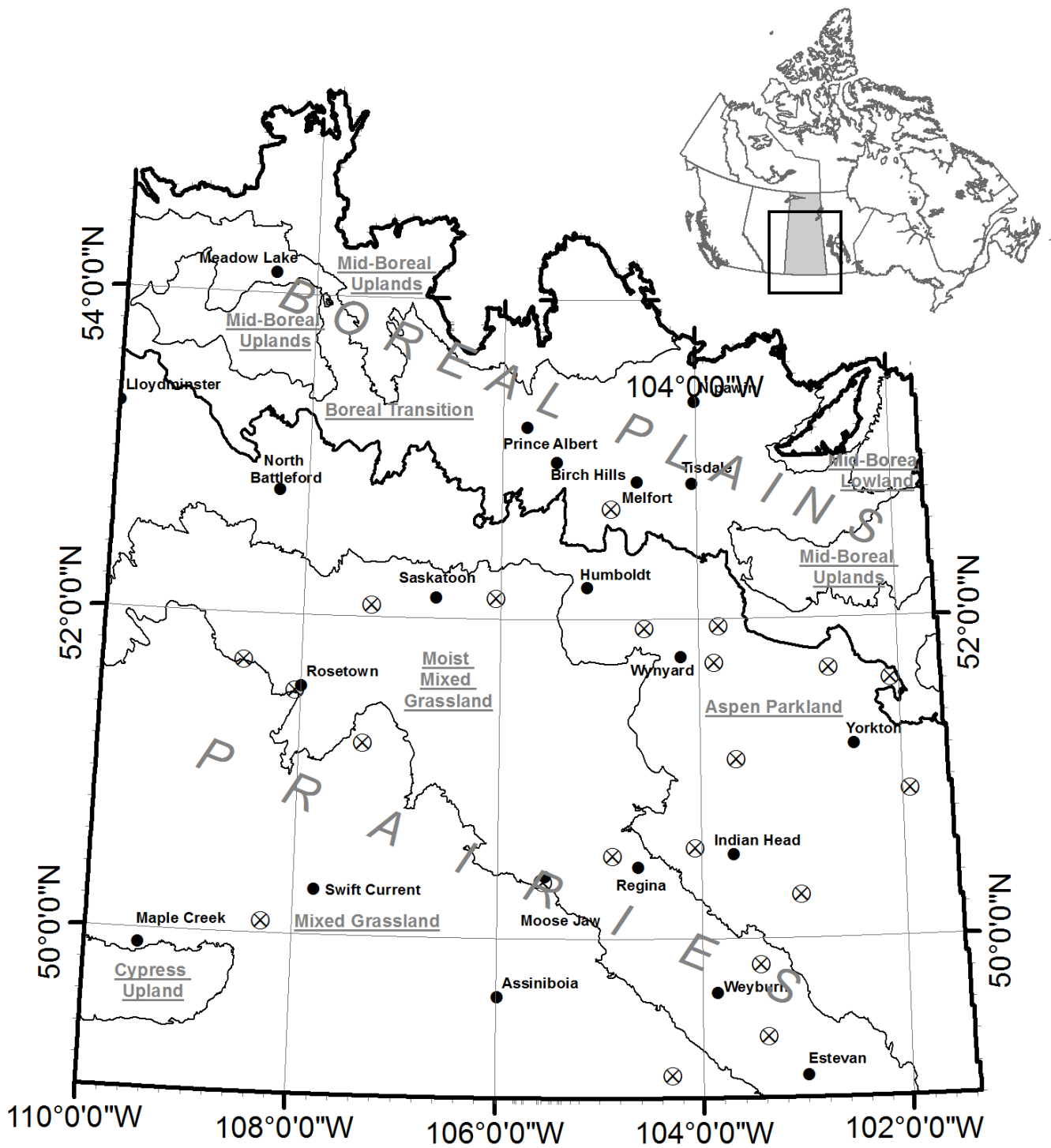


Figure 2.10.1

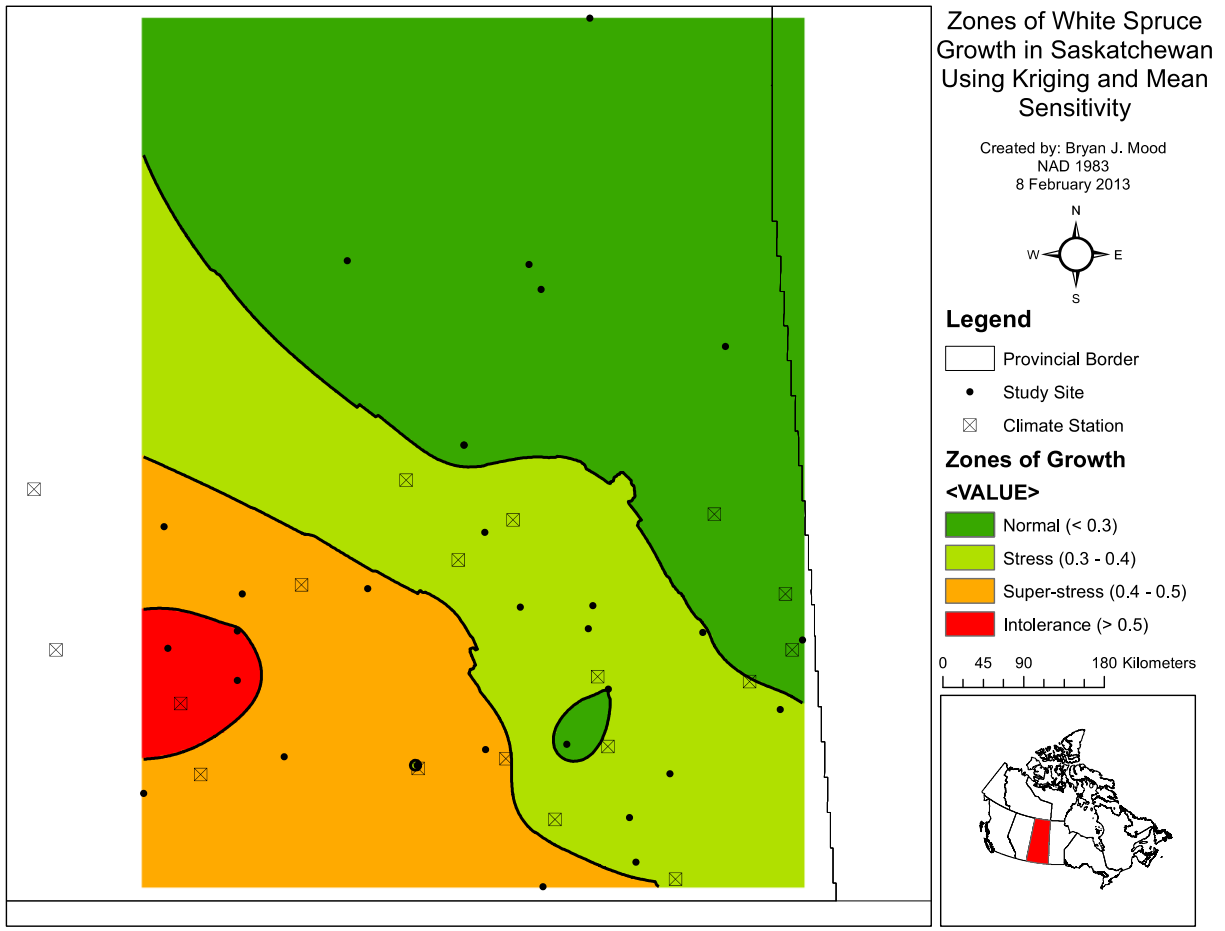


Figure 2.10.2

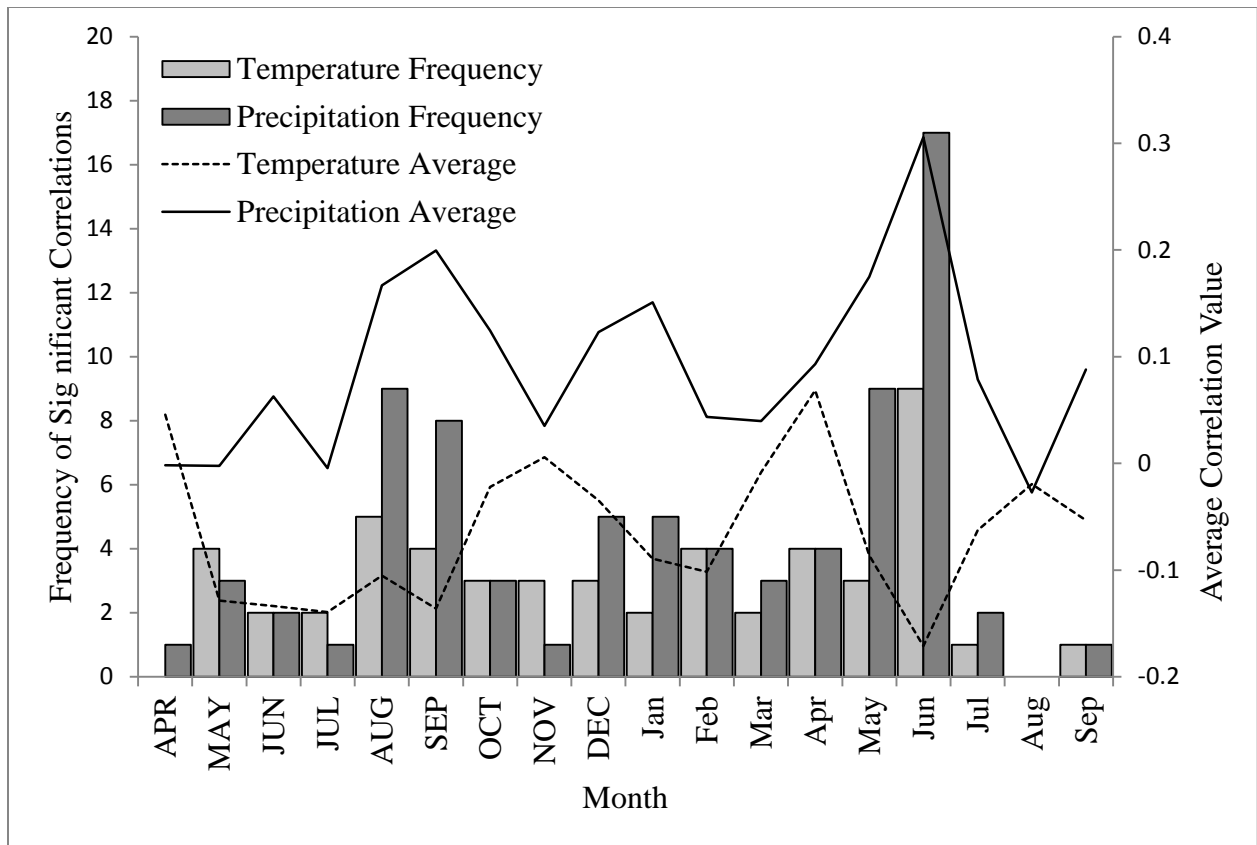


Figure 2.10.3

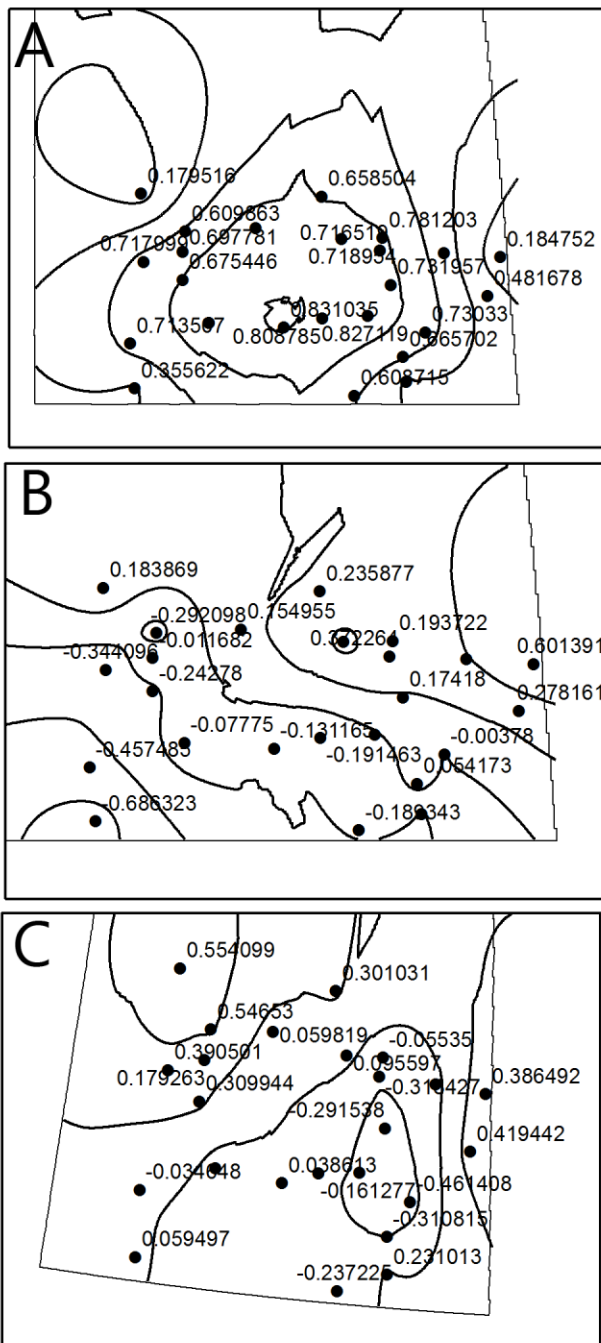


Figure 2.10.4

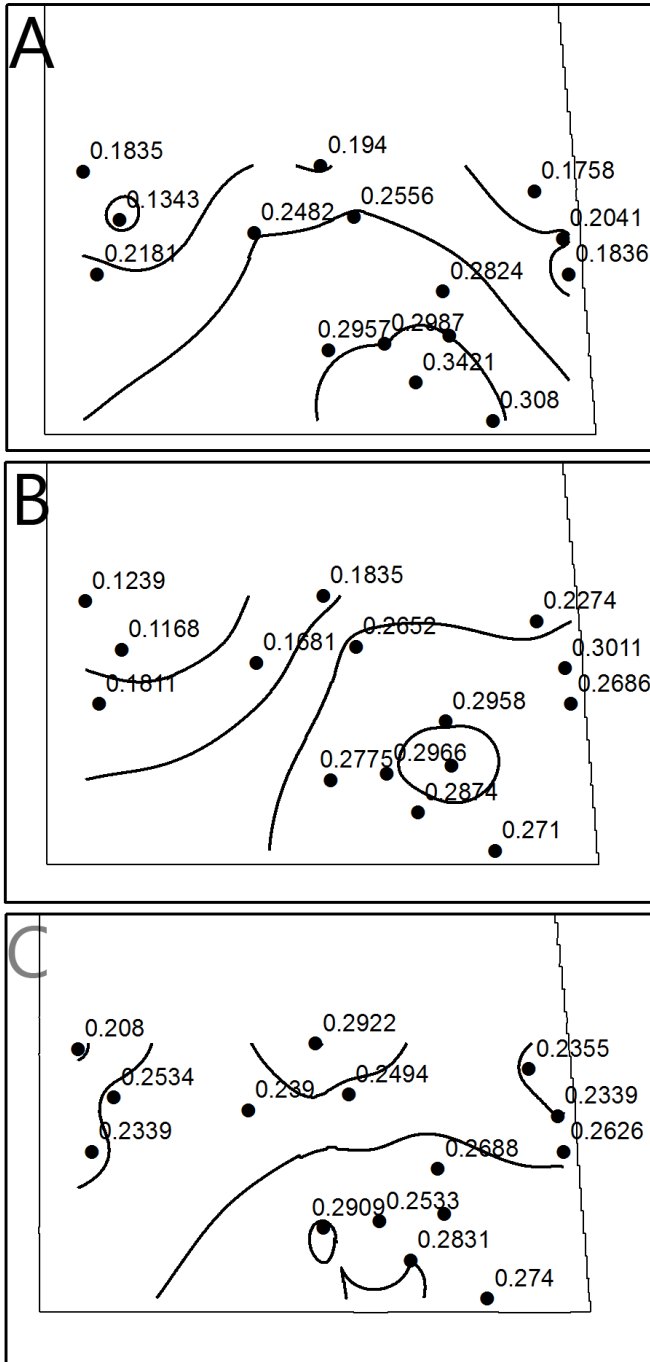


Figure 2.10.5

3.0

Conclusions

Tree-ring analysis has been able to determine several important ecological factors associated with the southern range limits of the Canadian boreal forest in addition to determining the general condition of white spruce shelterbelts throughout southern Saskatchewan. Both southern Saskatchewan and the southern limits of the boreal forest have been severely understudied presenting a large gap in understanding of shifting tree climate-envelopes as well as the condition of white spruce outside their natural range. The results and discussion presented in this these help to address this gap in knowledge and will aid in predicting future shifts in optimal habitat for white spruce due to changing weather patterns and increasing temperatures.

Dendroclimatic analysis demonstrates spring precipitation (May and June in this case) is a significant factor in the growth of white spruce throughout southern Saskatchewan. Increased precipitation should result in wider annual radial-growth. However, Schindler and Donahue (2006) have shown that spring precipitation will decrease in the future which will result in a negative effect on white spruce growth. Akinremi et al. (2001) demonstrate the same results but also suggest that winter precipitation will increase dramatically, and by doing so think that spring snowmelt will help to mitigate the effects of reduced spring precipitation in southern Saskatchewan on white spruce. June temperature has also been shown to have a large negative effect on the growth of white spruce, higher temperatures will result in the hindering of an annual radial-growth increment. Predicted increasing June temperatures over the next century (IPCC 2007) suggests this too will have a negative effect on white spruce radial growth.

Eigenvector analysis has demonstrated that May and June precipitation are the two most dominant factors in the growth of white spruce, accounting for 47% of variance in radial growth. These two factors are more prominent in south-central Saskatchewan where precipitation during the spring deviates above the national average by over 100 mm (Akinremi et al. 2001). To a lesser extent, soil (9.7%) and June temperature (8.8%) are also significant factors in the growth of white spruce. Extreme negative effects on white spruce growth were shown to be in the southern-most region of Saskatchewan, adjacent to the Canada-United States border, this is attributed to higher temperatures in this region due to weather systems coming from the United States during this time of the year.

Mean sensitivity was used to demarcate the current growth thresholds for white spruce in southern Saskatchewan and into the natural boreal forest using supplementary data from the ITRDB. A highly significant relationship was found between mean sensitivity correlated against longitude and latitude, producing a strong north-east to south-west gradient of increasing variability in annual radial growth. This gradient is observably similar to the current boreal forest ecotone demonstrating that the further white spruce is located from its natural range, or climate-envelope, the higher its physiological stress due to its susceptibility to climate variance. It is concluded that with the forecasted changes in precipitation and increases in temperature patterns in southern Saskatchewan, the primary factors relating to white spruce growth in this region, will have a generally negative effect on its radial growth in the future. It is speculated that white spruce's climate-envelope will continue to migrate northeastward as temperature increases and changes in precipitation patterns further exacerbate an inhospitable environment for its future growth.

3.1 References

- Akinremi, O.O., McGinn, S.M., and Cutforth, H.W. 2001. Seasonal and spatial patterns of rainfall trends on the Canadian Prairies. *Journal of Climate*, 14, 2177-2182.
- [IPCC] Intergovernmental Panel on Climate Change. 2007. Climate Change 2007: The Physical Science Basis. Summary for Policy Makers (17 November 2012; <http://www.ipcc.ch/>).
- Schindler, D.W. and Donahue, W.F. 2006. An impending water crisis in Canada's western prairie provinces. *PNAS*, 103(19), 7210-7216.

4.0 Appendices

Appendix A: Standardized Radial Growth Indices

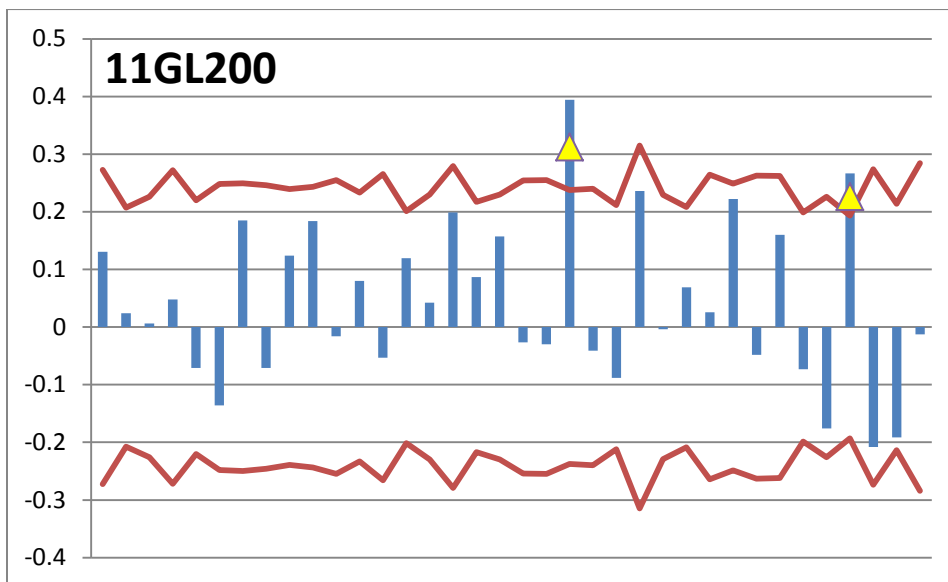
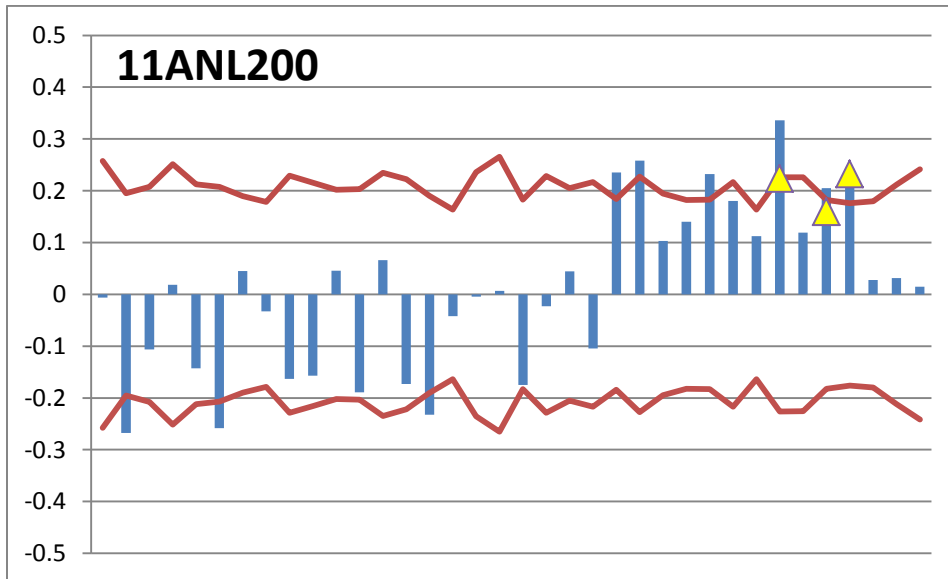
Year	11anl200	11gl200	11jl200	12abl200	12acl200	12adl200	12ael200
1976	2.201	1.02	0.776	1.185	1.256	1.84	1.579
1977	0.863	0.522	0.606	0.798	0.922	0.548	0.997
1978	1.303	0.718	1.04	1.028	1.017	1.015	0.558
1979	0.855	1.513	0.962	1.339	0.981	0.939	0.897
1980	0.5	0.636	0.935	0.829	0.983	0.283	0.65
1981	0.773	1.284	0.808	0.719	0.73	0.458	1.026
1982	0.965	0.592	1.025	1.096	0.975	0.969	1.015
1983	1.391	0.892	1.356	1.108	1.284	0.946	1.035
1984	0.861	1.123	0.36	0.74	0.765	0.496	0.636
1985	1.506	0.823	1.135	0.9	1.156	0.913	1.112
1986	0.78	0.932	1.475	0.963	1.144	0.741	1.168
1987	0.266	1.48	1.07	1.225	0.841	0.46	0.385
1988	0.486	0.913	0.37	0.771	0.641	0.444	0.802
1989	0.995	0.888	1.421	1.173	0.833	0.871	1.016
1990	0.673	1.243	1.088	1.016	0.864	0.792	1.344
1991	0.965	0.736	0.758	1.351	1.186	1.368	1.287
1992	0.664	0.671	0.686	0.691	1.024	0.691	1.162
1993	0.844	0.602	1.353	1.059	1.401	1.095	1.538
1994	1.598	0.739	1.128	1.336	1.308	1.745	1.852
1995	0.74	0.759	0.968	0.923	0.923	0.775	0.505
1996	1.099	0.871	0.823	0.851	1.044	1.152	0.942
1997	1.27	0.969	0.97	0.865	0.808	1.118	1.258
1998	0.75	1.155	0.397	0.815	0.747	0.737	1.041
1999	1.475	1.093	1.082	0.911	1.264	1.518	1.309
2000	1.222	1.164	0.645	1.017	1.097	1.547	1.059
2001	0.344	0.623	0.421	0.599	0.755	0.633	0.837
2002	0.617	0.32	0.494	0.903	0.583	0.673	0.929
2003	0.803	0.968	1.106	1.066	0.979	1.038	0.983
2004	0.891	0.955	0.789	1.163	0.944	0.829	0.722
2005	1.255	1.072	1.599	1.306	1.172	1.056	1.167
2006	1.243	1.579	1.486	0.637	1.072	1.118	0.649
2007	0.909	1.554	1.552	0.948	1.274	1.006	1.242

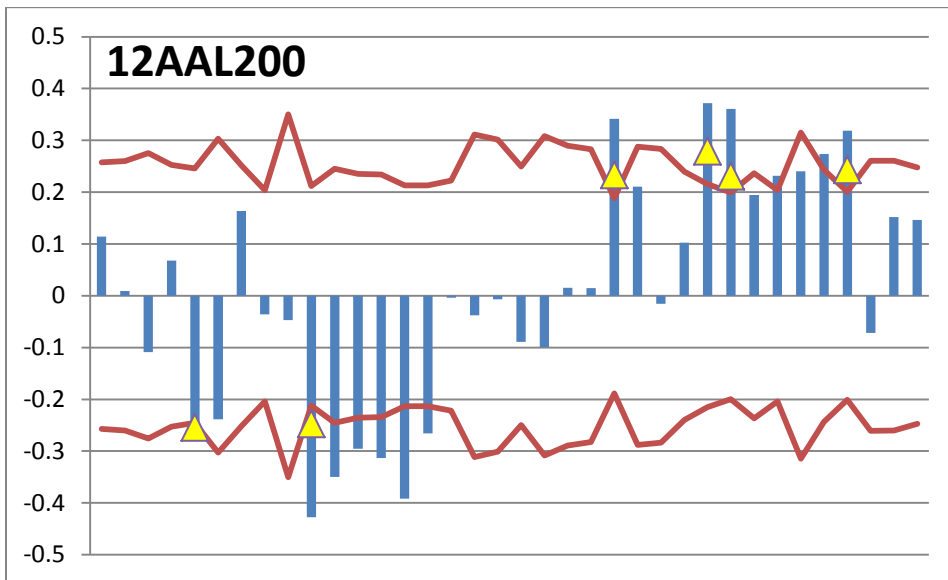
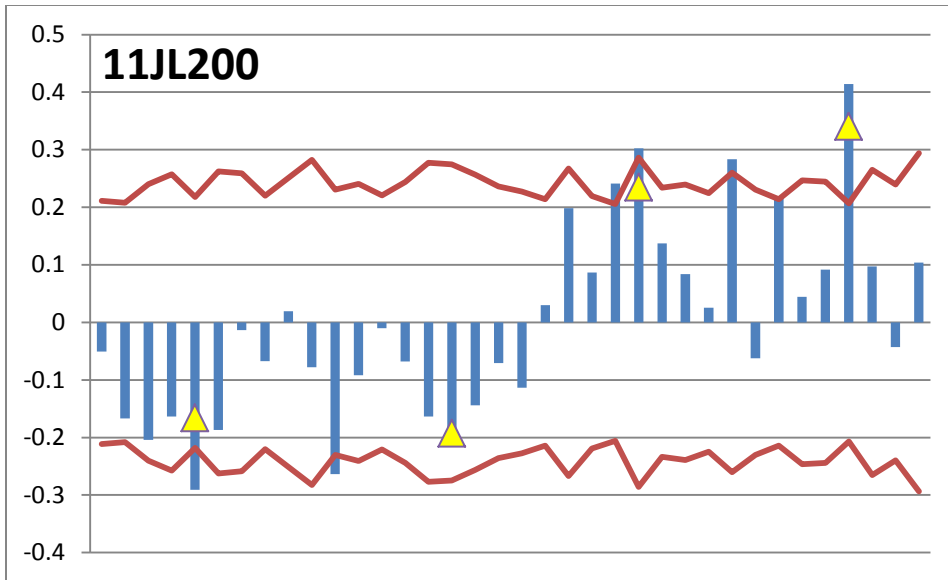
Year	12afl200	12ahl200	12ail200	12ajl200	12akl200	12all200	12aml200
1976	1.595	1.1	0.792	1.197	1.209	1.416	1.301
1977	0.838	0.899	0.746	0.656	0.532	0.494	0.977
1978	1.754	1.087	1.042	0.73	1.155	1.011	0.988
1979	0.664	0.805	0.827	0.736	0.828	0.775	0.805
1980	0.367	1.05	1.36	0.951	0.892	0.86	0.824
1981	0.884	1.014	1.103	0.899	1.013	0.628	0.742
1982	0.777	0.639	0.944	0.911	0.977	0.728	0.82
1983	1.16	1.13	1.038	0.899	1.167	1.25	1.013
1984	0.448	1.012	1.05	1.003	0.956	0.946	0.867
1985	0.949	1.159	0.947	0.894	1.053	1.127	0.885
1986	1.107	1.129	1.196	1.107	1.139	1.285	0.991
1987	0.341	0.743	0.859	0.844	0.84	0.776	0.801
1988	0.731	0.876	0.953	0.864	0.944	0.668	0.724
1989	0.709	0.733	0.783	0.98	0.605	0.978	0.935
1990	0.757	1.446	1.209	0.815	1.209	0.632	0.758
1991	0.936	1.107	1.061	1.026	1.008	1.113	0.976
1992	0.867	0.989	1.015	1.048	1.236	0.95	0.76
1993	1.04	0.82	1.104	1.039	1.298	1.203	0.994
1994	1.366	1.18	1.045	1.105	1.31	1.34	1.091
1995	0.882	0.928	1.007	0.746	0.883	0.407	0.901
1996	0.907	0.873	0.94	1.07	1.081	1.06	0.933
1997	0.717	1.179	1.24	1.146	0.761	0.884	0.966
1998	1.023	0.744	1.022	1.021	1.129	1.012	0.847
1999	1.264	1.212	1.14	1.242	1.125	1.31	1.123
2000	1.453	0.708	1.023	1.135	1.064	0.928	0.824
2001	0.596	0.727	0.842	0.666	0.479	0.877	0.634
2002	0.689	0.702	0.779	1.026	0.51	0.461	0.493
2003	0.784	0.804	0.757	0.759	0.765	0.764	1.349
2004	0.838	0.841	1.139	1.191	0.787	0.825	0.521
2005	0.94	1.017	0.804	0.971	0.937	1.153	1.28
2006	0.827	1.108	1.114	1.264	1.342	1.453	1.533
2007	0.863	1	0.985	0.825	1.107	1.116	1.021

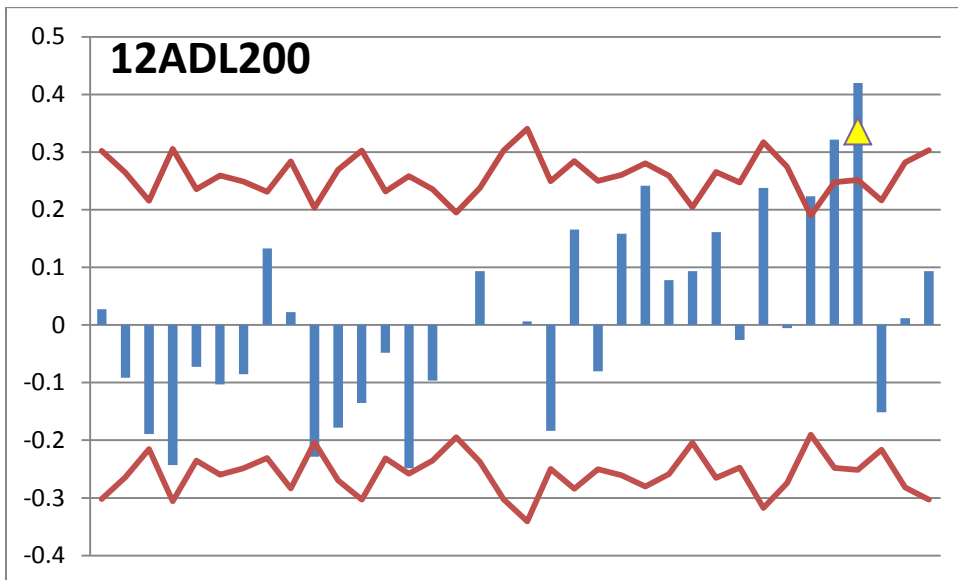
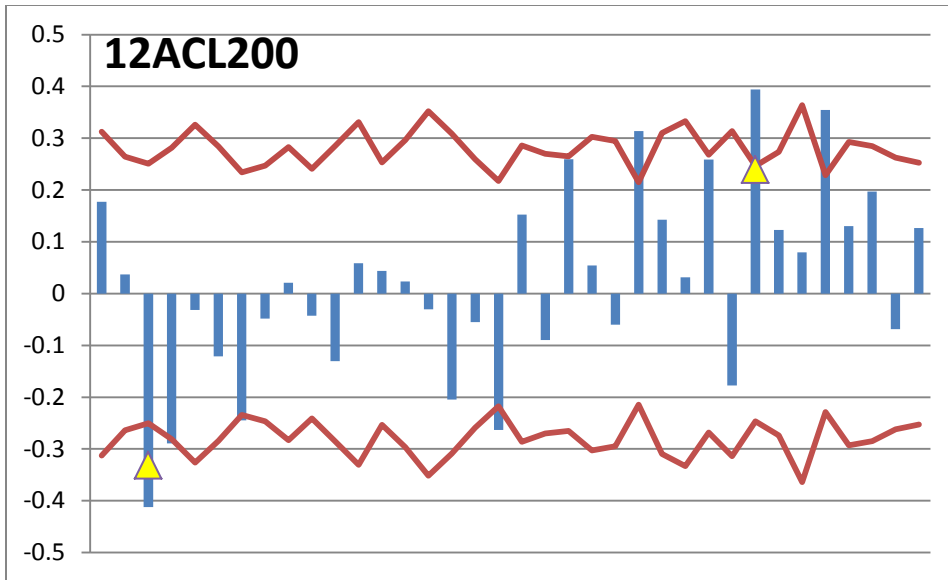
Year	12anl200	12gl200	12hl200	12ll200	12ml200	12nl200	12ol200	12ql200	12zl200
1976	1.175	1.307	1.155	0.816	1.177	1.28	1.364	1.211	0.873
1977	0.798	0.439	0.648	0.716	0.896	0.854	0.777	0.68	0.729
1978	1.326	1.155	1.207	1.084	1.312	1.206	1.133	1.059	1.125
1979	1.326	0.805	0.801	0.809	0.561	0.51	0.677	0.782	0.838
1980	0.564	0.668	0.766	1.029	0.727	0.405	0.771	0.684	0.796
1981	1.022	1.13	0.637	0.735	0.991	0.743	0.869	0.835	0.986
1982	1.229	0.97	1.068	1.308	0.787	0.689	0.92	1.083	1.378
1983	1.131	1.244	1.043	1.032	0.95	0.962	1.156	1.106	1.468
1984	0.523	0.754	1.087	0.973	0.706	0.597	1.004	0.803	0.627
1985	1.326	0.998	1.256	1.424	0.971	0.818	1.134	0.699	1.409
1986	1.083	0.86	0.82	1.476	1.173	1	1.024	0.958	1.113
1987	0.681	0.588	0.758	0.872	0.553	0.592	0.455	0.748	0.523
1988	0.337	0.825	0.994	0.65	0.781	0.449	0.971	0.624	0.401
1989	0.982	0.872	0.728	1.324	0.621	0.503	1.11	1.095	1.416
1990	0.917	0.698	0.883	0.877	0.838	0.503	0.704	0.855	1.22
1991	0.914	0.824	0.812	1.262	0.845	0.755	0.931	1.045	1.174
1992	0.498	1.007	0.621	0.647	1.251	0.743	1.096	1.018	0.74
1993	0.683	1.394	1.027	0.893	1.386	1.121	1.273	1.165	1.151
1994	1.53	1.489	0.938	1.087	1.379	1.138	1.146	1.236	1.49
1995	0.506	0.914	1.004	0.647	0.477	1.013	0.945	0.751	0.455
1996	1.221	1.419	0.862	0.813	0.901	0.624	0.963	0.853	1.185
1997	1.417	0.837	1.06	1.142	0.625	0.833	0.947	0.904	0.953
1998	0.883	0.937	0.778	0.891	0.656	0.899	1.137	1.011	0.257
1999	1.828	0.811	1.138	1.323	0.925	0.942	1.239	1.066	1.283
2000	0.486	0.988	1.009	1.11	1.03	1.205	1.054	1.25	0.581
2001	0.341	0.341	0.427	1.557	0.924	0.797	0.681	0.827	0.309
2002	0.606	0.753	0.708	0.632	0.865	0.66	0.847	0.673	0.397
2003	0.71	0.979	0.822	0.842	0.999	0.655	0.661	0.835	1.119
2004	0.674	0.946	0.784	1.191	0.698	0.9	1.056	0.934	0.898
2005	0.977	1.184	1.297	1.065	1.269	1.039	0.991	1.181	1.388
2006	1.12	1.711	1.728	1.04	1.085	1.318	1.387	1.21	1.251
2007	1.218	1.175	1.48	1.026	1.116	1.205	0.76	1.179	1.072

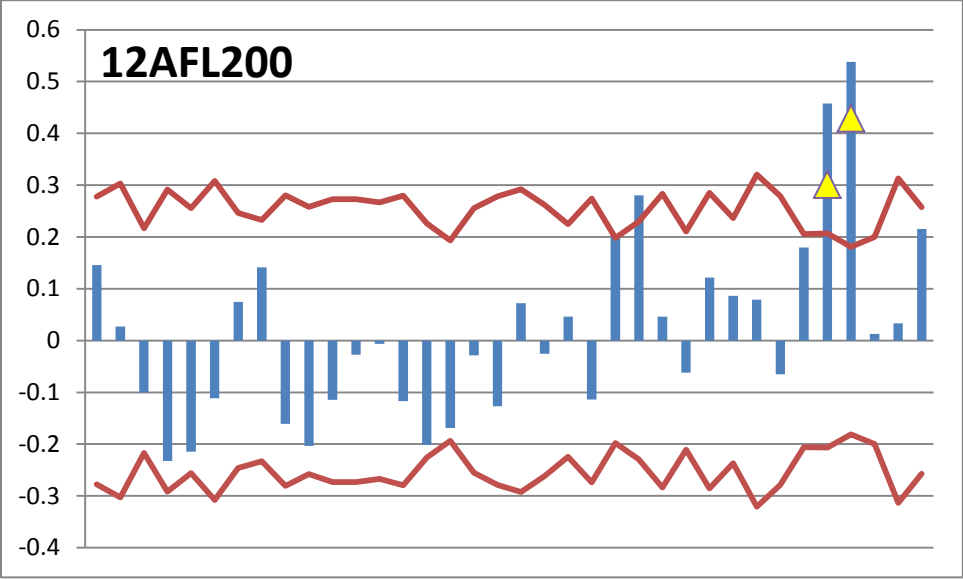
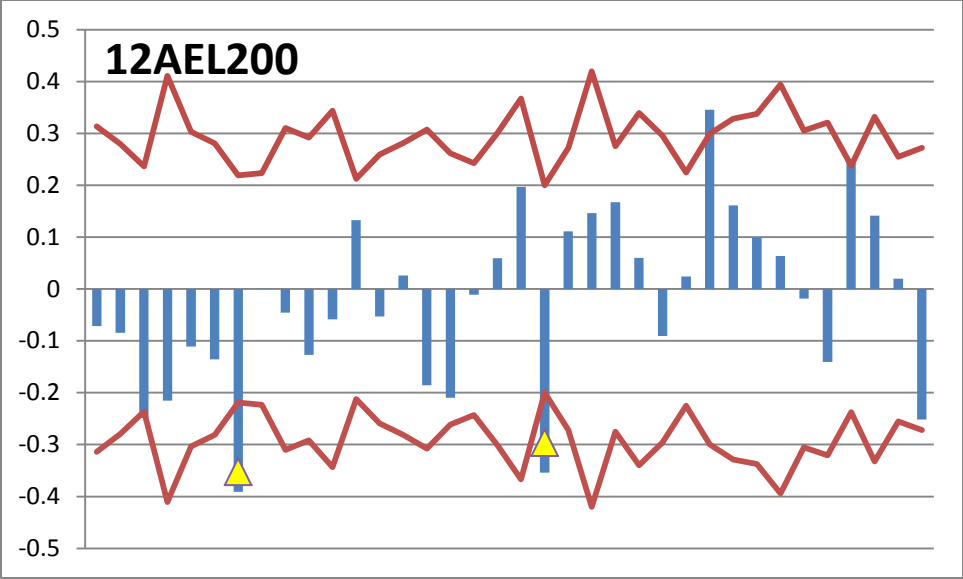
Appendix B: DendroCLIM2002 Figures

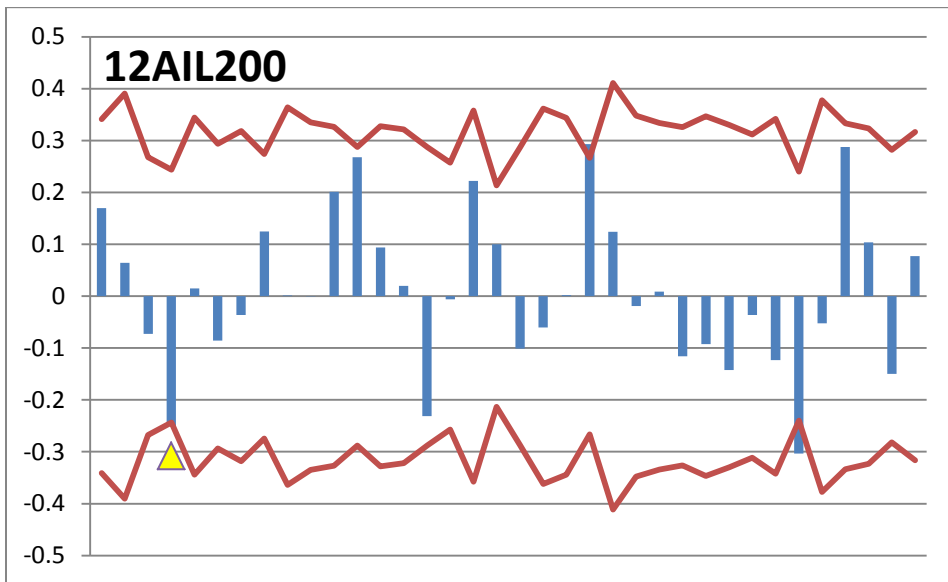
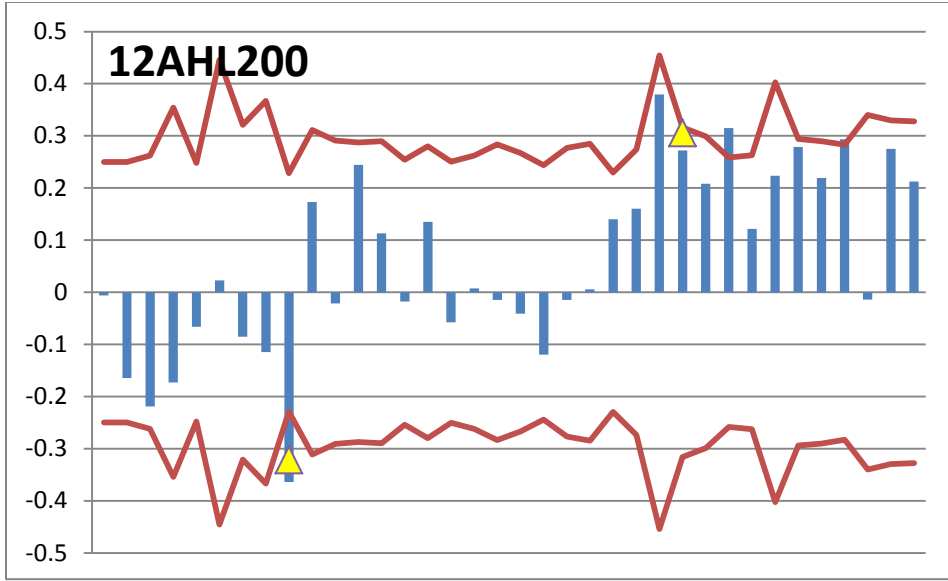
Yellow triangles represent significant response functions. Correlations (blue bars) that surpass the red bar indicates a significant correlation at the 95% level. Values start at “previous April temperature” to current September temperature” then “previous April precipitation” to “current September precipitation”.

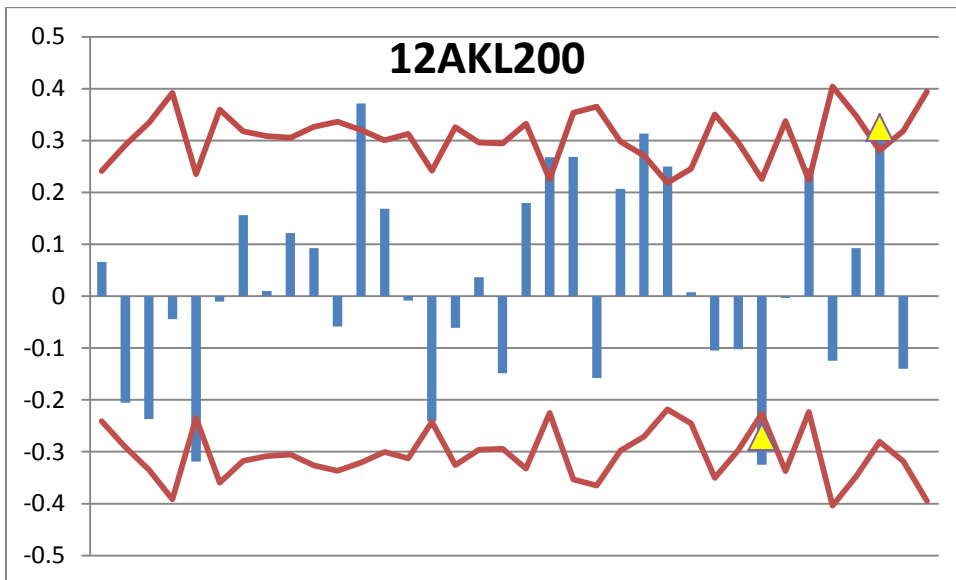
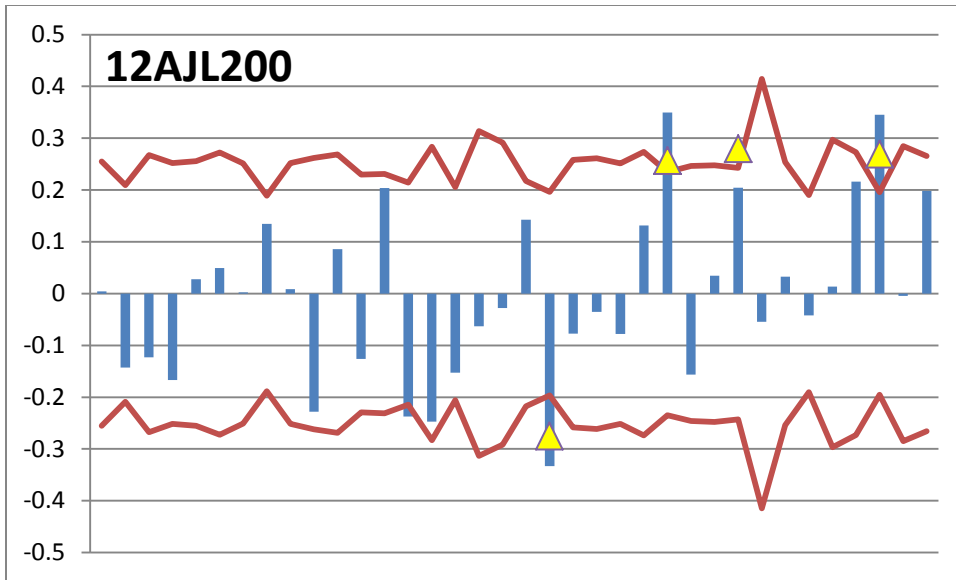


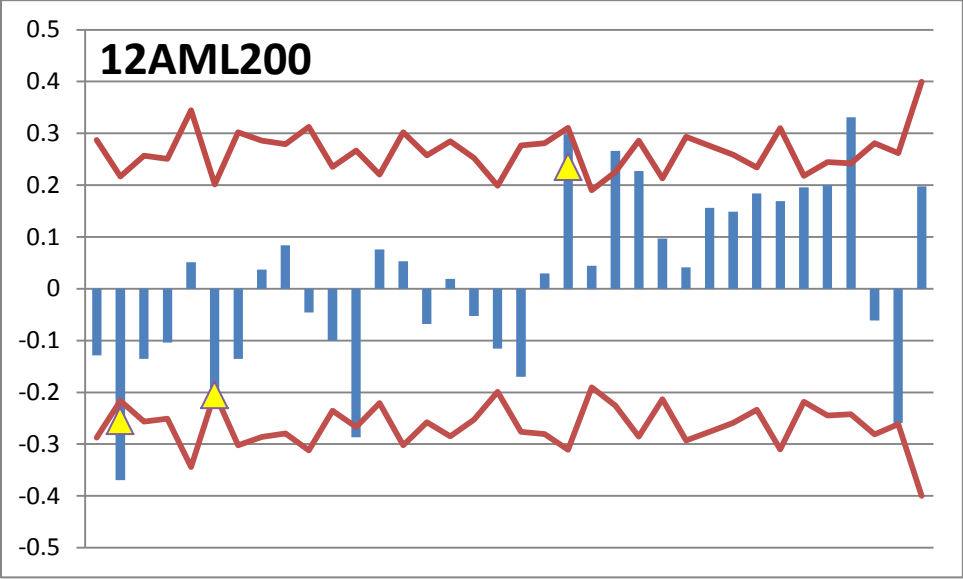
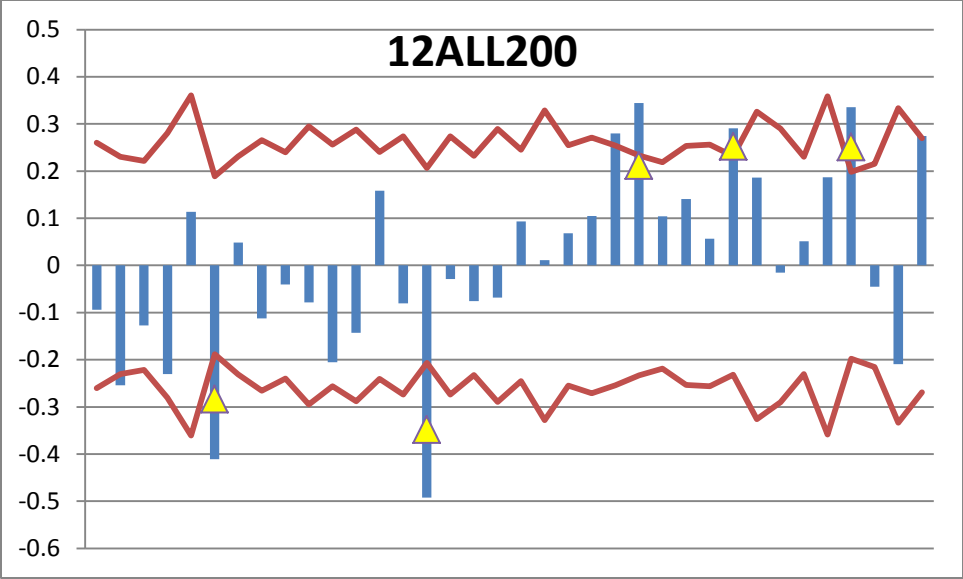


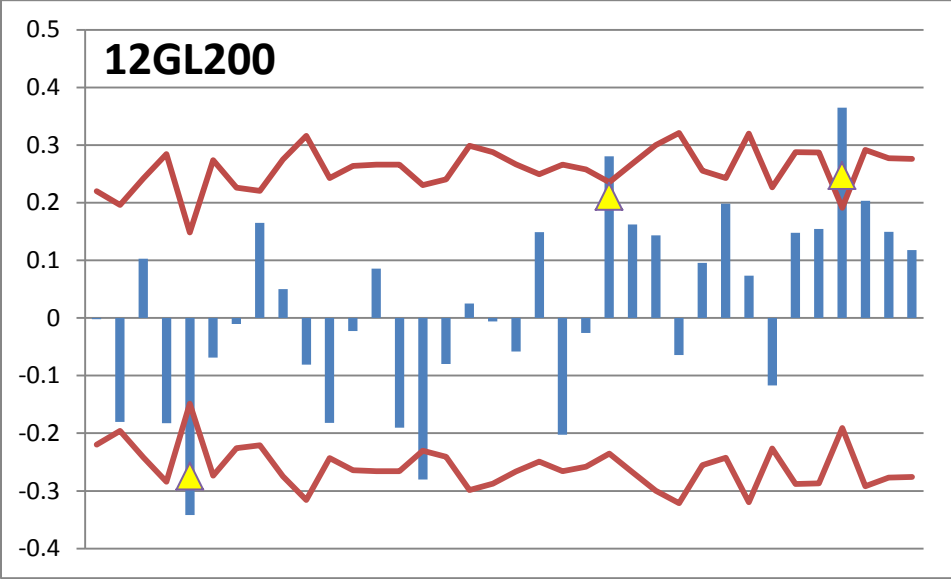
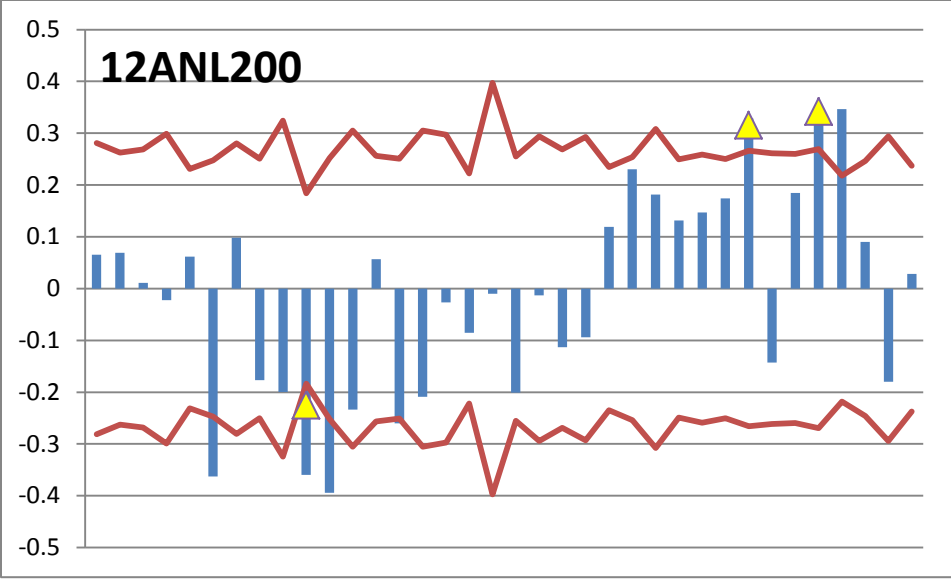


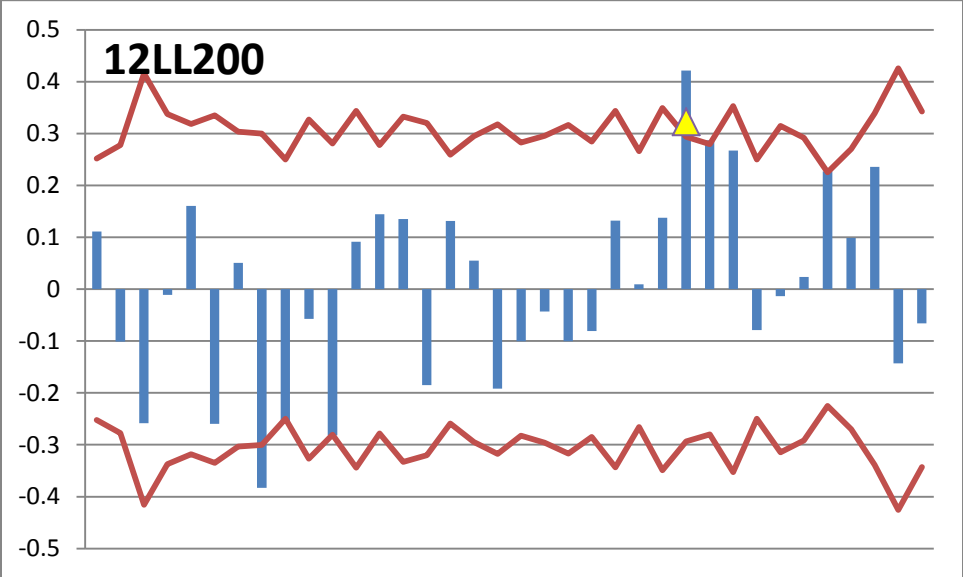
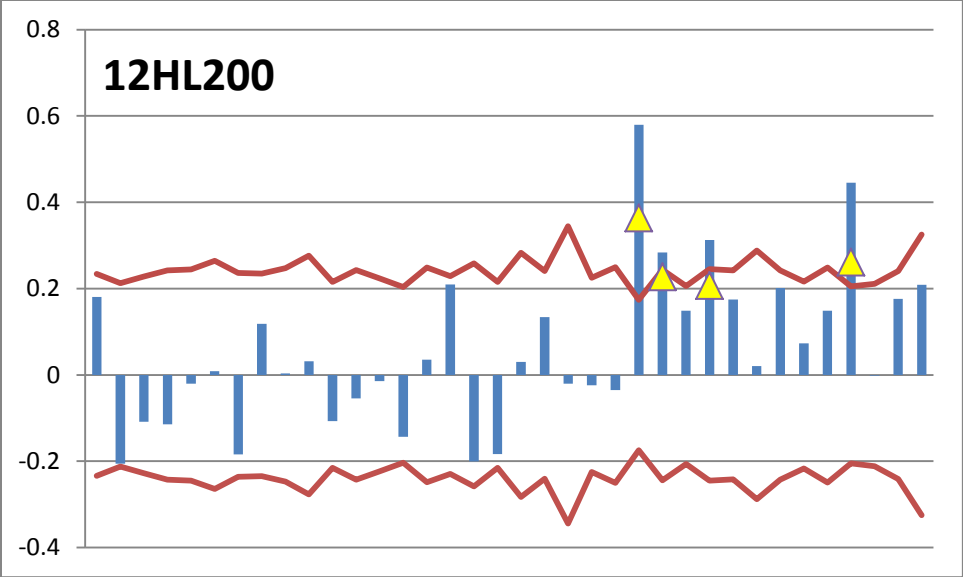


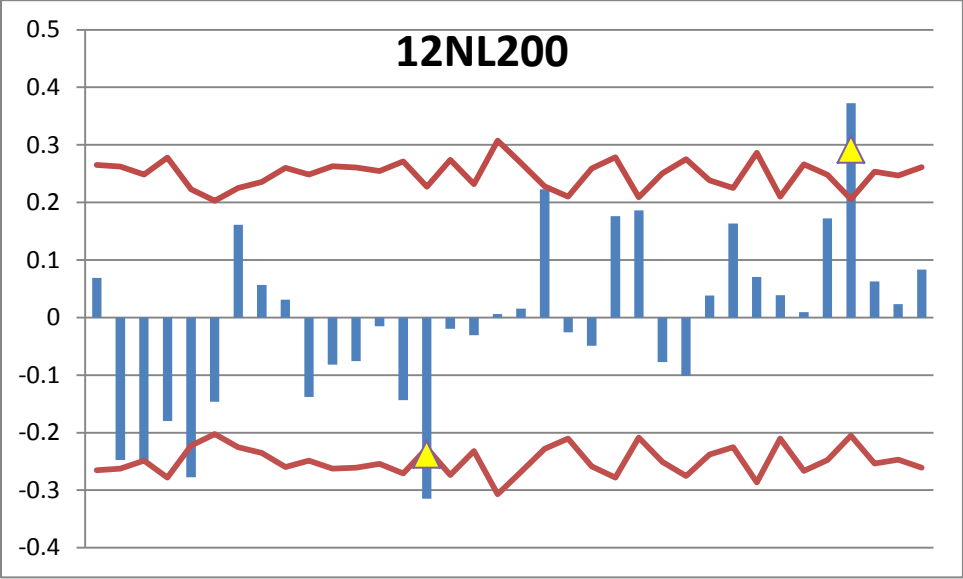
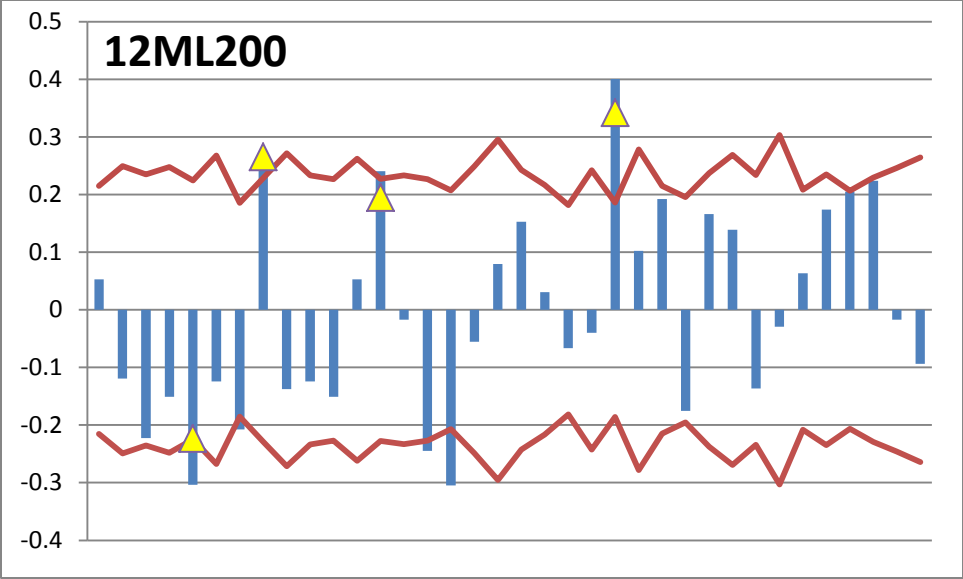


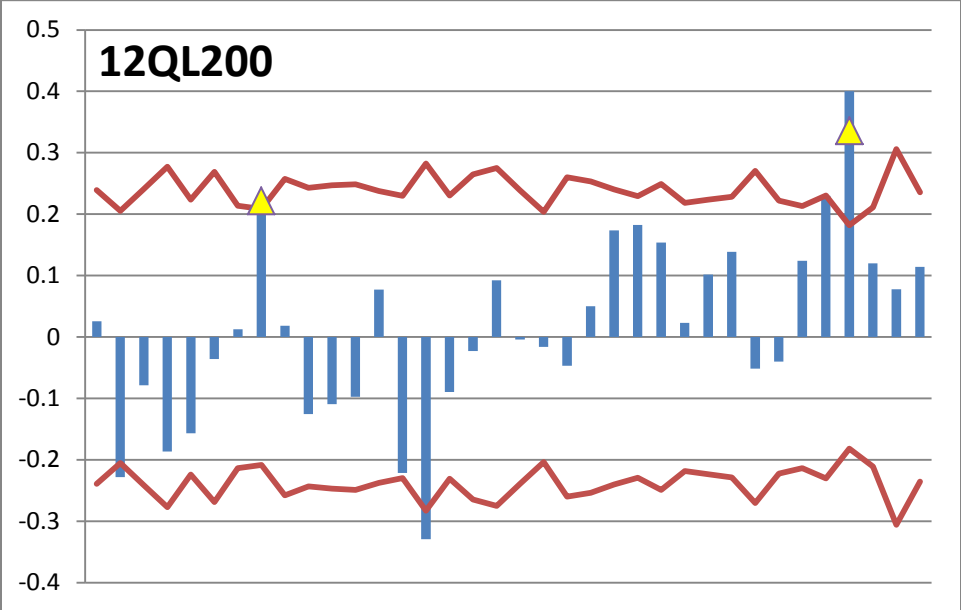
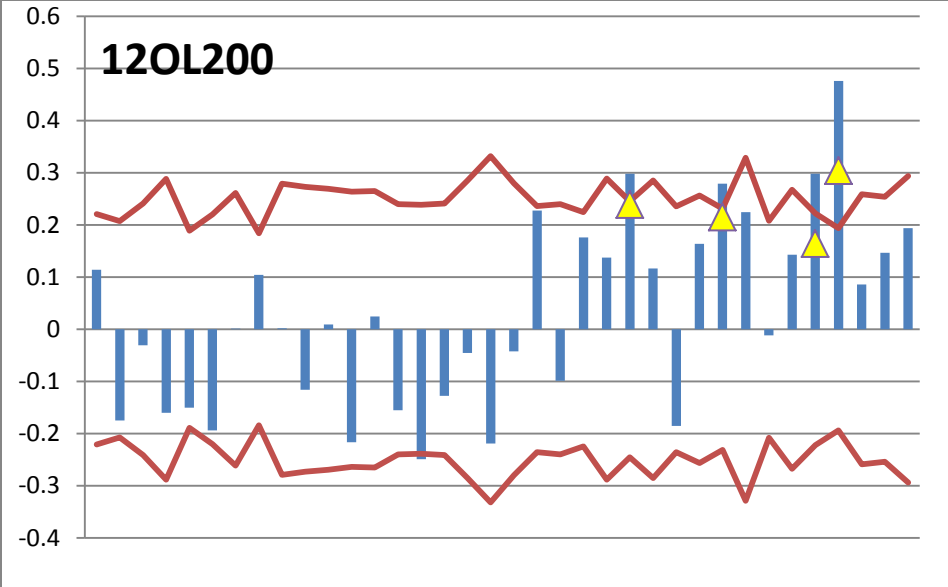


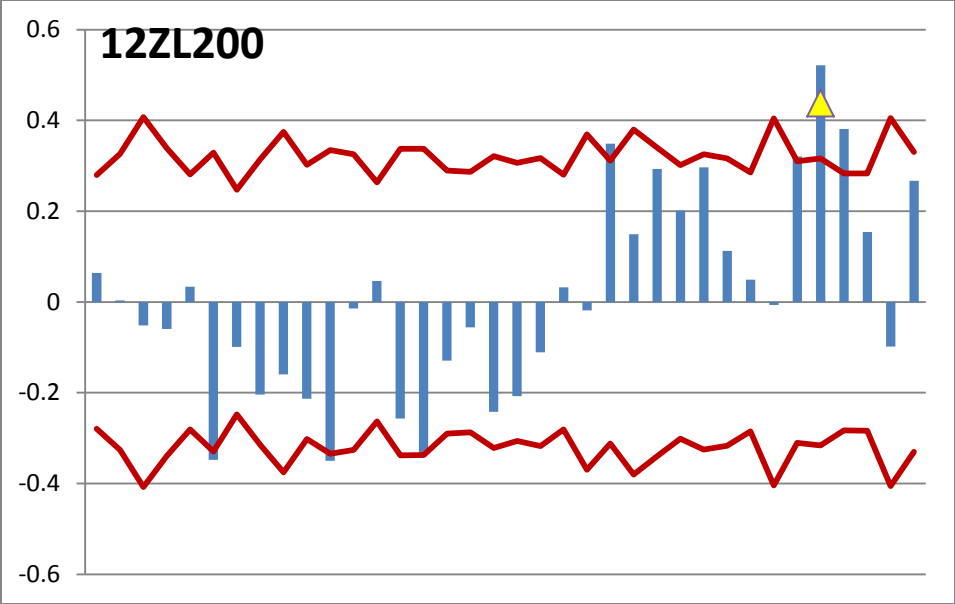












Appendix C: Moran's I Clustering Analysis Results

ObjectID = Abstract site number and location. The following are types of clustering classifications (COType) by Moran's I: HH = high value surrounded by high values (clustering), LL = low value surrounded by low values (clustering), LH = low value surrounding by high values (outlier), HL = high value surrounded by low values (outlier). Binary indicates weights associated with Global Moran's I. NS = not significant. LMiIndex = Local Moran's I Index, a relative measure used within the context of local Z score. LMiZScore = Z-score associated with LISA test, a standard statistical measure. LMiPValue = significance of clustering as indicated by LMiZScore.

ObjectID	HH	LL	HL	LH	HH- binary	LL- binary	HL- binary	LH- binary	summary
1					0	0	0	0	NS
2		1			0	1	0	0	NS
3					0	0	0	0	NS
4		1			0	1	0	0	NS
5				1	0	0	0	1	NS
6	1	1		1	0	1	0	1	NS
7	1	1		1	0	1	0	1	NS
8	1	1	4	1	0	1	1	1	HL
9					0	0	0	0	NS
10	3	1	1		1	1	0	0	HH
11	2			1	0	0	0	1	HH
12		1			0	1	0	0	NS
13	3	1		1	1	1	0	1	HH
14	1		1	1	0	0	0	1	NS
15					0	0	0	0	NS
16	1	1			0	1	0	0	NS
17	3				1	0	0	0	HH
18	1	1	1		0	1	0	0	NS
19	1		2	1	0	0	1	1	HL
20	3		1		1	0	0	0	HH
21		1	1		0	1	0	0	NS
22		1	3	1	0	1	1	1	HL
23					0	0	0	0	NS
24			1		0	0	0	0	NS

1975						
OBJECTID	SOURCE_ID	y1975	LMiIndex	LMiZScore	LMiPValue	COType
1	0	1.1	0.060235	0.119545	0.904843	
2	1	1.84	0.394513	0.384265	0.700781	
3	2	1.033	-0.09859	-0.06111	0.951274	
4	3	1.024	-0.99502	-0.43991	0.660002	
5	4	1.209	-0.50897	-0.20903	0.834423	
6	5	0.326	-4.25516	-2.73822	0.006177	LH
7	6	1.046	0.365027	0.321024	0.748192	
8	7	1.081	-0.02701	0.018262	0.985429	
9	8	1.197	-0.68322	-0.28322	0.777005	
10	9	1.185	0.012243	0.061777	0.950739	
11	10	1.182	-0.27633	-0.17703	0.859485	
12	11	0.958	-0.57745	-0.17319	0.862501	
13	12	1.133	0.012243	0.061777	0.950739	
14	13	1.416	-0.43782	-0.56337	0.573184	
15	14	1.301	-0.77794	-0.42985	0.667304	
16	15	0.995	0.285369	0.277099	0.781703	
17	16	0.792	-0.24837	-0.12911	0.897272	
18	17	0.873	-0.45479	-0.17655	0.859862	
19	18	0.973	-0.53921	-0.18589	0.852532	
20	19	1.136	-0.19081	-0.09082	0.927634	
21	20	1.019	0.15783	0.196934	0.843878	
22	21	1.595	-6.71306	-3.95102	0.000077	HL
23	22	1.256	1.263593	1.449133	0.1473	
24	23	1.175	-0.17709	-0.00186	0.998516	

1976						
OBJECTID	SOURCE_ID	y1976	LMiIndex	LMiZScore	LMiPValue	COType
1	0	0.899	0.258422	0.282497	0.777561	
2	1	0.548	-0.515293	-0.339111	0.734525	
3	2	1.155	-0.524914	-0.52921	0.596659	
4	3	1.211	0.441061	0.360096	0.718774	
5	4	0.532	-3.361615	-1.936349	0.052824	
6	5	0.816	-0.69903	-0.374628	0.707936	
7	6	1.177	0.644619	0.485528	0.627301	
8	7	2.201	-1.42462	-1.518196	0.128964	
9	8	0.656	-1.282338	-0.629378	0.529101	
10	9	0.798	0.471259	0.565816	0.571518	
11	10	1.02	-0.117204	-0.03498	0.972094	
12	11	1.28	0.34635	0.30958	0.756879	

13	12	0.569	0.471259	0.565816	0.571518
14	13	0.494	0.498382	0.738024	0.460499
15	14	0.977	-0.009528	0.079661	0.936506
16	15	1.364	0.300405	0.283779	0.776579
17	16	0.746	0.591577	0.53785	0.59068
18	17	0.729	0.54255	0.430267	0.667001
19	18	0.776	0.989843	0.665283	0.505869
20	19	1.579	0.092597	0.145816	0.884066
21	20	1.307	-0.063378	0.063108	0.949679
22	21	0.838	-0.497787	-0.197279	0.843608
23	22	0.922	0.147761	0.210216	0.833498
24	23	0.798	-0.911152	-0.429093	0.667855

1977

OBJECTID	SOURCE_ID	y1977	LMiIndex	LMiZScore	LMiPValue	COType
1	0	1.087	-0.16246	-0.06351	0.949357	
2	1	1.015	-0.15238	-0.05015	0.96	
3	2	0.648	-0.70621	-0.70404	0.481404	
4	3	0.68	-1.60768	-0.75754	0.448726	
5	4	1.155	-2.48907	-1.36861	0.171121	
6	5	0.716	-2.11164	-1.26649	0.205337	
7	6	0.896	-0.20377	-0.01985	0.98416	
8	7	0.863	-0.35924	-0.33545	0.737284	
9	8	0.73	1.117864	0.74524	0.456126	
10	9	1.028	0.455016	0.529573	0.596407	
11	10	0.522	0.878957	0.818486	0.413079	
12	11	0.854	0.206726	0.231368	0.817028	
13	12	1.438	0.455016	0.529573	0.596407	
14	13	1.011	-0.19798	-0.2188	0.826807	
15	14	0.988	0.102731	0.149052	0.881512	
16	15	0.777	1.548248	0.959277	0.337418	
17	16	1.042	-0.08158	0.004036	0.996779	
18	17	1.125	-0.5409	-0.22131	0.824852	
19	18	0.606	-0.93088	-0.39222	0.694892	
20	19	0.997	-0.15826	-0.06099	0.951364	
21	20	0.439	1.405202	0.916411	0.359451	
22	21	1.754	-5.64559	-3.19284	0.001408	HL
23	22	1.017	0.054922	0.104535	0.916744	
24	23	1.326	-0.87711	-0.39798	0.690648	

1978						
OBJECTID	SOURCE_ID	y1978	LMiIndex	LMiZScore	LMiPValue	COType
1	0	0.805	1.266809	1.038758	0.298916	
2	1	0.939	-0.06157	0.018696	0.985083	
3	2	1.207	-0.65314	-0.62099	0.534605	
4	3	1.059	0.497647	0.369501	0.711753	
5	4	0.828	-2.13203	-1.11835	0.263419	
6	5	1.084	-0.79183	-0.40722	0.683848	
7	6	1.312	-3.23724	-1.71771	0.08585	
8	7	1.303	2.080037	2.162995	0.030541	HH
9	8	0.736	-0.79154	-0.325	0.745183	
10	9	1.339	-0.33689	-0.29886	0.765043	
11	10	0.718	0.309049	0.317899	0.750561	
12	11	1.206	-1.06692	-0.40576	0.684918	
13	12	0.932	-0.33689	-0.29886	0.765043	
14	13	0.775	-0.1794	-0.18595	0.852483	
15	14	0.805	-0.86021	-0.44932	0.653204	
16	15	1.133	0.265577	0.249367	0.803076	
17	16	0.827	1.23478	0.974846	0.329636	
18	17	0.838	-0.02279	0.081668	0.93491	
19	18	1.04	-0.43302	-0.1186	0.905591	
20	19	0.558	-3.18598	-2.40336	0.016245	LH
21	20	1.155	0.012227	0.101758	0.918948	
22	21	0.664	-4.29551	-2.32307	0.020175	LH
23	22	0.981	0.000879	0.045182	0.963961	
24	23	1.326	0.373769	0.299307	0.764705	

1979						
OBJECTID	SOURCE_ID	y1979	LMiIndex	LMiZScore	LMiPValue	COType
1	0	1.05	2.119391	1.760216	0.078371	
2	1	0.283	-1.01773	-0.71205	0.476436	
3	2	0.801	-0.0042	0.041642	0.966783	
4	3	0.782	0.451567	0.356077	0.721782	
5	4	0.892	-0.41115	-0.14394	0.885548	
6	5	0.809	-0.03084	0.063544	0.949332	
7	6	0.561	1.143796	0.760212	0.447127	
8	7	0.855	-0.15169	-0.11472	0.90867	
9	8	0.951	0.732062	0.525988	0.598896	
10	9	0.829	-0.12739	-0.08895	0.929121	
11	10	1.513	1.285585	1.164034	0.24441	
12	11	0.51	1.343851	0.809704	0.418109	

13	12	0.385	-0.12739	-0.08895	0.929121	
14	13	0.86	0.086403	0.161488	0.871708	
15	14	0.824	-0.02226	0.069018	0.944974	
16	15	0.677	0.159578	0.199214	0.842094	
17	16	1.36	2.724895	2.154012	0.031239	HH
18	17	0.796	-0.05719	0.064157	0.948845	
19	18	0.962	0.981484	0.642825	0.520337	
20	19	0.897	-0.24894	-0.13381	0.893553	
21	20	0.805	-0.00043	0.097838	0.92206	
22	21	0.367	2.978137	1.831264	0.067061	
23	22	0.983	-1.16733	-1.19135	0.233515	
24	23	0.564	-0.65818	-0.27358	0.784404	

1980

OBJECTID	SOURCE_ID	y1980	LMiIndex	LMiZScore	LMiPValue	COType
1	0	1.014	2.384975	1.907421	0.056465	
2	1	0.458	1.437106	1.127473	0.259542	
3	2	0.766	-0.14083	-0.09962	0.920647	
4	3	0.684	1.96019	1.139778	0.254378	
5	4	1.013	-2.80002	-1.50415	0.132543	
6	5	1.029	-0.68162	-0.34075	0.73329	
7	6	0.727	-0.16346	0.003417	0.997273	
8	7	0.5	-1.74282	-1.73885	0.08206	
9	8	0.899	0.117222	0.173753	0.862059	
10	9	0.719	-0.38971	-0.35429	0.723123	
11	10	0.636	-1.20005	-0.92682	0.354022	
12	11	0.405	-1.23459	-0.49033	0.623903	
13	12	1.001	-0.38971	-0.35429	0.723123	
14	13	0.628	-0.48298	-0.57818	0.563145	
15	14	0.742	-0.71734	-0.36283	0.716728	
16	15	0.771	0.141238	0.184147	0.853897	
17	16	1.103	2.688096	2.055736	0.039807	HH
18	17	0.986	1.019932	0.678677	0.497341	
19	18	0.935	0.377183	0.307516	0.75845	
20	19	0.65	-0.6606	-0.44958	0.653014	
21	20	0.668	0.274398	0.250105	0.802505	
22	21	0.884	-0.7052	-0.30314	0.761779	
23	22	0.73	0.52043	0.57702	0.563925	
24	23	1.022	0.008001	0.099796	0.920506	

1981						
OBJECTID	SOURCE_ID	y1981	LMiIndex	LMiZScore	LMiPValue	COType
1	0	0.639	0.014945	0.076772	0.938804	
2	1	0.969	-0.05019	0.027549	0.978021	
3	2	0.637	-0.36276	-0.3311	0.740569	
4	3	0.835	0.680147	0.471578	0.637227	
5	4	0.977	-0.37998	-0.12333	0.901848	
6	5	0.735	-0.03096	0.062237	0.950373	
7	6	0.991	-0.56811	-0.22654	0.820779	
8	7	0.773	-1.21856	-1.21856	0.22301	
9	8	0.911	0.140132	0.188278	0.850658	
10	9	1.096	0.432414	0.493502	0.621657	
11	10	1.284	2.310981	1.99751	0.045769	HH
12	11	0.743	0.368423	0.308607	0.757619	
13	12	1.029	0.432414	0.493502	0.621657	
14	13	0.728	0.50411	0.703728	0.481601	
15	14	0.82	-1.783	-1.03393	0.30117	
16	15	0.869	0.052794	0.138544	0.889809	
17	16	0.944	-0.11805	-0.02342	0.981313	
18	17	1.378	4.199029	2.525946	0.011538	HH
19	18	0.808	-2.59369	-1.2695	0.204261	
20	19	1.026	-0.34918	-0.21	0.833663	
21	20	1.13	-1.1226	-0.54433	0.586215	
22	21	0.777	1.575129	0.996466	0.319023	
23	22	0.975	0.047215	0.09405	0.925069	
24	23	1.229	0.482095	0.36391	0.715924	

1982						
OBJECTID	SOURCE_ID	y1982	LMiIndex	LMiZScore	LMiPValue	COType
1	0	1.13	-0.31827	-0.18711	0.851571	
2	1	0.946	-0.73106	-0.49066	0.623668	
3	2	1.068	0.084391	0.134945	0.892655	
4	3	1.083	-0.75843	-0.29654	0.766818	
5	4	1.167	-1.54513	-0.80795	0.41912	
6	5	1.308	-1.18315	-0.669	0.503496	
7	6	0.787	-2.73187	-1.47771	0.139484	
8	7	0.965	-0.18419	-0.1485	0.881949	
9	8	0.899	1.607071	1.017042	0.309133	
10	9	1.108	-0.05908	-0.01647	0.986859	
11	10	0.592	-4.00893	-3.34273	0.000829	LH
12	11	0.689	0.670638	0.465682	0.641442	

13	12	1.009	-0.05908	-0.01647	0.986859	
14	13	1.25	-0.07822	-0.05812	0.953656	
15	14	1.013	-0.39549	-0.16844	0.866237	
16	15	0.92	1.295542	0.816901	0.413984	
17	16	1.038	0.007079	0.071641	0.942887	
18	17	1.468	-3.74923	-2.10391	0.035386	HL
19	18	1.025	-0.10127	0.056966	0.954572	
20	19	1.015	-0.02627	0.045097	0.964029	
21	20	0.97	0.93468	0.638948	0.522856	
22	21	1.16	-0.91316	-0.43161	0.666028	
23	22	1.284	-0.62645	-0.61523	0.538403	
24	23	1.131	0.711481	0.498351	0.618236	

1983

OBJECTID	SOURCE_ID	y1983	LMiIndex	LMiZScore	LMiPValue	COType
1	0	1.012	0.284714	0.289035	0.772554	
2	1	0.496	-0.2582	-0.12879	0.89752	
3	2	1.043	0.075287	0.123664	0.90158	
4	3	1.106	-1.3433	-0.60518	0.545061	
5	4	0.956	0.428826	0.34497	0.730116	
6	5	1.032	-0.45708	-0.20511	0.837483	
7	6	0.95	-0.01712	0.086923	0.930732	
8	7	1.391	-2.34572	-2.3972	0.016521	HL
9	8	1.003	0.911894	0.619121	0.535836	
10	9	0.74	1.402242	1.505349	0.132234	
11	10	0.892	-0.04677	0.025902	0.979335	
12	11	0.962	0.29265	0.271391	0.786089	
13	12	0.259	1.402242	1.505349	0.132234	
14	13	0.946	0.156716	0.250865	0.801918	
15	14	0.867	0.124872	0.160315	0.872632	
16	15	1.156	2.085811	1.234358	0.217069	
17	16	1.05	0.338705	0.320512	0.74858	
18	17	0.627	0.006329	0.100093	0.920269	
19	18	1.356	-3.95693	-2.00086	0.045407	HL
20	19	1.035	0.24481	0.258894	0.795716	
21	20	1.244	1.775157	1.113136	0.265649	
22	21	0.448	-2.27579	-1.2081	0.22701	
23	22	0.765	0.761746	0.838436	0.401785	
24	23	0.523	-2.92029	-1.52869	0.126341	

1984						
OBJECTID	SOURCE_ID	y1984	LMiIndex	LMiZScore	LMiPValue	COType
1	0	1.159	-0.15587	-0.05782	0.953888	
2	1	0.913	-0.04028	0.035526	0.97166	
3	2	1.087	0.298045	0.360063	0.718799	
4	3	0.803	1.418278	0.874647	0.381765	
5	4	1.053	-0.54826	-0.22357	0.823093	
6	5	0.973	-0.30712	-0.11218	0.910677	
7	6	0.706	1.644081	1.045066	0.295992	
8	7	0.861	-0.57598	-0.56141	0.574518	
9	8	0.894	0.196714	0.222513	0.823914	
10	9	0.9	-0.03422	0.009759	0.992212	
11	10	1.123	-0.60202	-0.44547	0.655979	
12	11	0.597	1.340878	0.805175	0.420718	
13	12	0.986	-0.03422	0.009759	0.992212	
14	13	1.127	-1.5825	-2.05622	0.039761	HL
15	14	0.885	-0.28393	-0.09746	0.922358	
16	15	1.004	-0.66767	-0.25158	0.801362	
17	16	0.947	0.01566	0.078113	0.937737	
18	17	1.409	-0.92283	-0.44398	0.657053	
19	18	0.36	-12.0242	-6.36549	1.95E-10	LH
20	19	0.636	1.027028	0.887874	0.374608	
21	20	0.754	0.746149	0.529347	0.596564	
22	21	0.949	-0.0859	0.047984	0.961728	
23	22	1.156	-0.11492	-0.07532	0.939958	
24	23	1.326	-1.79905	-0.91397	0.36073	

1985						
OBJECTID	SOURCE_ID	y1985	LMiIndex	LMiZScore	LMiPValue	COType
1	0	1.129	0.166278	0.197267	0.843618	
2	1	0.741	3.02778	2.358101	0.018368	LL
3	2	1.256	0.261216	0.319464	0.749374	
4	3	0.699	6.881303	3.797466	0.000146	LL
5	4	1.139	-0.12476	0.024297	0.980615	
6	5	1.424	-0.56207	-0.27272	0.785071	
7	6	0.971	-0.01575	0.088211	0.929708	
8	7	1.506	-0.00576	0.039542	0.968457	
9	8	1.107	-0.07579	0.068856	0.945103	
10	9	0.963	-0.15288	-0.11471	0.908676	
11	10	0.823	-0.52538	-0.37838	0.705149	
12	11	0.818	2.389519	1.331763	0.182937	

13	12	1.13	-0.15288	-0.11471	0.908676
14	13	1.285	0.224728	0.34245	0.732011
15	14	0.991	-0.20317	-0.04595	0.963346
16	15	1.134	-0.82754	-0.33712	0.736027
17	16	1.196	0.211593	0.226252	0.821005
18	17	1.113	-0.20518	-0.02285	0.981768
19	18	1.135	-0.2181	-0.00598	0.995225
20	19	1.112	0.1861	0.213866	0.830651
21	20	0.998	0.323745	0.283653	0.776675
22	21	1.107	-0.24482	-0.04388	0.965001
23	22	1.144	-0.56537	-0.54719	0.584246
24	23	1.083	-0.00561	0.094222	0.924932

1986

OBJECTID	SOURCE_ID	y1986	LMiIndex	LMiZScore	LMiPValue	COType
1	0	0.743	0.056257	0.109768	0.912592	
2	1	0.46	-0.25638	-0.12771	0.89838	
3	2	0.82	0.018827	0.065023	0.948155	
4	3	0.958	-0.3378	-0.0695	0.944595	
5	4	0.84	-0.07024	0.055856	0.955456	
6	5	1.476	0.451037	0.365869	0.714462	
7	6	1.173	1.448102	0.924309	0.355325	
8	7	0.78	0.198816	0.252865	0.800372	
9	8	0.844	-0.03397	0.091968	0.926723	
10	9	1.225	-2.17273	-2.22214	0.026273	HL
11	10	0.932	0.201333	0.234694	0.814445	
12	11	1	-0.48046	-0.11741	0.906533	
13	12	0.328	-2.17273	-2.22214	0.026273	LH
14	13	0.776	-0.51985	-0.63817	0.523364	
15	14	0.801	-0.05061	0.050227	0.959941	
16	15	1.024	0.227723	0.233637	0.815266	
17	16	0.859	0.023081	0.082966	0.933878	
18	17	0.523	-1.54062	-0.79965	0.423913	
19	18	1.475	-4.29301	-2.18399	0.028962	HL
20	19	1.168	2.929441	2.387011	0.016985	HH
21	20	0.86	-0.03032	0.079432	0.936688	
22	21	0.341	-6.64942	-3.7228	0.000197	LH
23	22	0.841	0.144507	0.196186	0.844463	
24	23	0.681	-0.19666	-0.01268	0.98988	

1987						
OBJECTID	SOURCE_ID	y1987	LMiIndex	LMiZScore	LMiPValue	COType
1	0	0.876	1.025162	0.896363	0.370058	
2	1	0.444	0.004318	0.070663	0.943665	
3	2	0.758	0.215298	0.277797	0.781167	
4	3	0.748	-0.48481	-0.15118	0.879837	
5	4	0.944	-1.26622	-0.65366	0.51333	
6	5	0.872	-1.01329	-0.56963	0.568931	
7	6	0.553	0.025979	0.114356	0.908955	
8	7	0.266	2.114461	2.316558	0.020527	LL
9	8	0.864	0.058008	0.146435	0.883577	
10	9	0.771	-0.13898	-0.10252	0.918346	
11	10	1.48	1.308426	1.19775	0.231013	
12	11	0.592	-0.14033	0.054881	0.956233	
13	12	0.562	-0.13898	-0.10252	0.918346	
14	13	0.668	-0.11104	-0.10352	0.917553	
15	14	0.724	-0.1102	0.013057	0.989581	
16	15	0.455	-0.76187	-0.307	0.758846	
17	16	0.953	1.239243	1.028072	0.303915	
18	17	0.401	-2.78684	-1.56071	0.118592	
19	18	1.07	0.58432	0.432104	0.665665	
20	19	0.385	-0.20932	-0.10316	0.917836	
21	20	0.588	-0.08039	0.051906	0.958603	
22	21	0.731	-0.00712	0.095032	0.924289	
23	22	0.641	0.187011	0.247432	0.804573	
24	23	0.337	1.574297	0.997955	0.3183	

1988						
OBJECTID	SOURCE_ID	y1988	LMiIndex	LMiZScore	LMiPValue	COType
1	0	0.733	-0.11314	-0.02368	0.98111	
2	1	0.871	-0.1022	-0.01151	0.990812	
3	2	0.994	-0.55816	-0.53851	0.590227	
4	3	0.624	1.481352	0.903319	0.366356	
5	4	0.605	0.224471	0.227455	0.820069	
6	5	0.65	0.694939	0.520517	0.602703	
7	6	0.781	0.546052	0.409749	0.681989	
8	7	0.486	-0.77236	-0.76262	0.445692	
9	8	0.98	-0.89081	-0.38731	0.698528	
10	9	1.173	2.569981	2.734429	0.006248	HH
11	10	0.913	0.015919	0.078889	0.93712	
12	11	0.449	1.847359	1.056412	0.290779	

13	12	1.343	2.569981	2.734429	0.006248	HH
14	13	0.978	-0.78961	-0.9954	0.319543	
15	14	0.935	0.349315	0.302551	0.762231	
16	15	0.971	-1.42156	-0.65782	0.510651	
17	16	0.783	-0.02626	0.045829	0.963446	
18	17	1.416	-1.60534	-0.83908	0.401426	
19	18	0.37	-7.19301	-3.74132	0.000183	LH
20	19	0.802	0.152549	0.186789	0.851825	
21	20	0.825	0.099316	0.154132	0.877505	
22	21	0.709	1.707824	1.080264	0.280024	
23	22	0.833	-0.00402	0.041287	0.967066	
24	23	0.982	-0.34865	-0.09766	0.922205	

1989

OBJECTID	SOURCE_ID	y1989	LMiIndex	LMiZScore	LMiPValue	COType
1	0	1.446	0.918259	0.776563	0.437416	
2	1	0.792	-0.11406	-0.02012	0.983949	
3	2	0.728	-0.88362	-0.86278	0.388257	
4	3	1.095	-2.13699	-1.01725	0.309036	
5	4	1.209	-2.0716	-1.0914	0.275095	
6	5	1.324	-2.67979	-1.58115	0.113843	
7	6	0.621	-1.84344	-0.9437	0.345324	
8	7	0.995	-0.02328	0.020745	0.983448	
9	8	0.815	-0.74955	-0.30389	0.761214	
10	9	1.016	-0.17996	-0.14016	0.888532	
11	10	0.888	-0.70054	-0.51613	0.605766	
12	11	0.503	-0.66727	-0.20911	0.834359	
13	12	0.758	-0.17996	-0.14016	0.888532	
14	13	0.632	-1.83261	-2.3265	0.019991	LH
15	14	0.758	-2.0933	-1.2174	0.223452	
16	15	1.11	-0.68807	-0.25744	0.796836	
17	16	1.209	1.341612	1.061858	0.2883	
18	17	1.22	0.679956	0.48559	0.627257	
19	18	1.421	-2.13337	-1.017	0.309152	
20	19	1.016	0.058785	0.11033	0.912147	
21	20	0.872	0.22611	0.223526	0.823125	
22	21	0.757	0.836071	0.569509	0.56901	
23	22	0.864	0.23464	0.285612	0.775174	
24	23	0.917	-0.34616	-0.09478	0.924493	

1990						
OBJECTID	SOURCE_ID	y1990	LMiIndex	LMiZScore	LMiPValue	COType
1	0	1.107	0.224226	0.239649	0.810601	
2	1	1.368	0.416404	0.375679	0.707154	
3	2	0.883	-0.0337	0.010095	0.991945	
4	3	0.855	1.525232	0.917629	0.358812	
5	4	1.008	-0.33825	-0.09889	0.921224	
6	5	0.877	-0.31998	-0.11816	0.905941	
7	6	0.838	-0.02208	0.083527	0.933431	
8	7	0.673	0.492196	0.553248	0.580093	
9	8	1.026	-0.51742	-0.17661	0.859815	
10	9	1.351	-0.7222	-0.70099	0.483312	
11	10	1.243	1.189896	1.055906	0.291011	
12	11	0.503	7.030593	3.63777	0.000275	LL
13	12	0.89	-0.7222	-0.70099	0.483312	
14	13	1.113	0.180282	0.279497	0.779863	
15	14	0.976	-0.06396	0.041442	0.966943	
16	15	0.704	4.850409	2.706957	0.00679	LL
17	16	1.061	0.200287	0.214593	0.830084	
18	17	1.174	0.737661	0.521186	0.602237	
19	18	1.088	0.799859	0.533847	0.593447	
20	19	1.344	-1.75849	-1.31508	0.188484	
21	20	0.698	4.24115	2.508152	0.012136	LL
22	21	0.936	0.956948	0.641058	0.521484	
23	22	1.186	1.431545	1.523414	0.127655	
24	23	0.914	0.08991	0.145858	0.884033	

1991						
OBJECTID	SOURCE_ID	y1991	LMiIndex	LMiZScore	LMiPValue	COType
1	0	0.989	0.662515	0.58229	0.560371	
2	1	0.691	-1.37661	-0.96404	0.335027	
3	2	0.812	-0.62698	-0.60364	0.546083	
4	3	1.045	-1.32742	-0.59376	0.552674	
5	4	1.236	-1.70434	-0.88644	0.375379	
6	5	1.262	3.002876	1.956149	0.050447	
7	6	0.845	-0.88187	-0.40406	0.686166	
8	7	0.965	-0.7193	-0.69915	0.484458	
9	8	1.048	0.312202	0.283385	0.776881	
10	9	0.691	1.481961	1.578097	0.114543	
11	10	0.736	0.887855	0.805558	0.420497	
12	11	0.755	-1.7428	-0.7484	0.454219	

13	12	0.571	1.481961	1.578097	0.114543	
14	13	0.95	-0.15308	-0.15454	0.877182	
15	14	0.76	2.024934	1.345612	0.178427	
16	15	0.931	0.441328	0.346592	0.728897	
17	16	1.015	0.794623	0.659834	0.50936	
18	17	0.74	2.708524	1.660107	0.096892	
19	18	0.758	2.349058	1.357023	0.174773	
20	19	1.287	3.201219	2.580836	0.009856	HH
21	20	0.824	-0.60681	-0.24948	0.802991	
22	21	0.867	-0.17193	-0.00182	0.998547	
23	22	1.024	-0.63914	-0.61622	0.537746	
24	23	0.498	3.03498	1.776529	0.075645	

1992

OBJECTID	SOURCE_ID	y1992	LMiIndex	LMiZScore	LMiPValue	COType
1	0	0.82	-0.49885	-0.31974	0.749167	
2	1	1.095	0.877192	0.709854	0.477794	
3	2	0.621	-2.06157	-2.05464	0.039913	LH
4	3	1.018	0.155703	0.190278	0.849091	
5	4	1.298	-2.46455	-1.30702	0.191206	
6	5	0.647	-3.03441	-1.78721	0.073903	
7	6	1.251	-0.46153	-0.16343	0.870178	
8	7	0.664	1.771297	1.847645	0.064653	
9	8	1.039	-0.13463	0.035076	0.972018	
10	9	1.059	0.308296	0.358146	0.720233	
11	10	0.671	0.887304	0.792953	0.427804	
12	11	0.743	-2.28519	-1.00851	0.313209	
13	12	1.221	0.308296	0.358146	0.720233	
14	13	1.203	-0.93506	-1.15518	0.248018	
15	14	0.994	-0.06031	0.043155	0.965577	
16	15	1.096	0.320103	0.278151	0.780896	
17	16	1.104	-0.24267	-0.1149	0.908527	
18	17	1.151	-2.54692	-1.3567	0.174875	
19	18	0.686	1.436249	0.861704	0.38885	
20	19	1.162	-0.32257	-0.18577	0.852622	
21	20	1.007	0.083527	0.141787	0.887247	
22	21	1.04	-0.26916	-0.05651	0.954936	
23	22	1.401	0.815097	0.874126	0.382049	
24	23	0.683	2.475879	1.447535	0.147747	

1993						
OBJECTID	SOURCE_ID	y1993	LMiIndex	LMiZScore	LMiPValue	COType
1	0	1.18	0.292096	0.298706	0.765163	
2	1	1.745	-0.01978	0.051191	0.959172	
3	2	1.027	-0.24572	-0.2135	0.830938	
4	3	1.165	-0.80674	-0.32263	0.746977	
5	4	1.31	-0.13502	0.01842	0.985303	
6	5	0.893	-3.20774	-1.95618	0.050444	
7	6	1.386	-0.04559	0.0715	0.942999	
8	7	0.844	-1.85633	-1.91378	0.055648	
9	8	1.105	0.389516	0.331354	0.740376	
10	9	1.336	0.040101	0.088232	0.929691	
11	10	0.602	-3.26169	-2.70819	0.006765	LH
12	11	1.121	-0.34029	-0.04721	0.962342	
13	12	1.263	0.040101	0.088232	0.929691	
14	13	1.34	0.150994	0.24673	0.805117	
15	14	1.091	-1.56164	-0.90979	0.362933	
16	15	1.273	-0.03721	0.091437	0.927145	
17	16	1.045	0.590767	0.517062	0.605112	
18	17	1.49	-1.0579	-0.5238	0.600417	
19	18	1.353	-0.25113	-0.02383	0.980991	
20	19	1.538	-1.02375	-0.75403	0.450829	
21	20	1.394	-0.31804	-0.08645	0.931105	
22	21	1.366	-0.77625	-0.35232	0.724597	
23	22	1.308	0.57521	0.653131	0.513671	
24	23	1.53	-0.81491	-0.36089	0.718184	

1994						
OBJECTID	SOURCE_ID	y1994	LMiIndex	LMiZScore	LMiPValue	COType
1	0	0.928	0.106259	0.149893	0.880848	
2	1	0.775	-0.31448	-0.17236	0.863155	
3	2	0.938	0.046471	0.094372	0.924813	
4	3	1.236	0.706397	0.489872	0.624223	
5	4	0.883	-0.63861	-0.27536	0.783036	
6	5	1.087	0.902351	0.652922	0.513806	
7	6	1.379	3.211475	1.940415	0.052329	
8	7	1.598	-2.41513	-2.48828	0.012836	HL
9	8	0.746	-1.33999	-0.63999	0.52218	
10	9	0.923	0.156263	0.209563	0.834008	

11	10	0.739	0.632004	0.600044	0.548476	
12	11	1.138	0.586347	0.421222	0.673592	
13	12	0.709	0.156263	0.209563	0.834008	
14	13	0.407	-0.52213	-0.64457	0.519204	
15	14	0.901	0.649241	0.492907	0.622078	
16	15	1.146	0.679064	0.47918	0.63181	
17	16	1.007	-0.04119	0.034627	0.972376	
18	17	0.455	2.825962	1.748291	0.080413	
19	18	1.128	-2.04712	-0.98756	0.323367	
20	19	1.852	3.149733	2.574506	0.010038	HH
21	20	1.489	-0.08418	0.048744	0.961122	
22	21	0.882	-0.76017	-0.34125	0.732918	
23	22	0.923	0.119642	0.171141	0.864112	
24	23	0.506	-0.47517	-0.16875	0.865995	

1995

OBJECTID	SOURCE_ID	y1995	LMiIndex	LMiZScore	LMiPValue	COType
1	0	0.873	-0.19549	-0.08848	0.929496	
2	1	1.152	-0.29033	-0.15332	0.878147	
3	2	1.004	0.343702	0.404133	0.686114	
4	3	0.751	0.519683	0.388271	0.697814	
5	4	1.081	0.725468	0.517931	0.604506	
6	5	0.647	6.290535	4.040714	0.000053	LL
7	6	0.477	9.704269	5.642559	1.68E-08	LL
8	7	0.74	-1.42228	-1.43918	0.1501	
9	8	1.07	0.274029	0.264005	0.791775	
10	9	0.851	-0.28881	-0.25608	0.79789	
11	10	0.759	-1.10857	-0.86751	0.385665	
12	11	1.013	0.233961	0.242298	0.808548	
13	12	1.078	-0.28881	-0.25608	0.79789	
14	13	1.06	0.133399	0.220813	0.825237	
15	14	0.933	0.181956	0.196587	0.84415	
16	15	0.945	0.139777	0.186191	0.852294	
17	16	0.94	0.047895	0.101711	0.918985	
18	17	1.185	1.543908	0.994895	0.319786	
19	18	0.968	0.639975	0.452729	0.650743	
20	19	0.505	7.349622	5.890846	3.84E-09	LL
21	20	0.914	-0.08037	0.050726	0.959543	
22	21	0.907	0.301536	0.270179	0.787022	
23	22	1.044	0.737883	0.815575	0.414742	
24	23	1.221	1.093961	0.707156	0.479469	

1996						
OBJECTID	SOURCE_ID	y1996	LMiIndex	LMiZScore	LMiPValue	COType
1	0	1.179	2.296723	1.87872	0.060282	
2	1	1.118	-0.99739	-0.68798	0.491462	
3	2	0.862	0.504853	0.57378	0.566116	
4	3	0.853	1.298713	0.805709	0.42041	
5	4	0.761	-0.34016	-0.10109	0.919481	
6	5	0.813	1.222744	0.853463	0.393402	
7	6	0.901	0.814837	0.563712	0.57295	
8	7	1.099	1.477537	1.591606	0.111473	
9	8	1.146	2.47507	1.496228	0.134593	
10	9	0.865	0.104517	0.154864	0.876927	
11	10	0.871	0.330311	0.344077	0.730788	
12	11	0.624	-0.84429	-0.30114	0.763309	
13	12	0.921	0.104517	0.154864	0.876927	
14	13	0.884	0.218688	0.333812	0.73852	
15	14	0.966	0.011815	0.089718	0.92851	
16	15	0.963	0.000837	0.111405	0.911295	
17	16	1.24	2.644846	2.06715	0.038719	HH
18	17	0.953	-0.0652	0.058804	0.953108	
19	18	0.823	-0.9903	-0.41955	0.674811	
20	19	0.942	0.113051	0.155429	0.876482	
21	20	1.419	-4.24376	-2.34304	0.019127	HL
22	21	0.717	3.853343	2.315584	0.02058	LL
23	22	0.808	-0.58251	-0.56405	0.572721	
24	23	1.417	-0.18109	-0.00401	0.996799	

1997						
OBJECTID	SOURCE_ID	y1997	LMiIndex	LMiZScore	LMiPValue	COType
1	0	0.744	-0.73775	-0.53181	0.594858	
2	1	0.737	0.534647	0.483399	0.628812	
3	2	1.06	0.721952	0.825604	0.409028	
4	3	0.904	-0.00221	0.112419	0.910491	
5	4	1.129	0.343278	0.304143	0.761018	
6	5	1.142	0.952121	0.701422	0.483039	
7	6	0.625	-3.86589	-2.17043	0.029974	LH
8	7	1.27	-0.15552	-0.12086	0.903805	
9	8	1.021	-0.27147	-0.0417	0.966736	
10	9	0.815	0.485096	0.570128	0.56859	

11	10	0.969	-0.62356	-0.4739	0.635574
12	11	0.833	-0.55579	-0.15888	0.873766
13	12	0.637	0.485096	0.570128	0.56859
14	13	1.012	0.116825	0.205658	0.837057
15	14	0.847	0.698938	0.537377	0.591006
16	15	0.947	0.168971	0.207043	0.835975
17	16	1.022	-0.10368	-0.01312	0.989533
18	17	0.257	-0.56177	-0.23658	0.812984
19	18	0.97	-0.78168	-0.31499	0.75277
20	19	1.258	-0.08982	-0.00592	0.995278
21	20	0.837	-0.41211	-0.14346	0.885925
22	21	1.023	-0.26296	-0.05562	0.955642
23	22	0.747	0.535644	0.62465	0.5322
24	23	0.883	0.114993	0.165565	0.868498

1998

OBJECTID	SOURCE_ID	y1998	LMiIndex	LMiZScore	LMiPValue	COType
1	0	1.212	0.268608	0.282486	0.77757	
2	1	1.518	0.475185	0.432141	0.665638	
3	2	0.778	-0.12769	-0.08973	0.9285	
4	3	1.011	-0.0052	0.109764	0.912596	
5	4	1.125	-0.23558	-0.04084	0.967424	
6	5	0.891	0.710696	0.539128	0.589798	
7	6	0.656	0.739693	0.528544	0.597121	
8	7	0.75	-2.91122	-3.05567	0.002245	LH
9	8	1.242	-0.18469	0.007916	0.993683	
10	9	0.911	-0.39681	-0.37649	0.706556	
11	10	1.155	-0.38712	-0.26558	0.790565	
12	11	0.899	-0.33008	-0.0423	0.966259	
13	12	1.281	-0.39681	-0.37649	0.706556	
14	13	1.31	-1.40588	-1.84104	0.065616	
15	14	1.123	0.092309	0.142769	0.886472	
16	15	1.137	-0.13286	0.039641	0.968379	
17	16	1.14	0.160041	0.19005	0.849269	
18	17	1.283	0.296983	0.274053	0.784043	
19	18	0.397	-9.67124	-5.13933	2.76E-07	LH
20	19	1.041	0.332878	0.335794	0.737025	
21	20	0.937	-0.04638	0.071436	0.94305	
22	21	1.264	-1.79482	-0.9503	0.341958	
23	22	1.264	0.866477	0.969586	0.332252	
24	23	1.828	-6.9058	-3.81934	0.000133	HL

1999						
OBJECTID	SOURCE_ID	y1999	LMiIndex	LMiZScore	LMiPValue	COType
1	0	0.708	-0.29462	-0.16531	0.868698	
2	1	1.547	0.533911	0.464572	0.642237	
3	2	1.138	0.027515	0.073521	0.94139	
4	3	1.066	0.26358	0.250037	0.802558	
5	4	1.064	-0.00704	0.091959	0.926729	
6	5	1.323	2.146116	1.422601	0.154851	
7	6	0.925	-1.5417	-0.77903	0.435961	
8	7	1.475	-3.3029	-3.37547	0.000736	HL
9	8	1.135	-0.56928	-0.20577	0.836972	
10	9	1.017	0.099218	0.147777	0.882518	
11	10	1.093	-0.2342	-0.13077	0.895956	
12	11	0.942	-0.66324	-0.20832	0.834979	
13	12	0.764	0.099218	0.147777	0.882518	
14	13	0.928	-0.04893	-0.01882	0.984988	
15	14	0.824	2.943956	1.921166	0.05471	
16	15	1.239	-0.57041	-0.19598	0.844623	
17	16	1.023	0.066454	0.114862	0.908554	
18	17	0.581	4.410971	2.645609	0.008154	LL
19	18	1.082	-0.68697	-0.25506	0.798678	
20	19	1.309	0.635611	0.565011	0.572066	
21	20	0.811	-0.62853	-0.26208	0.793261	
22	21	1.453	0.492219	0.377253	0.705985	
23	22	1.097	0.374199	0.432549	0.665342	
24	23	0.486	1.602717	0.98445	0.324893	

2000						
OBJECTID	SOURCE_ID	y2000	LMiIndex	LMiZScore	LMiPValue	COType
1	0	0.727	0.117236	0.154078	0.877547	
2	1	0.633	-0.80736	-0.53026	0.595931	
3	2	1.009	-0.769	-0.73846	0.460232	
4	3	1.25	2.137334	1.227871	0.219495	
5	4	0.479	-3.68695	-2.00178	0.045308	LH
6	5	1.11	0.821927	0.585972	0.557894	
7	6	1.03	1.835898	1.122207	0.261774	
8	7	1.222	-2.28084	-2.27726	0.02277	HL
9	8	0.666	-1.16423	-0.52898	0.596817	
10	9	0.599	1.084372	1.147964	0.250983	

11	10	1.164	-2.38968	-1.8995	0.057498
12	11	1.205	1.004755	0.619459	0.535613
13	12	0.394	1.084372	1.147964	0.250983
14	13	0.877	-0.09775	-0.0811	0.935361
15	14	0.634	2.485351	1.609448	0.107518
16	15	1.054	1.293855	0.79364	0.427404
17	16	0.842	-0.073	0.010197	0.991863
18	17	0.309	3.260434	1.95209	0.050927
19	18	0.645	1.579541	0.936649	0.348939
20	19	1.059	1.396286	1.144462	0.252431
21	20	0.988	0.319253	0.274197	0.783932
22	21	0.596	-3.33525	-1.78141	0.074846
23	22	0.755	0.132514	0.179131	0.857834
24	23	0.341	2.55529	1.490574	0.136073

2001

OBJECTID	SOURCE_ID	y2001	LMiIndex	LMiZScore	LMiPValue	COType
1	0	0.702	0.063225	0.121351	0.903412	
2	1	0.673	-0.00684	0.063582	0.949302	
3	2	0.427	0.635763	0.748572	0.454115	
4	3	0.827	0.578853	0.437428	0.6618	
5	4	0.51	1.28732	0.882871	0.377305	
6	5	1.557	4.417777	3.00348	0.002669	HH
7	6	0.924	3.562374	2.230239	0.025731	HH
8	7	0.344	0.390498	0.478272	0.632456	
9	8	1.026	-0.538	-0.19747	0.843462	
10	9	0.903	0.774059	0.900983	0.367596	
11	10	0.623	0.450149	0.467532	0.640118	
12	11	0.797	-0.09631	0.078857	0.937146	
13	12	0.961	0.774059	0.900983	0.367596	
14	13	0.461	0.656548	0.959545	0.337283	
15	14	0.493	1.709146	1.214794	0.224444	
16	15	0.681	0.001646	0.116302	0.907413	
17	16	0.779	0.413903	0.397955	0.690663	
18	17	0.397	2.380266	1.549394	0.121286	
19	18	0.421	2.964104	1.766151	0.07737	
20	19	0.837	2.12389	1.841117	0.065604	
21	20	0.341	-1.0023	-0.50015	0.616969	
22	21	0.689	-0.01933	0.08976	0.928477	
23	22	0.583	0.024548	0.07497	0.940238	
24	23	0.606	1.247187	0.828858	0.407184	

2002

OBJECTID	SOURCE_ID	y2002	LMiIndex	LMiZScore	LMiPValue	COType
1	0	0.804	0.012493	0.07627	0.939203	
2	1	1.038	0.154256	0.184142	0.853901	
3	2	0.708	0.096645	0.148211	0.882175	
4	3	0.673	-0.40541	-0.10667	0.915048	
5	4	0.765	0.233248	0.234669	0.814465	
6	5	0.632	-0.55577	-0.27085	0.78651	
7	6	0.865	-0.27134	-0.05882	0.953095	
8	7	0.617	0.406661	0.47612	0.633988	
9	8	0.759	0.227802	0.240602	0.809863	
10	9	1.066	1.279634	1.399479	0.161669	
11	10	0.32	0.537458	0.524113	0.600199	
12	11	0.66	0.837858	0.551373	0.581377	
13	12	1.047	1.279634	1.399479	0.161669	
14	13	0.764	0.242997	0.369815	0.711519	
15	14	1.349	-1.21464	-0.6904	0.489943	
16	15	0.847	-0.32197	-0.0637	0.949208	
17	16	0.757	0.06339	0.114843	0.908568	
18	17	1.119	-1.81324	-0.96898	0.332555	
19	18	0.494	-1.58777	-0.74564	0.455883	
20	19	0.929	-0.32241	-0.19249	0.847354	
21	20	0.753	0.243555	0.239204	0.810947	
22	21	0.784	0.215037	0.22292	0.823597	
23	22	0.979	0.812752	0.90565	0.36512	
24	23	0.71	-0.7148	-0.30501	0.760358	

2003

OBJECTID	SOURCE_ID	y2003	LMiIndex	LMiZScore	LMiPValue	COType
1	0	0.841	-0.87321	-0.61575	0.538059	
2	1	0.829	0.029955	0.08722	0.930496	
3	2	0.822	0.251525	0.304549	0.760708	
4	3	0.835	0.87339	0.572254	0.567149	
5	4	0.787	1.442008	0.925491	0.35471	
6	5	0.842	-0.21805	-0.0546	0.95646	
7	6	0.999	-0.30613	-0.07734	0.938349	
8	7	0.803	0.640453	0.706064	0.480148	
9	8	1.191	-1.45467	-0.69564	0.486651	
10	9	1.163	2.625609	2.75546	0.00586	HH

11	10	0.968	0.444641	0.434892	0.66364	
12	11	0.655	0.707068	0.476865	0.633457	
13	12	1.218	2.625609	2.75546	0.00586	HH
14	13	0.825	-0.36555	-0.43059	0.666768	
15	14	0.521	0.139799	0.168394	0.866273	
16	15	0.661	0.46909	0.360895	0.718177	
17	16	1.139	1.767822	1.385592	0.165871	
18	17	0.898	-0.01311	0.088174	0.929738	
19	18	1.106	-3.75845	-1.88252	0.059764	
20	19	0.983	0.098743	0.142224	0.886902	
21	20	0.979	-0.82736	-0.37444	0.708078	
22	21	0.838	0.432344	0.342181	0.732214	
23	22	0.944	-0.09827	-0.05656	0.954895	
24	23	0.674	1.769007	1.073781	0.28292	

2004

OBJECTID	SOURCE_ID	y2004	LMiIndex	LMiZScore	LMiPValue	COType
1	0	1.017	-0.00889	0.058204	0.953585	
2	1	1.056	0.069657	0.117515	0.906451	
3	2	0.784	0.415559	0.476782	0.633516	
4	3	0.934	0.79797	0.534818	0.592775	
5	4	0.937	0.639155	0.465893	0.641291	
6	5	1.191	-2.75717	-1.64575	0.099816	
7	6	0.698	1.781965	1.110658	0.266715	
8	7	0.891	0.10953	0.158923	0.873728	
9	8	0.971	0.345858	0.302981	0.761904	
10	9	1.306	3.248113	3.418835	0.000628	HH
11	10	0.955	-0.11961	-0.03517	0.971947	
12	11	0.9	0.759645	0.505265	0.613372	
13	12	1.504	3.248113	3.418835	0.000628	HH
14	13	1.153	-0.56572	-0.69516	0.486958	
15	14	1.28	0.651521	0.489924	0.624187	
16	15	1.056	-0.34428	-0.07482	0.940355	
17	16	0.804	0.207062	0.220837	0.825218	
18	17	1.388	-0.42546	-0.15031	0.880521	
19	18	0.789	-3.36523	-1.68193	0.092582	
20	19	0.722	0.738446	0.647719	0.517166	
21	20	0.946	0.306093	0.271356	0.786116	
22	21	0.94	0.565547	0.420134	0.674387	
23	22	1.172	0.145228	0.196001	0.844608	
24	23	0.977	-0.25184	-0.04329	0.965471	

2005						
OBJECTID	SOURCE_ID	y2005	LMiIndex	LMiZScore	LMiPValue	COType
1	0	1.108	-0.05626	0.021375	0.982946	
2	1	1.118	0.053967	0.107271	0.914573	
3	2	1.297	0.546151	0.621764	0.534096	
4	3	1.181	-0.2437	-0.01942	0.984505	
5	4	1.342	-0.39584	-0.13435	0.893128	
6	5	1.065	0.419687	0.349356	0.726821	
7	6	1.269	-0.93183	-0.43933	0.66042	
8	7	1.255	-0.07881	-0.03725	0.970284	
9	8	1.264	-0.72471	-0.29612	0.767139	
10	9	0.637	3.596171	3.838005	0.000124	LL
11	10	1.072	-0.92306	-0.71833	0.472555	
12	11	1.039	0.470957	0.364179	0.715723	
13	12	0.835	3.596171	3.838005	0.000124	LL
14	13	1.453	2.205592	2.976158	0.002918	HH
15	14	1.533	3.972506	2.605579	0.009171	HH
16	15	0.991	-0.72333	-0.2819	0.778017	
17	16	1.114	-0.05233	0.026298	0.979019	
18	17	1.251	1.404923	0.921817	0.356623	
19	18	1.599	5.472478	3.059757	0.002215	HH
20	19	1.167	0.001291	0.067124	0.946482	
21	20	1.184	-0.00482	0.094874	0.924414	
22	21	0.827	0.524702	0.401781	0.687844	
23	22	1.072	0.073608	0.123468	0.901736	
24	23	1.12	-0.81751	-0.36202	0.717337	

2006						
OBJECTID	SOURCE_ID	y2006	LMiIndex	LMiZScore	LMiPValue	COType
1	0	1	1.187357	0.998614	0.317981	
2	1	1.006	-0.32886	-0.182	0.855579	
3	2	1.728	-0.49176	-0.46695	0.640538	
4	3	1.21	-0.11278	0.050544	0.959688	
5	4	1.107	-1.26758	-0.63832	0.523262	
6	5	1.04	1.659264	1.124177	0.260937	
7	6	1.085	1.029664	0.684126	0.493895	
8	7	1.243	0.048522	0.09583	0.923655	
9	8	0.825	-2.21372	-1.12371	0.261135	
10	9	0.948	-0.13573	-0.09609	0.923451	

11	10	1.579	1.280601	1.140645	0.254017
12	11	1.318	0.287826	0.269035	0.787902
13	12	1.214	-0.13573	-0.09609	0.923451
14	13	1.116	-0.18951	-0.20342	0.838807
15	14	1.021	-0.55228	-0.26498	0.791025
16	15	1.387	1.082997	0.694242	0.48753
17	16	0.985	1.328944	1.066722	0.286097
18	17	1.072	-0.75241	-0.34057	0.733428
19	18	1.486	0.670578	0.468345	0.639537
20	19	0.649	1.50368	1.25482	0.209543
21	20	1.711	-0.02287	0.083573	0.933395
22	21	0.863	0.161459	0.189376	0.849797
23	22	1.274	-0.23772	-0.20233	0.83966
24	23	1.218	0.0941	0.149227	0.881373

2007

OBJECTID	SOURCE_ID	y2007	LMiIndex	LMiZScore	LMiPValue	COType
1	0	0.746	-0.23893	-0.12098	0.903705	
2	1	0.696	0.606056	0.51516	0.60644	
3	2	1.48	1.508718	1.596381	0.110403	
4	3	1.179	-1.05055	-0.44494	0.656361	
5	4	1.262	1.658655	1.046836	0.295175	
6	5	1.026	0.005422	0.084372	0.93276	
7	6	1.116	0.160827	0.18648	0.852067	
8	7	0.909	0.283636	0.336426	0.736549	
9	8	1.094	-0.17785	0.011484	0.990836	
10	9	0.641	-0.02115	0.022966	0.981676	
11	10	1.554	2.776022	2.367733	0.017897	HH
12	11	1.205	0.226983	0.236348	0.813161	
13	12	1.025	-0.02115	0.022966	0.981676	
14	13	0.753	-1.53946	-1.9501	0.051164	
15	14	0.864	-0.39626	-0.16509	0.868876	
16	15	0.76	-2.76291	-1.3651	0.17222	
17	16	1.018	0.008032	0.070619	0.9437	
18	17	0.861	-1.36244	-0.68755	0.491738	
19	18	1.552	-1.45107	-0.65755	0.510828	
20	19	1.242	0.273034	0.277934	0.781062	
21	20	1.175	0.480355	0.367897	0.712949	
22	21	0.783	-1.36952	-0.68143	0.4956	
23	22	0.726	1.306233	1.388132	0.165096	
24	23	0.835	-0.25935	-0.04707	0.962458	

Appendix D: Eigenvector analysis data tables

NAME	ST_ID	LAT (DD)	LON (DD)	ELEV (M)
Cote	4011846	51.52	-101.78	450
Estevan	4012400	49.22	-102.97	581
Hudson Bay	4083324	52.82	-102.32	358
Indian Head	4013480	50.55	-103.65	579
Kelliher	4013660	51.25	-103.75	676
Kindersley	4043900	51.52	-109.18	694
Moose Jaw	4015322	50.33	-105.55	577
Pelly	4086000	52.08	-101.87	509
Pilger	4056120	52.42	-105.15	552
Prince Albert	4056240	53.22	-105.67	428
Regina	4016560	50.43	-104.67	577
Saskatoon	4057120	52.17	-106.72	504
Scott	4047241	52.37	-108.83	660
Waseca	4048520	53.13	-109.40	638
Yellow Grass	4019040	49.82	-104.18	580

P_JAN_AVG	P_FEB_AVG	P_MAR_AVG	P_APR_AVG	P_MAY_AVG
25.02	17.49	24.58	22.47	44.22
30.85	23.22	29.58	36.34	60.97
24.68	20.88	30.00	31.13	45.08
28.19	21.11	29.09	29.10	55.54
27.84	20.11	31.43	32.07	54.16
22.77	15.98	21.64	27.35	38.63
21.79	16.35	21.43	27.58	53.38
30.18	24.71	38.45	33.25	49.46
26.98	21.27	27.59	30.77	44.87
25.81	20.49	25.34	30.88	44.74
27.33	21.23	28.38	28.55	54.66
26.03	20.86	24.10	27.63	45.67
20.43	14.16	18.31	23.97	35.73
25.86	15.77	26.81	29.69	41.37
22.99	16.72	23.96	32.11	57.64

P_JUN_AVG	P_JUL_AVG	P_AUG_AVG	P_SEP_AVG	P_OCT_AVG
79.93	68.99	64.18	47.48	26.14
82.00	67.98	54.37	41.97	28.15
78.36	86.44	66.01	54.81	31.99
80.39	64.59	57.54	41.54	27.38
81.03	70.51	65.48	44.50	30.72
66.32	59.68	42.34	32.26	17.17
80.92	67.19	49.70	40.47	21.07
85.90	89.87	64.65	55.06	31.11
73.10	71.50	58.09	44.51	26.14
73.49	76.83	61.79	43.71	28.84
80.34	66.37	48.63	37.98	25.67
65.86	61.91	44.29	36.01	22.07
68.94	67.29	48.90	33.55	16.28
79.75	81.69	68.60	39.78	22.90
80.27	67.97	47.69	44.89	24.57

P_NOV_AVG	P_DEC_AVG	T_JAN_AVG	T_FEB_AVG	T_MAR_AVG
22.96	28.43	-19.81	-15.38	-8.57
25.16	28.82	-15.76	-11.81	-5.36
26.96	30.01	-19.69	-15.15	-8.53
23.19	32.21	-17.65	-13.84	-7.70
21.63	29.47	-17.83	-13.84	-7.68
18.17	24.78	-15.53	-11.60	-5.70
18.70	21.38	-14.46	-10.37	-4.67
30.95	31.66	-19.62	-15.38	-9.48
19.36	25.03	-19.39	-14.76	-8.47
23.84	29.50	-16.26	-12.35	-6.20
20.78	27.68	-18.68	-14.23	-8.05
21.16	27.39	-17.41	-13.39	-7.49
17.17	19.46	-12.84	-9.09	-4.15
21.54	24.83	-17.22	-12.72	-7.04
18.56	22.06	-15.90	-11.92	-5.86

T_APR_AVG	T_MAY_AVG	T_JUN_AVG	T_JUL_AVG	T_AUG_AVG
2.80	10.67	15.52	18.05	16.85
4.37	11.31	16.19	19.18	18.26
1.92	9.51	14.65	17.31	15.88
2.52	9.91	14.60	17.16	16.34
2.70	10.17	14.99	17.59	16.66
4.10	11.04	15.47	18.20	17.46
4.60	11.52	16.50	19.33	18.49
1.09	9.04	13.90	16.70	15.43
2.68	10.27	15.03	17.66	16.41
4.07	11.29	16.13	18.95	18.13
2.79	10.83	15.38	17.84	16.98
3.24	10.35	14.71	17.16	16.30
4.31	10.71	15.28	18.32	17.80
3.23	10.49	14.55	16.97	15.95
4.13	11.25	16.23	18.95	18.12

T_SEP_AVG	T_OCT_AVG	T_NOV_AVG	T_DEC_AVG	T_JAN_PCA
10.86	4.08	-6.67	-15.35	0.21
12.26	5.74	-4.08	-11.89	0.24
9.94	3.43	-7.09	-15.81	0.24
10.62	3.74	-6.02	-13.79	0.24
10.64	3.94	-6.00	-13.90	0.25
11.53	4.89	-4.95	-11.82	0.27
12.47	5.89	-3.67	-10.56	0.28
9.55	3.10	-7.28	-15.76	0.24
10.44	3.72	-6.84	-15.33	0.26
11.94	5.07	-4.83	-12.35	0.26
11.08	4.16	-6.49	-14.59	0.26
10.48	3.85	-6.24	-13.65	0.27
11.93	5.62	-3.45	-9.44	0.28
10.41	4.04	-6.25	-13.55	0.28
12.02	5.24	-4.55	-11.99	0.27

T_FEB_PCA	T_MAR_PCA	T_APR_PCA	T_MAY_PCA	T_JUN_PCA
0.24	0.24	0.28	0.28	0.26
0.28	0.28	0.24	0.26	0.27
0.24	0.23	0.26	0.27	0.24
0.27	0.28	0.26	0.27	0.28
0.26	0.25	0.28	0.28	0.27
0.26	0.27	0.25	0.23	0.23
0.27	0.27	0.25	0.26	0.29
0.23	0.24	0.24	0.26	0.23
0.25	0.25	0.27	0.26	0.25
0.26	0.28	0.26	0.27	0.29
0.25	0.25	0.29	0.27	0.25
0.25	0.26	0.25	0.21	0.24
0.27	0.26	0.24	0.24	0.25
0.25	0.24	0.24	0.21	0.21
0.28	0.27	0.26	0.26	0.28

T_JUL_PCA	T_AUG_PCA	T_SEP_PCA	T_OCT_PCA	T_NOV_PCA
0.26	0.25	0.23	0.27	0.25
0.28	0.24	0.24	0.24	0.26
0.24	0.24	0.21	0.25	0.24
0.26	0.25	0.26	0.27	0.26
0.28	0.26	0.27	0.27	0.26
0.25	0.27	0.28	0.25	0.27
0.29	0.27	0.27	0.27	0.26
0.24	0.23	0.24	0.27	0.23
0.23	0.24	0.25	0.25	0.26
0.28	0.26	0.26	0.25	0.26
0.24	0.27	0.25	0.26	0.26
0.23	0.27	0.27	0.26	0.28
0.26	0.28	0.31	0.28	0.26
0.21	0.27	0.26	0.25	0.27
0.29	0.26	0.26	0.24	0.26

T_DEC_PCA	P_JAN_PCA	P_FEB_PCA	P_MAR_PCA	P_APR_PCA
0.26	0.24	0.16	0.27	0.12
0.25	0.26	0.25	0.18	0.24
0.25	0.21	0.18	0.31	0.21
0.25	0.27	0.33	0.31	0.28
0.25	0.28	0.25	0.32	0.31
0.26	0.25	0.23	0.16	0.16
0.26	0.19	0.18	0.14	0.24
0.25	0.22	0.30	0.47	0.20
0.27	0.25	0.36	0.31	0.41
0.25	0.18	0.25	0.18	0.25
0.26	0.26	0.22	0.23	0.25
0.26	0.27	0.27	0.21	0.26
0.26	0.24	0.20	0.12	0.17
0.28	0.28	0.17	0.19	0.20
0.26	0.28	0.23	0.18	0.31

P_MAY_PCA	P_JUN_PCA	P_JUL_PCA	P_AUG_PCA	P_SEP_PCA
0.18	0.27	0.32	0.21	0.23
0.31	0.27	0.27	0.17	0.28
0.18	0.23	0.21	0.28	0.25
0.30	0.32	0.25	0.29	0.31
0.28	0.30	0.27	0.34	0.31
0.22	0.18	0.18	0.15	0.17
0.30	0.28	0.22	0.27	0.29
0.20	0.30	0.39	0.25	0.28
0.26	0.27	0.28	0.27	0.20
0.19	0.18	0.24	0.27	0.23
0.30	0.30	0.27	0.24	0.27
0.25	0.17	0.16	0.20	0.21
0.13	0.12	0.20	0.20	0.17
0.18	0.12	0.17	0.25	0.19
0.34	0.29	0.23	0.21	0.31

<u>P_OCT_PCA</u>	<u>P_NOV_PCA</u>	<u>P_DEC_PCA</u>
0.15	0.29	0.20
0.21	0.32	0.25
0.28	0.25	0.12
0.30	0.27	0.37
0.31	0.29	0.31
0.15	0.19	0.29
0.26	0.25	0.21
0.22	0.35	0.20
0.31	0.20	0.22
0.31	0.20	0.13
0.30	0.26	0.30
0.26	0.23	0.22
0.14	0.16	0.19
0.14	0.24	0.20
0.25	0.22	0.18

Appendix E: Tree-Ring Annual Growth Estimator (TRiAGE) Program

“#” and grey text indicate comments explaining the program. This program can also be found at <http://www.mta.ca/madlab/GHG/Model/program-send.php/>.

```
<?php
    error_reporting(E_ALL);
    ini_set('display_errors','1');
#####
#           CGCM Future Radial Tree-ring Growth Modeller       v1.03d   #
#                                     By Jobs and Cee-Doc          #
#####

#### REFERENCE #####
# GCM 0 = A1B
# GCM 1 = A2
# GCM 2 = B1
# TREEn in alphabetical order (caragana at end)
# LOC0 = NW
# LOC1 = NE
# LOC2 = SW
# LOC3 = SE (not implemented)
#####

##### Functions #####

### FUTURE GROWTH - NOT USED###

function displayFuture($a,$im){
    #define the image type
    header('Content-Type: image/png');
    #define the line color when "drawing"
    $line_color = imagecolorallocate($im, 0, 0, 0);
    #primary hard-coded variables used to start future growth
    #model for x,y
    $x1 = 590;
    $y1 = 275;

    #forloop for arrays key = index, value is STD ring width
    foreach($a as $key=>$value) {
        #creates second value associated with creating the
        #line before drawing it
        $x2 = ($key*5)+590;
        $y2 = 525-($value*275);
        #draws line using 4 coords, the image, and line color
        imageline($im, $x1, $y1, $x2, $y2, $line_color);
        #following 2 lines replace original $x1, $y1 with
        #current $x2,$y2 values... forloop continues until n=N
        $x1 = ($key*5)+590;
        $y1 = 525-($value*275);
    }
}
```

```

# Each tree has its own function due to the differing input requires for each
#tree species and thus all have the same hardcoded inputs for each of the 9
#tree species. The only difference is the hardcoded integers and called
#parameters.
### TREE 0 - ACCUTE WILLOW ###
  #function name for acute willow
  function displayTree0($a,$im) {

    #define image type
    header('Content-Type: image/png');
    #define line color, in this case blue. Different for each
    #species
    $line_color = imagecolorallocate($im, 0, 0, 255);

    #define hardcoded primary x,y variables with xn,yn which
    #make the line 2px thick
    $x1 = 315;
    $y1 = 275;
    $x1n = 315+1;
    $y1n = 275+1;
    #call array text file from folder for prior growth
    $a_willow = array_map ('trim', file('a_willow.txt'));

    #forloop for measured acute willow growth
    foreach($a_willow as $key=>$value) {

      #creates second value associated with creating the
      #line before drawing it
      $x2 = ($key*5)+315;
      $y2 = 525-($value*275);
      $x2n = ($key*5)+315+1;
      $y2n = 525-($value*275)+1;

      #draws line using 4 coords, the image, and line color
      imageline($im, $x1, $y1, $x2, $y2, $line_color);
      imageline($im, $x1n, $y1n, $x2n, $y2n, $line_color);

      #following 2 lines replace original $x1, $y1 with
      #current $x2,$y2 values... forloop continues until n=N
      $x1 = ($key*5)+315;
      $y1 = 525-($value*275);
      $x1n = ($key*5)+315+1;
      $y1n = 525-($value*275)+1;
    }

    #forloop for projected acute willow growth under different
    #GCMs.
    foreach($a as $key=>$value) {

      #creates second value associated with creating the
      #line before drawing it
      $x2 = ($key*5)+590;
      $y2 = 525-($value*275);
      $x2n = ($key*5)+590+1;
      $y2n = 525-($value*275)+1;
    }
  }

```

```

        #draws line using 4 coords, the image, and line color
        imageline($im, $x1, $y1, $x2, $y2, $line_color);
        imageline($im, $x1n, $y1n, $x2n, $y2n, $line_color);

        #following 2 lines replace original $x1, $y1 with
        #current $x2,$y2 values... forloop continues until n=N
        $x1 = ($key*5)+590;
        $y1 = 525-($value*275);
        $x1n = ($key*5)+590+1;
        $y1n = 525-($value*275)+1;
    }
}

### TREE 1 - COLORADO SPRUCE###

function displayTree1($a,$im) {

    header('Content-Type: image/png');
    $line_color = imagecolorallocate($im, 255, 0, 0);

    $x1 = 305;
    $y1 = 275;
    $x1n = 305+1;
    $y1n = 275+1;
    $c_spruce = array_map ('trim', file('c_spruce.txt'));

    foreach($c_spruce as $key=>$value) {

        $x2 = ($key*5)+305;
        $y2 = 525-($value*275);
        $x2n = ($key*5)+305+1;
        $y2n = 525-($value*275)+1;

        imageline($im, $x1, $y1, $x2, $y2, $line_color);
        imageline($im, $x1n, $y1n, $x2n, $y2n, $line_color);

        $x1 = ($key*5)+305;
        $y1 = 525-($value*275);
        $x1n = ($key*5)+305+1;
        $y1n = 525-($value*275)+1;
    }

    foreach($a as $key=>$value) {

        $x2 = ($key*5)+590;
        $y2 = 525-($value*275);
        $x2n = ($key*5)+590+1;
        $y2n = 525-($value*275)+1;

        imageline($im, $x1, $y1, $x2, $y2, $line_color);
        imageline($im, $x1n, $y1n, $x2n, $y2n, $line_color);

        $x1 = ($key*5)+590;
        $y1 = 525-($value*275);
        $x1n = ($key*5)+590+1;
        $y1n = 525-($value*275)+1;
    }
}

```

```

    }

#### TREE2 - GREEN ASH ####

function displayTree2($a,$im) {

    header('Content-Type: image/png');
    $line_color = imagecolorallocate($im, 57, 181, 74);

    $x1 = 115;
    $y1 = 275;
    $x1n = 115+1;
    $y1n = 275+1;
    $g_ash = array_map ('trim', file('g_ash.txt'));

    foreach($g_ash as $key=>$value) {

        $x2 = ($key*5)+115;
        $y2 = 525-($value*275);
        $x2n = ($key*5)+115+1;
        $y2n = 525-($value*275)+1;

        imageline($im, $x1, $y1, $x2, $y2, $line_color);
        imageline($im, $x1n, $y1n, $x2n, $y2n, $line_color);

        $x1 = ($key*5)+115;
        $y1 = 525-($value*275);
        $x1n = ($key*5)+115+1;
        $y1n = 525-($value*275)+1;

    }

    foreach($a as $key=>$value) {

        $x2 = ($key*5)+590;
        $y2 = 525-($value*275);
        $x2n = ($key*5)+590+1;
        $y2n = 525-($value*275)+1;

        imageline($im, $x1, $y1, $x2, $y2, $line_color);
        imageline($im, $x1n, $y1n, $x2n, $y2n, $line_color);

        $x1 = ($key*5)+590;
        $y1 = 525-($value*275);
        $x1n = ($key*5)+590+1;
        $y1n = 525-($value*275)+1;

    }

}

```

```

#### TREE 3 - HYBRID POPLAR ####

```

```

function displayTree3($a,$im) {

```

```

header('Content-Type: image/png');
$line_color = imagecolorallocate($im, 99, 4, 96);

$x1 = 105;
$y1 = 275;
$x1n = 105+1;
$y1n = 275+1;
$h_poplar = array_map ('trim', file('h_poplar.txt'));

foreach($h_poplar as $key=>$value) {

    $x2 = ($key*5)+105;
    $y2 = 525-($value*275);
    $x2n = ($key*5)+105+1;
    $y2n = 525-($value*275)+1;

    imageline($im, $x1, $y1, $x2, $y2, $line_color);
    imageline($im, $x1n, $y1n, $x2n, $y2n, $line_color);

    $x1 = ($key*5)+105;
    $y1 = 525-($value*275);
    $x1n = ($key*5)+105+1;
    $y1n = 525-($value*275)+1;
}

foreach($a as $key=>$value) {

    $x2 = ($key*5)+590;
    $y2 = 525-($value*275);
    $x2n = ($key*5)+590+1;
    $y2n = 525-($value*275)+1;

    imageline($im, $x1, $y1, $x2, $y2, $line_color);
    imageline($im, $x1n, $y1n, $x2n, $y2n, $line_color);

    $x1 = ($key*5)+590;
    $y1 = 525-($value*275);
    $x1n = ($key*5)+590+1;
    $y1n = 525-($value*275)+1;
}
}

```

```

### TREE 4 - MANITOBA MAPLE ###

```

```

function displayTree4($a,$im) {

    header('Content-Type: image/png');
    $line_color = imagecolorallocate($im, 0, 0, 0);

```

```

$x1 = 310;
$y1 = 275;
$x1n = 310+1;
$y1n = 275+1;
$m_maple = array_map ('trim', file('m_maple.txt'));

foreach($m_maple as $key=>$value) {

    $x2 = ($key*5)+310;
    $y2 = 525-($value*275);
    $x2n = ($key*5)+310+1;
    $y2n = 525-($value*275)+1;

    imageline($im, $x1, $y1, $x2, $y2, $line_color);
    imageline($im, $x1n, $y1n, $x2n, $y2n, $line_color);

    $x1 = ($key*5)+310;
    $y1 = 525-($value*275);
    $x1n = ($key*5)+310+1;
    $y1n = 525-($value*275)+1;
}

foreach($a as $key=>$value) {

    $x2 = ($key*5)+590;
    $y2 = 525-($value*275);
    $x2n = ($key*5)+590+1;
    $y2n = 525-($value*275)+1;

    imageline($im, $x1, $y1, $x2, $y2, $line_color);
    imageline($im, $x1n, $y1n, $x2n, $y2n, $line_color);

    $x1 = ($key*5)+590;
    $y1 = 525-($value*275);
    $x1n = ($key*5)+590+1;
    $y1n = 525-($value*275)+1;
}

}

```

```

### TREE 5 - SCOTS PINE ###

```

```

function displayTree5($a,$im) {

    header('Content-Type: image/png');
    $line_color = imagecolorallocate($im, 117, 76, 36);

    $x1 = 175;
    $y1 = 275;
    $x1n = 175+1;
    $y1n = 275+1;
}

```

```

$s_pine = array_map ('trim', file('s_pine.txt'));

foreach($s_pine as $key=>$value) {

    $x2 = ($key*5)+175;
    $y2 = 525-($value*275);
    $x2n = ($key*5)+175+1;
    $y2n = 525-($value*275)+1;

    imageline($im, $x1, $y1, $x2, $y2, $line_color);
    imageline($im, $x1n, $y1n, $x2n, $y2n, $line_color);

    $x1 = ($key*5)+175;
    $y1 = 525-($value*275);
    $x1n = ($key*5)+175+1;
    $y1n = 525-($value*275)+1;
}

foreach($a as $key=>$value) {

    $x2 = ($key*5)+590;
    $y2 = 525-($value*275);
    $x2n = ($key*5)+590+1;
    $y2n = 525-($value*275)+1;

    imageline($im, $x1, $y1, $x2, $y2, $line_color);
    imageline($im, $x1n, $y1n, $x2n, $y2n, $line_color);

    $x1 = ($key*5)+590;
    $y1 = 525-($value*275);
    $x1n = ($key*5)+590+1;
    $y1n = 525-($value*275)+1;
}

}

```

TREE 6 - SIBERIAN ELM

```

function displayTree6($a,$im) {

    header('Content-Type: image/png');
    $line_color = imagecolorallocate($im, 0, 118, 163);

    $x1 = 320;
    $y1 = 275;
    $x1n = 305+1;
    $y1n = 275+1;

    $s_elm = array_map ('trim', file('s_elm.txt'));

    foreach($s_elm as $key=>$value) {

        $x2 = ($key*5)+320;

```

```

        $y2 = 525-($value*275);
        $x2n = ($key*5)+320+1;
        $y2n = 525-($value*275)+1;

        imageline($im, $x1, $y1, $x2, $y2, $line_color);
        imageline($im, $x1n, $y1n, $x2n, $y2n, $line_color);

        $x1 = ($key*5)+320;
        $y1 = 525-($value*275);
        $x1n = ($key*5)+320+1;
        $y1n = 525-($value*275)+1;
    }

}

```

TREE 7 - WHITE SPRUCE

```

function displayTree7($a,$im) {

    header('Content-Type: image/png');
    $line_color = imagecolorallocate($im, 0, 88, 38);

    $x1 = 265;
    $y1 = 275;
    $x1n = 265+1;
    $y1n = 275+1;
    $w_spruce = array_map ('trim', file('w_spruce.txt'));

    foreach($w_spruce as $key=>$value) {

        $x2 = ($key*5)+265;
        $y2 = 525-($value*275);
        $x2n = ($key*5)+265+1;
        $y2n = 525-($value*275)+1;

        imageline($im, $x1, $y1, $x2, $y2, $line_color);
        imageline($im, $x1n, $y1n, $x2n, $y2n, $line_color);

        $x1 = ($key*5)+265;
        $y1 = 525-($value*275);
        $x1n = ($key*5)+265+1;
        $y1n = 525-($value*275)+1;
    }

    foreach($a as $key=>$value) {

        $x2 = ($key*5)+590;
        $y2 = 525-($value*275);
        $x2n = ($key*5)+590+1;
        $y2n = 525-($value*275)+1;

        imageline($im, $x1, $y1, $x2, $y2, $line_color);
        imageline($im, $x1n, $y1n, $x2n, $y2n, $line_color);
    }
}

```

```

        $x1 = ($key*5)+590;
        $y1 = 525-($value*275);
        $x1n = ($key*5)+590+1;
        $y1n = 525-($value*275)+1;
    }

}

```

```
### TREE 8 - CARAGANA ###
```

```

function displayTree8($a,$im) {

    header('Content-Type: image/png');
    $line_color = imagecolorallocate($im, 242, 101, 34);

    $x1 = 425;
    $y1 = 275;
    $x1n = 425+1;
    $y1n = 275+1;
    foreach($a as $key=>$value) {

        $x2 = ($key*5)+425;
        $y2 = 525-($value*275);
        $x2n = ($key*5)+425+1;
        $y2n = 525-($value*275)+1;

        imageline($im, $x1, $y1, $x2, $y2, $line_color);
        imageline($im, $x1n, $y1n, $x2n, $y2n, $line_color);

        $x1 = ($key*5)+425;
        $y1 = 525-($value*275);
        $x1n = ($key*5)+425+1;
        $y1n = 525-($value*275)+1;
    }

}

```

```
#Attempt to create 3 separate images depending on GCM scenario called
```

```
### WORK IN PROGRESS ###
```

```

function process_data ($values) {

    $gcm = $_GET['gcm'];
    $tree = $_GET['tree'];
    $loc = $_GET['loc'];

    $alb = imagecreatefromPNG('alb-chart.png');
    $a2 = imagecreatefromPNG('a2-chart.png');
    $b1 = imagecreatefromPNG('b1-chart.png');
    $im = imagecreatefromPNG('chart2.png');
}

```

```
##### ARRAYS #####
```

#The following lines are used to extract information from .txt files. The
#information contained in these .txt files are the future radial growth
#projections for each species. To modify the current graphics, weights, or
#variables being called simply replace one of the .txt files with a new one.

```
### TREE ARRAYS ###
```

```
$s_elm = array_map ('trim', file('s_elm.txt'));
$scaragana = array_map ('trim', file('caragana.txt'));
```

```
### A1B SCENARIO ARRAYS ###
```

```
$alb_willow = array_map ('trim', file('alb_willow.txt'));
$alb_cspruce = array_map ('trim', file('alb_cspruce.txt'));
$alb_gash = array_map ('trim', file('alb_gash.txt'));
$alb_hpoplar = array_map ('trim', file('alb_hpoplar.txt'));
$alb_mmaple = array_map ('trim', file('alb_mmaple.txt'));
$alb_spine = array_map ('trim', file('alb_spine.txt'));
$alb_wspruce = array_map ('trim', file('alb_wspruce.txt'));
```

```
### A2 SCENARIO ARRAYS ###
```

```
$a2_willow = array_map ('trim', file('a2_willow.txt'));
$a2_cspruce = array_map ('trim', file('a2_cspruce.txt'));
$a2_gash = array_map ('trim', file('a2_gash.txt'));
$a2_hpoplar = array_map ('trim', file('a2_hpoplar.txt'));
$a2_mmaple = array_map ('trim', file('a2_mmaple.txt'));
$a2_spine = array_map ('trim', file('a2_spine.txt'));
$a2_wspruce = array_map ('trim', file('a2_wspruce.txt'));
```

```
### B1 SCENARIO ARRAYS ###
```

```
$b1_willow = array_map ('trim', file('b1_awillow.txt'));
$b1_cspruce = array_map ('trim', file('b1_cspruce.txt'));
$b1_gash = array_map ('trim', file('b1_gash.txt'));
$b1_hpoplar = array_map ('trim', file('b1_hpoplar.txt'));
$b1_mmaple = array_map ('trim', file('b1_mmaple.txt'));
$b1_spine = array_map ('trim', file('b1_spine.txt'));
$b1_wspruce = array_map ('trim', file('b1_wspruce.txt'));
```

```
### IF STATEMENTS FOR GRAPHING ###
```

```
#primary if statement, $n is the tree species field name e.g., $n  

#could be 'tree0' which is acute willow. This process is repeated  

#for each tree species and examines all the variations starting  

#from tree species then GCM selected and finally the location  

#(not yet implemented).  

foreach ($tree as $m=>$n) {
```

```
### ACCUTE WILLOW ###
```

```
    if($n == 'tree0'){  
        foreach ($gcm as $a=>$b) {  
            if($b == 'gcm0') {  
                foreach( $loc as $y=>$z){
```

```

        if($z == 'loc0'){

displayTree0($a1b_willow,$sim);

        }
    }
    foreach( $loc as $y=>$z){
        if($z == 'loc1'){

displayTree0($a1b_willow,$sim);

        }
    }
    foreach( $loc as $y=>$z){
        if($z == 'loc2'){

displayTree0($a1b_willow,$sim);

        }
    }
}
foreach ($gcm as $a=>$b) {
    if($b == 'gcm1') {

        foreach( $loc as $y=>$z){
            if($z == 'loc0'){
                displayTree0($a2_willow,$sim);
            }
        }
        foreach( $loc as $y=>$z){
            if($z == 'loc1'){
                displayTree0($a2_willow,$sim);
            }
        }
        foreach( $loc as $y=>$z){
            if($z == 'loc2'){
                displayTree0($a2_willow,$sim);
            }
        }
    }
}
foreach ($gcm as $a=>$b) {
    if($b == 'gcm2') {

        foreach( $loc as $y=>$z){
            if($z == 'loc0'){
                displayTree0($b1_willow,$sim);
            }
        }
        foreach( $loc as $y=>$z){
            if($z == 'loc1'){
                displayTree0($b1_willow,$sim);
            }
        }
        foreach( $loc as $y=>$z){
            if($z == 'loc2'){
                displayTree0($b1_willow,$sim);
            }
        }
    }
}

```

```

    }
  }
}
}
}

```

```
### COLORADO SPRUCE ###
```

```

if($n == 'tree1'){
  foreach ($gcm as $a=>$b) {
    if($b == 'gcm0') {
      foreach( $loc as $y=>$z){
        if($z == 'loc0'){
          displayTree1($a1b_cspruce,$sim);
        }
      }
      foreach( $loc as $y=>$z){
        if($z == 'loc1'){
          displayTree1($a1b_cspruce,$sim);
        }
      }
      foreach( $loc as $y=>$z){
        if($z == 'loc2'){
          displayTree1($a1b_cspruce,$sim);
        }
      }
    }
  }
  foreach ($gcm as $a=>$b) {
    if($b == 'gcm1') {
      foreach( $loc as $y=>$z){
        if($z == 'loc0'){
          displayTree1($a2_cspruce,$sim);
        }
      }
      foreach( $loc as $y=>$z){
        if($z == 'loc1'){
          displayTree1($a2_cspruce,$sim);
        }
      }
      foreach( $loc as $y=>$z){
        if($z == 'loc2'){
          displayTree1($a2_cspruce,$sim);
        }
      }
    }
  }
}
}

```

```

    }
  }
  foreach ($gcm as $a=>$b) {
    if($b == 'gcm2') {

      foreach( $loc as $y=>$z){
        if($z == 'loc0'){

displayTree1($b1_cspruce,$sim);

        }
      }
      foreach( $loc as $y=>$z){
        if($z == 'loc1'){

displayTree1($b1_cspruce,$sim);

        }
      }
      foreach( $loc as $y=>$z){
        if($z == 'loc2'){

displayTree1($b1_cspruce,$sim);

        }
      }
    }
  }
}

```

```
### GREEN ASH ###
```

```

if($n == 'tree2') {

  foreach ($gcm as $a=>$b) {
    if($b == 'gcm0') {

      foreach( $loc as $y=>$z){
        if($z == 'loc0'){
          displayTree2($alb_gash,$sim);
        }
      }
      foreach( $loc as $y=>$z){
        if($z == 'loc1'){
          displayTree2($alb_gash,$sim);
        }
      }
      foreach( $loc as $y=>$z){
        if($z == 'loc2'){
          displayTree2($alb_gash,$sim);
        }
      }
    }
  }
  foreach ($gcm as $a=>$b) {
    if($b == 'gcm1') {

```

```

        foreach( $loc as $y=>$z){
            if($z == 'loc0'){
                displayTree2($a2_gash,$sim);
            }
        }
        foreach( $loc as $y=>$z){
            if($z == 'loc1'){
                displayTree2($a2_gash,$sim);
            }
        }
        foreach( $loc as $y=>$z){
            if($z == 'loc2'){
                displayTree2($a2_gash,$sim);
            }
        }
    }
}
foreach ($gcm as $a=>$b) {
    if($b == 'gcm2') {

        foreach( $loc as $y=>$z){
            if($z == 'loc0'){
                displayTree2($b1_gash,$sim);
            }
        }
        foreach( $loc as $y=>$z){
            if($z == 'loc1'){
                displayTree2($b1_gash,$sim);
            }
        }
        foreach( $loc as $y=>$z){
            if($z == 'loc2'){
                displayTree2($b1_gash,$sim);
            }
        }
    }
}
}
}

```

HYBRID POPLAR

```

    if($n == 'tree3'){

        foreach ($gcm as $a=>$b) {
            if($b == 'gcm0') {

                foreach( $loc as $y=>$z){
                    if($z == 'loc0'){

displayTree3($a1b_hpoplar,$sim);

                    }
                }
            }
        }
    }
}

```

```

displayTree3($a1b_hpoplar,$sim);
    }
    }
    foreach( $loc as $y=>$z){
        if($z == 'loc2'){

displayTree3($a1b_hpoplar,$sim);
    }
    }
}
foreach ($gcm as $a=>$b) {
    if($b == 'gcm1') {

        foreach( $loc as $y=>$z){
            if($z == 'loc0'){

displayTree3($a2_hpoplar,$sim);
    }
    }
    foreach( $loc as $y=>$z){
        if($z == 'loc1'){

displayTree3($a2_hpoplar,$sim);
    }
    }
    foreach( $loc as $y=>$z){
        if($z == 'loc2'){

displayTree3($a2_hpoplar,$sim);
    }
    }
}
foreach ($gcm as $a=>$b) {
    if($b == 'gcm2') {

        foreach( $loc as $y=>$z){
            if($z == 'loc0'){

displayTree3($b1_hpoplar,$sim);
    }
    }
    foreach( $loc as $y=>$z){
        if($z == 'loc1'){

displayTree3($b1_hpoplar,$sim);
    }
    }
    foreach( $loc as $y=>$z){
        if($z == 'loc2'){

displayTree3($b1_hpoplar,$sim);
    }
    }
}
}

```

```
    }  
  }  
}  
  
### MANITOBA MAPLE ###
```

```
  if($n == 'tree4'){  
    foreach ($gcm as $a=>$b) {  
      if($b == 'gcm0') {  
        foreach( $loc as $y=>$z){  
          if($z == 'loc0'){  
  
displayTree4($a1b_mmaple,$sim);  
  
          }  
        }  
        foreach( $loc as $y=>$z){  
          if($z == 'loc1'){  
  
displayTree4($a1b_mmaple,$sim);  
  
          }  
        }  
        foreach( $loc as $y=>$z){  
          if($z == 'loc2'){  
  
displayTree4($a1b_mmaple,$sim);  
  
          }  
        }  
      }  
    }  
    foreach ($gcm as $a=>$b) {  
      if($b == 'gcm1') {  
        foreach( $loc as $y=>$z){  
          if($z == 'loc0'){  
            displayTree4($a2_mmaple,$sim);  
          }  
        }  
        foreach( $loc as $y=>$z){  
          if($z == 'loc1'){  
            displayTree4($a2_mmaple,$sim);  
          }  
        }  
        foreach( $loc as $y=>$z){  
          if($z == 'loc2'){  
            displayTree4($a2_mmaple,$sim);  
          }  
        }  
      }  
    }  
    foreach ($gcm as $a=>$b) {  
      if($b == 'gcm2') {
```



```

    }
  }
  foreach ($gcm as $a=>$b) {
    if($b == 'gcm1') {

      foreach( $loc as $y=>$z){
        if($z == 'loc0'){
          displayTree6($s_elm,$sim);
        }
      }
      foreach( $loc as $y=>$z){
        if($z == 'loc1'){
          displayTree6($s_elm,$sim);
        }
      }
      foreach( $loc as $y=>$z){
        if($z == 'loc2'){
          displayTree6($s_elm,$sim);
        }
      }
    }
  }
  foreach ($gcm as $a=>$b) {
    if($b == 'gcm2') {

      foreach( $loc as $y=>$z){
        if($z == 'loc0'){
          displayTree6($s_elm,$sim);
        }
      }
      foreach( $loc as $y=>$z){
        if($z == 'loc1'){
          displayTree6($s_elm,$sim);
        }
      }
      foreach( $loc as $y=>$z){
        if($z == 'loc2'){
          displayTree6($s_elm,$sim);
        }
      }
    }
  }
}

```

```
### WHITE SPRUCE ###
```

```

if($n == 'tree7'){

  foreach ($gcm as $a=>$b) {
    if($b == 'gcm0') {

      foreach( $loc as $y=>$z){
        if($z == 'loc0'){

          displayTree7($alb_wspruce,$sim);
        }
      }
    }
  }
}

```

```

    }
    }
    foreach( $loc as $y=>$z){
        if($z == 'loc1'){

displayTree7($a1b_wspruce,$sim);

        }
    }
    foreach( $loc as $y=>$z){
        if($z == 'loc2'){

displayTree7($a1b_wspruce,$sim);

        }
    }
}
foreach ($gcm as $a=>$b) {
    if($b == 'gcm1') {

        foreach( $loc as $y=>$z){
            if($z == 'loc0'){

displayTree7($a2_wspruce,$sim);

            }
        }
        foreach( $loc as $y=>$z){
            if($z == 'loc1'){

displayTree7($a2_wspruce,$sim);

            }
        }
        foreach( $loc as $y=>$z){
            if($z == 'loc2'){

displayTree7($a2_wspruce,$sim);

            }
        }
    }
}
foreach ($gcm as $a=>$b) {
    if($b == 'gcm2') {

        foreach( $loc as $y=>$z){
            if($z == 'loc0'){

displayTree7($b1_wspruce,$sim);

            }
        }
        foreach( $loc as $y=>$z){
            if($z == 'loc1'){

displayTree7($b1_wspruce,$sim);

            }
        }
        foreach( $loc as $y=>$z){
            if($z == 'loc2'){

```

```

displayTree7($b1_wspruce,$sim);
    }
}
}
}
}

```

```

### CARAGANA ###

```

```

if($n == 'tree8'){
    foreach ($gcm as $a=>$b) {
        if($b == 'gcm0') {
            foreach( $loc as $y=>$z){
                if($z == 'loc0'){
                    displayTree8($caragana,$sim);
                }
            }
            foreach( $loc as $y=>$z){
                if($z == 'loc1'){
                    displayTree8($caragana,$sim);
                }
            }
            foreach( $loc as $y=>$z){
                if($z == 'loc2'){
                    displayTree8($caragana,$sim);
                }
            }
        }
    }
    foreach ($gcm as $a=>$b) {
        if($b == 'gcm1') {
            foreach( $loc as $y=>$z){
                if($z == 'loc0'){
                    displayTree8($caragana,$sim);
                }
            }
            foreach( $loc as $y=>$z){
                if($z == 'loc1'){
                    displayTree8($caragana,$sim);
                }
            }
            foreach( $loc as $y=>$z){
                if($z == 'loc2'){
                    displayTree8($caragana,$sim);
                }
            }
        }
    }
    foreach ($gcm as $a=>$b) {
        if($b == 'gcm2') {

```



```

        $treeChkBox[] = &HTML_QuickForm::createElement('advcheckbox',
'TREE7', null, 'WHITE SPRUCE',null,'tree7');
        $treeChkBox[] = &HTML_QuickForm::createElement('advcheckbox',
'TREE8', null, 'CARAGANA (no future growth)',null,'tree8');

        $form->addGroup($treeChkBox, 'tree', null, '<br>');
        $form->addGroupRule('tree', 'Please check at least one box',
'required', null, 1);

        $form->addElement('header', 'TheHeader', 'Global Climate Model');
        $gcmChkBox[] = &HTML_QuickForm::createElement('advcheckbox', 'GCM0',
null, 'A1B (middle)',null,'gcm0');
        $gcmChkBox[] = &HTML_QuickForm::createElement('advcheckbox', 'GCM1',
null, 'A2 (high)',null,'gcm1');
        $gcmChkBox[] = &HTML_QuickForm::createElement('advcheckbox', 'GCM2',
null, 'B1 (low)',null,'gcm2');

        $form->addGroup($gcmChkBox, 'gcm', null, '<br>');
        $form->addGroupRule('gcm', 'Please check at least one box', 'required',
null, 1);

        $form->addElement('header', 'TheHeader', 'Saskatchewan Location');
        $locChkBox[] = &HTML_QuickForm::createElement('advcheckbox', 'LOC0',
null, 'NORTH-WEST', null, 'loc0');
        $locChkBox[] = &HTML_QuickForm::createElement('advcheckbox', 'LOC1',
null, 'NORTH-EAST', null, 'loc1');
        $locChkBox[] = &HTML_QuickForm::createElement('advcheckbox', 'LOC2',
null, 'SOUTH-WEST', null, 'loc2');
        $locChkBox[] = &HTML_QuickForm::createElement('advcheckbox', 'LOC3',
null, 'SOUTH-EAST(not working)', null, 'loc3');

        $form->addGroup($locChkBox, 'loc', null, '<br>');
        $form->addGroupRule('loc', 'Please check at least one box', 'required',
null, 1);

#validate form
$form->addElement('reset', 'btnClear', 'Clear');
        $form->addElement('submit', 'btnSubmit', 'Submit');

        if ($form->validate()) {
            $form->freeze();
            $form->process('process_data', false);
            $form->process('process_datas', false);
        }
        else {
            $form->setDefaults($user);
            $form->display();
        }
?>

```